

AD-A034 943

AIR FORCE INST OF TECH WRIGHT-PATTERSON AFB OHIO SCH--ETC F/G 20/4  
NUMERICAL SOLUTION OF THE COMPRESSIBLE BOUNDARY LAYER EQUATIONS--ETC(U)  
DEC 76 C R BLAKE  
GA/MC/76D-4

UNCLASSIFIED

NL

1 of 2  
ADA034943



ADA034943



COPY AVAILABLE TO DDC DOES NOT  
PERMIT FULLY LEGIBLE PRODUCTION



DDC  
RECEIVED  
JAN 28 1977  
REGULATORY

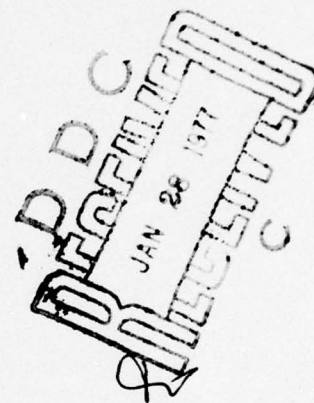
UNITED STATES AIR FORCE  
AIR UNIVERSITY  
AIR FORCE INSTITUTE OF TECHNOLOGY  
Wright-Patterson Air Force Base, Ohio

**DISTRIBUTION STATEMENT A**  
Approved for public release;  
Distribution Unlimited



GA/MC/76D-4

1



NUMERICAL SOLUTION OF THE COMPRESS-  
IBLE BOUNDARY LAYER EQUATIONS OVER  
AXISYMMETRIC SURFACES

THESIS

GA/MC/76D-4

Charles R. Blake  
Capt USAF

Approved for public release; distribution unlimited

14 GA/MC/76D-4

6 NUMERICAL SOLUTION OF THE COMPRESSIBLE  
BOUNDARY LAYER EQUATIONS OVER  
AXISYMMETRIC SURFACES.

THESIS 9 Master's thesis

Presented to the Faculty of the School of Engineering  
of the Air Force Institute of Technology  
Air University  
in Partial Fulfillment of the  
Requirements for the Degree of  
Master of Science

11 Dec 76

12 1210

by

10 Charles R./Blake B.S.  
Capt USAF

SEARCHED		SERIALIZED	
INDEXED		FILED	
DEC 1976			
AFIT			
BY			
REMARKS			
A			

## Preface

The subject of this study was suggested by Dr. J. S. Shang of the Air Force Flight Dynamics Laboratory in order to further validate numerical solutions of aerodynamic boundary layer flows. The study was accomplished by building upon a computer solution method developed by Dr. Shang. The study allowed me to apply much of my recent academic training.

I am indebted to Dr. Shang and Lt John Shea, my advisor, for their assistance and encouragement in all phases of this project. I am most grateful for the patience and understanding of my wife, Becki, throughout my study.



## Contents

Preface . . . . .	ii
List of Symbols . . . . .	v
List of Figures . . . . .	ix
Abstract . . . . .	xi
I. Introduction . . . . .	1
Purpose of the Study . . . . .	1
Existing Numerical Solution . . . . .	1
Modified Numerical Solution . . . . .	2
Outline of the Report . . . . .	3
II. Mathematical Formulation of the Problem . . . . .	4
Governing Equations . . . . .	4
Transformation of Independent Variables . . . . .	6
Transverse Curvature Correction . . . . .	9
Method of Modelling Body Geometry . . . . .	10
Representation of Turbulence Produced Terms . . . . .	12
Boundary Conditions . . . . .	15
III. Solution Technique . . . . .	18
Grid Generation in the Transformed Plane . . . . .	18
Finite Difference Approximations . . . . .	20
Matrix Method of Solution . . . . .	21
Logic of the Numerical Solution Procedure . . . . .	24
IV. Validation of New Solution . . . . .	34
Comparison with Experimental Results . . . . .	34
Turbulent Flow over a Waisted Body of Revolution . . . . .	34
Laminar Flow over a Spherically Blunted Cone . . . . .	36
Comparison of Accuracy with Other Computer Solutions . . . . .	38
V. Conclusions . . . . .	51
Bibliography . . . . .	52
Appendix A: Development of Two-Dimensional and Axisymmetric Boundary Layer Equations . . . . .	54
Appendix B: Three Point Finite Difference Approximations and Linearization of the Transformed Boundary Layer Equations . . . . .	63

Appendix C: Four Point Finite Difference Approximations for Evaluating Wall Derivatives. .	75
Appendix D: Computer Program Listing . . . . .	77
Vita . . . . .	106

## List of Symbols

### English Letters

<u>A</u>	A three dimensional vector used for illustration in Appendix A
$A_{11n}, A_{12n}, \dots A_{33n}$	Coefficients of linearized difference equations (B-53), (B-54), and (B-55)
$B_{11n}, B_{12n}, \dots B_{33n}$	
$C_{11n}, C_{12n}, \dots C_{33n}$	
$D_{1n}, D_{2n}, D_{3n}$	
$A_i, B_i, C_i$	Coefficients of radius equation (27)
$C_f$	Skin friction coefficient $\tau / \frac{1}{2} \rho_\infty u_\infty^2$
$C_p$	Specific heat at constant pressure
$e$	Specific internal energy of a fluid
$F$	Non-dimensional velocity $u/u_e$
$F_{conv}$	Defined by equation (62)
$FM1$	Defined by equation (B-24)
$FM2$	Defined by equation (B-25)
$FY$	Defined by equation (B-26)
$G, H$	Variables used for illustration purposes in Appendix B
$h$	Enthalpy ( $e + p/\rho$ )
$h_c$	Heat transfer coefficient
$h_x, h_y, h_z$	Scaling factors for orthogonal curvilinear coordinates defined by equations (A-12), (A-13), and (A-14)
<u>I</u>	Intermittency factor defined by equation (43)



$I_d$	Identity matrix
$\hat{i}, \hat{j}, \hat{k}$	Unit vector along orthogonal curvilinear coordinate axis
$K$	Parameter in grid equation (55)
$K_1$	Constant of inner layer eddy viscosity equation (37)
$K_2$	Constant of outer layer eddy viscosity equation (38)
$K_c$	Longitudinal curvature
$k$	Thermal conductivity
$L_R$	Reference length used in free stream Reynolds number
$l$	Defined by equation (16)
$l_m$	Mixing length used in equation (33)
$M$	Mach number
$m, n$	Grid indices of Fig. 3
$\hat{n}$	Unit normal vector of Fig. 21
$P$	Pressure
$P_1, P_2$	Defined by equations (39) and (40)
$Pr$	Prandtl number
$Pr_t$	Turbulent Prandtl number
$R$	Gas constant of equation (5)
$Re_\infty$	Free stream Reynolds number
$r$	Radius defined by equation (21)
$r_0$	Radius of an axisymmetric body (Fig. 1)
$r_s$	Radius of a sphere
$S$	Surface of a fluid element (Fig. 21)

$St$	Stanton number defined by equation (69)
$T$	Temperature
$TM_1$	Defined by equation (B-27)
$TM_2$	Defined by equation (B-28)
$TY$	Defined by equation (B-29)
$t$	Transverse curvature parameter
$u$	Velocity component in $X$ direction
$v$	Defined by equation (15)
$\underline{v}$	Three dimensional velocity vector used in Appendix A
$v$	Velocity component in $Y$ direction
$\tilde{v}$	Normal velocity defined by equation (A-25)
$X$	Coordinate axis of Fig. 1
$X_t$	Surface location where transition from laminar to turbulent flow begins
$Y$	Coordinate axis of Fig. 1
$Y_1, Y_2 \dots Y_{10}$	Defined by equations (B-14) through (B-22)
$Z$	Axis of symmetry

#### Greek Letters

$\alpha$	Defined by equation (19)
$\beta$	Defined by equation (18)
$\gamma$	Ratio of specific heats
$\delta$	Boundary layer thickness
$\delta_1$	Displacement thickness
$\epsilon$	Eddy viscosity defined by equation (33)
$\bar{\epsilon}, \hat{\epsilon}$	Eddy viscosity terms defined by equations (A-29) and (A-30)

$\eta$	Transformed $y$ coordinate
$\theta$	Non-dimensional temperature $T/T_e$
$\mu$	Molecular viscosity
$\xi$	Transformed $x$ coordinate
$\rho$	Density
$\underline{\underline{\sigma}}$	Shear stress tensor defined by equation (A-4)
$\tau_w$	Wall shear defined by equation (35)
$\tau$	Variable used for volume in Appendix A
$\underline{\underline{I}}$	Rate of strain tensor
$\psi$	Scalar variable used for illustration in Appendix A
$\phi$	Angle of surface tangent (See Fig. 1)

#### Subscripts

$e$	Boundary layer edge
$m$	Surface station in $\xi$ direction
$n$	Grid point in $\eta$ direction
Ref	Reference conditions
w	Wall values
o	Total or stagnation conditions
$\infty$	Free stream conditions

#### Superscripts

$j$	Index which determines two-dimensional or axisymmetric flow
*	Transpose of a matrix
'	Turbulent fluctuations
—	Time averaged



## List of Figures

<u>Figure</u>		<u>Page</u>
1	Surface Coordinate System . . . . .	6
2	Radius Curve Fitting . . . . .	11
3	Grid in the Transformed Plane . . . . .	19
4	Physical Quantities Describing The Problem .	24
5	Grid for Starting Solution . . . . .	27
6	Flow Diagram of Computer Program . . . . .	32
7	Geometry of Axisymmetric Waisted Body . . . .	40
8	Mach Number Distribution on Waisted Body . .	41
9	Momentum Thickness on Waisted Body for $M_\infty = 1.398$ . . . . .	42
10	Local Skin Friction Coefficient on Waisted body for $M_\infty = 1.398$ . . . . .	42
11	Momentum Thickness on Waisted Body for $M_\infty = 1.7$ . . . . .	43
12	Local Skin Friction Coefficient on Waisted body for $M_\infty = 1.7$ . . . . .	43
13	Velocity Profile on Waisted Body for $z = 24$ in . . . . .	44
14	Velocity Profile on Waisted Body for $z = 42$ in . . . . .	44
15	Velocity Profile on Waisted Body for $z = 50$ in . . . . .	45
16	Geometry of Spherically Blunted Cone . . . .	46
17	Pressure Distribution on Spherically Blunted Cone . . . . .	47
18	Non-Dimensional Heat Transfer Rate on Spherically Blunted Cone . . . . .	48
19	Comparison of Momentum Thickness for Differ- ent Methods of Solution . . . . .	49

<u>Figure</u>		<u>Page</u>
20	Comparison of Skin Friction Coefficient for Different Methods of Solution . . . . .	50
21	Finite Region of Flow Field . . . . .	54
22	Orthogonal Curvilinear Coordinates for an Axisymmetric Body . . . . .	57

Abstract

A numerical solution of the compressible boundary layer equations was developed for flows over either two-dimensional or axisymmetric surfaces. The solution method is an extension of a computer solution developed by Dr. J. S. Shang of the Air Force Flight Dynamics Laboratory. The solution method is capable of solving for boundary layer parameters in either laminar or turbulent flows. In the case of turbulent flow, closure is achieved by use of a two-layered eddy viscosity model. The boundary layer equations are solved by a numerical marching procedure. A Mangler-Levy-Lees transformation of independent variables is used to improve the efficiency of the numerical solution. The transformed boundary layer equations are then linearized by a three point finite difference scheme. The linearized equations are solved by a matrix solution technique. Comparisons of computed boundary layer parameters with experimentally determined parameters were made for both laminar and turbulent flows over axisymmetric bodies. The comparisons show the numerical solution to be very accurate.



NUMERICAL SOLUTION OF THE COMPRESSIBLE  
BOUNDARY LAYER EQUATIONS OVER  
AXISYMMETRIC SURFACES

I. Introduction

Purpose of the Study

The purpose of this study was to develop a numerical solution for compressible boundary layer flow over axisymmetric surfaces. This solution was to be applicable to both laminar and turbulent flows. This study was accomplished by expanding an existing numerical solution procedure developed by Dr. J. S. Shang of the Air Force Flight Dynamics Laboratory.

Existing Numerical Solution Procedure. The existing numerical solution as developed by Dr. Shang was capable of solving for boundary layer parameters either in a two-dimensional case or the limited axisymmetric case of conical flow. This numerical solution procedure has been shown to yield accurate results for compressible boundary layers in both the laminar and turbulent flow cases with pressure gradients and heat transfer at the surface.

The original algorithm made use of a transformation of independent variables in the boundary layer equations to transform the boundary layer equations into a coordinate plane in which efficient numerical computation was possible. This transformation was considered only in two-dimensional or conical axisymmetric flows where the cone radius could be represented as a linear function of distance along the surface.

The transformation also employed the assumption that the boundary layer thickness was negligible in comparison with the radius of the cone.

The transformed boundary layer equations were linearized by using a finite difference method of approximating derivatives within the equations. These equations were then solved by a matrix method, and the boundary layer parameters of interest were obtained by an inverse transformation.

Modified Numerical Solution Procedure. The numerical solution developed in this report follows the same general method of solution as the existing solution procedure. The primary difference between this solution and the existing solution is that a more general transformation of independent variables is used. By generalizing the transformation, boundary layer flows over arbitrary axisymmetric bodies can be considered.

The transformation of independent variables used in this report represents the axisymmetric body radius as a polynomial function of distance along intervals of the axis of symmetry. Using this model of the radius, the transformation of independent variables, required for efficient numerical computation, can be applied to arbitrary bodies of revolution.

The new solution is also improved, particularly in the case of slender bodies of revolution, by accounting for the transverse curvature effects. These effects were ignored in the existing solution by assuming the boundary layer thickness to be negligible in comparison with the radius of

the axisymmetric body.

The boundary layer equations were then transformed by this new transformation, and the resulting equations were linearized by using a finite difference method of approximating derivatives. These linearized equations were then solved by the same matrix method of solution as used in the existing solution. The inverse of this new transformation produced the boundary layer parameters of interest.

### Outline of the Report

This report is written to describe the modelling and numerical solution of the boundary layer equations over axisymmetric or two-dimensional surfaces. The solution procedure described in this report was implemented in a computer program listed in Appendix D.

The equations necessary to model the boundary layer flow for either two-dimensional or axisymmetric flows are given in Chapter II. The transformations required for numerical computation purposes are also given in this chapter.

Chapter III provides the actual mechanics involved in the numerical solution. The logic of this numerical solution as implemented in the computer program is also given.

Chapter IV presents the results of two test cases used to validate the numerical solution procedure. A comparison of accuracy with two other numerical solution methods is also made.

Chapter V contains conclusions and recommendations resulting from this study.



## II. Mathematical Formulation of the Problem

### Governing Equations

The boundary layer equations describing conservation of mass, momentum, and energy as developed in Appendix A are

$$\frac{\partial}{\partial x} [r^j \bar{\rho} \bar{u}] + \frac{\partial}{\partial y} [r^j \bar{\rho} \tilde{v}] = 0 \quad (1)$$

$$\bar{\rho} \bar{u} \frac{\partial \bar{u}}{\partial x} + \bar{\rho} \tilde{v} \frac{\partial \bar{u}}{\partial y} = -\bar{\rho} \frac{\partial \bar{p}}{\partial x} + \frac{1}{r^j} \frac{\partial}{\partial y} \left[ r^j \mu \bar{\epsilon} \frac{\partial \bar{u}}{\partial y} \right] \quad (2)$$

$$\begin{aligned} \bar{\rho} \bar{u} \frac{\partial}{\partial x} [c_p \bar{T}] + \bar{\rho} \tilde{v} \frac{\partial}{\partial y} [c_p \bar{T}] &= \bar{u} \frac{\partial \bar{p}}{\partial x} + \mu \bar{\epsilon} \left[ \frac{\partial \bar{u}}{\partial y} \right]^2 \\ &+ \frac{1}{r^j} \frac{\partial}{\partial y} \left[ \frac{r^j \mu \hat{\epsilon}}{\rho_r} \frac{\partial}{\partial y} (c_p \bar{T}) \right] \end{aligned} \quad (3)$$

This set of equations can be used to describe either laminar or turbulent boundary layers. The eddy viscosity terms  $\bar{\epsilon}$  and  $\hat{\epsilon}$  reduce to a value of unity for laminar flow. Also the normal velocity term  $\tilde{v}$ , which is the sum of  $\bar{v}$  and  $\frac{\rho' v'}{\bar{\rho}}$ , reduces to  $\bar{v}$  for laminar flow.

The superscript  $j$  in equations (1), (2), and (3) allows the equations to be used for either two-dimensional or axisymmetric flow. For the two dimensional case,  $j$  is set equal to zero to remove the radius  $r$  from the equations. For the axisymmetric case,  $j$  is given the value of unity.

In equations (2) and (3),  $\bar{\epsilon}$  and  $\hat{\epsilon}$  are considered as

known functions of  $\bar{\rho}$ ,  $\bar{u}$ , and  $\gamma$  and will be discussed later in this chapter. The pressure gradient is known from the inviscid Euler equation (Ref 14:21) given as

$$\frac{\partial \bar{P}}{\partial x} = -\rho_e u_e \frac{\partial u_e}{\partial x} \quad (4)$$

since flow properties outside the boundary layer can be determined by inviscid flow theory.

Equations (1), (2), and (3) then contain five unknowns:  $\bar{u}$ ,  $\bar{\rho}$ ,  $\bar{v}$ ,  $\mu$ , and  $\bar{T}$ . The perfect gas law and Sutherland's viscosity law (Ref 17:19), given by equations (5) and (6) respectively, are used to express  $\mu$  and  $\bar{\rho}$  as functions of  $\bar{T}$  and thus reduce the unknowns to  $\bar{u}$ ,  $\bar{v}$ , and  $\bar{T}$ .

$$\bar{P} = \bar{\rho} R \bar{T} \quad (5)$$

$$\frac{\mu}{\mu_{\text{Ref}}} = \left[ \frac{\bar{T} (^{\circ}\text{R})}{T_{\text{Ref}} (^{\circ}\text{R})} \right]^{\frac{3}{2}} \left[ \frac{T_{\text{Ref}} (^{\circ}\text{R}) + 198.6 ^{\circ}\text{R}}{\bar{T} (^{\circ}\text{R}) + 198.6 ^{\circ}\text{R}} \right] \quad (6)$$

The pressure  $\bar{P}$  is a known quantity outside the boundary layer. The pressure within the boundary layer can be considered constant in a direction normal to the surface bordering the boundary layer; therefore, equation (5) reduces to a relation between  $\bar{\rho}$  and  $\bar{T}$ .

The use of equations (4), (5), and (6) can, therefore, be seen to reduce equations (1), (2), and (3) to a set of three equations in three unknowns.

### Transformation of Independent Variables

The governing equations (1), (2), and (3) have a singularity at the stagnation point ( $r=0$ ) for axisymmetric flow. In order to remove the singularity and also to remove most of the variation in boundary layer thickness along the surface, a Mangler-Levy-Lees transformation (Ref 2:261)

$$\xi(X) = \int_0^X \rho_e u_e \mu_e \left( \frac{r_0}{L_R} \right) dX \quad (7)$$

$$\eta(X, Y) = \frac{\rho_e u_e}{(2\xi)^{1/2}} \left( \frac{r_0}{L_R} \right) \int_0^Y \left( \frac{r}{r_0} \right) \left( \frac{\rho}{\rho_e} \right) dY \quad (8)$$

was introduced. The removal of most of the variation in boundary layer thickness improves the efficiency of numerical solution of the boundary layer equations.

The quantities  $r$ ,  $r_0$ ,  $X$ , and  $Y$  in equations (7) and (8) are those shown in Fig. 1. The orthogonal coordinate system  $X, Y$  is a surface coordinate system in which the

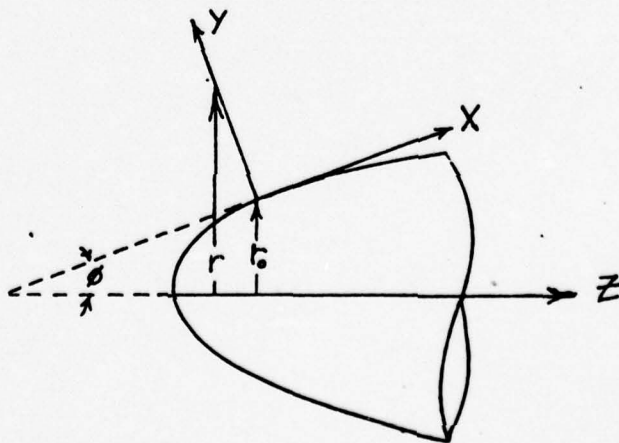


Fig. 1. Surface Coordinate System



X axis is tangent to the surface and points in the stream-wise direction while the Y axis is perpendicular to the surface. The term  $r$  is the distance from the centerline to any point on the Y axis measured perpendicular to the axis of symmetry. The term  $L_R$  is the reference length used in computing the free stream Reynolds number. The ratio  $\frac{r}{L_R}$  in equation (8) is known as the transverse curvature parameter and will be represented as  $\tau$ .

The partial derivative operators associated with equations (7) and (8) are

$$\left(\frac{\partial}{\partial x}\right)_y = \rho_e \mu_e u_e \left(\frac{r_o}{L_R}\right)^{2j} \left[ \left(\frac{\partial}{\partial \xi}\right)_\eta + \left(\frac{\partial \eta}{\partial \xi}\right)_\eta \left(\frac{\partial}{\partial \eta}\right)_\xi \right] \quad (9)$$

$$\left(\frac{\partial}{\partial y}\right)_x = \frac{\rho u_e}{(2\xi)^{1/2}} \left(\frac{r}{L_R}\right)^j \left(\frac{\partial}{\partial \eta}\right)_\xi \quad (10)$$

The governing equations (1), (2), and (3) are now transformed from physical surface coordinates  $X, Y$  to the transformed coordinates  $\xi, \eta$ . The transformed boundary layer equations are

$$F + 2\xi \frac{\partial F}{\partial \xi} + \frac{\partial V}{\partial \eta} = 0 \quad (11)$$

$$\begin{aligned} \frac{\partial}{\partial \eta} \left[ 1 \bar{E} \tau^{2j} \frac{\partial F}{\partial \eta} \right] - V \frac{\partial F}{\partial \eta} + \beta [\theta - F^2] \\ = 2\xi F \frac{\partial F}{\partial \xi} \end{aligned} \quad (12)$$

$$\frac{\partial}{\partial \eta} \left[ l \frac{\hat{\epsilon}}{\rho_r} t^{2j} \frac{\partial \theta}{\partial \eta} \right] - V \frac{\partial \theta}{\partial \eta} + l \bar{\epsilon} t^{2j} \alpha \left( \frac{\partial F}{\partial \eta} \right)^2 = 2 \xi F \frac{\partial \theta}{\partial \xi} \quad (13)$$

where the following definitions have been used.

$$F = \frac{\bar{U}}{u_e} \quad (14)$$

$$V = \frac{2\xi}{\rho_e u_e \mu_e \left( \frac{r_0}{L_R} \right)^{2j}} \left[ \frac{\partial \eta}{\partial X} F + \frac{1}{(2\xi)^{1/2}} (r_0^{2j} \bar{\rho} \tilde{v}) \right] \quad (15)$$

$$l = \frac{\bar{\rho} \bar{\mu}}{\rho_e \mu_e} \quad (16)$$

$$\theta = \frac{\bar{T}}{T_e} \quad (17)$$

$$\beta = \frac{2\xi}{u_e} \frac{\partial u_e}{\partial \xi} \quad (18)$$

$$\alpha = \frac{u_e}{C_p T_e} \quad (19)$$

When equations (5) and (6) are applied to equation (16), the expression for  $l$  becomes

$$l = \theta^{1/2} \left[ \frac{1 + \frac{198.6^\circ R}{T_e (^\circ R)}}{\theta + \frac{198.6^\circ R}{T_e (^\circ R)}} \right] \quad (20)$$

Given this relation for  $l$  and assuming  $\tau$ ,  $\bar{\epsilon}$ , and  $\hat{\epsilon}$  can

be expressed as functions of  $F$ ,  $\Theta$ , and  $V$ , equations (11), (12), and (13) become a set of three non-linear differential equations in three unknowns  $F$ ,  $\Theta$ , and  $V$ . The expressions for  $t$ ,  $\bar{\epsilon}$ , and  $\hat{\epsilon}$  are developed in detail later in this chapter.

#### Transverse Curvature Correction

The existing numerical solution prior to modification assumed that the transverse curvature parameter  $t$  was equal unity. The solution developed in this report retains the transverse curvature effect in the solution of the boundary layer equations. Since the parameter  $t$  is the ratio of  $\frac{r}{r_0}$ , an expression for  $t$  is found by observing from Fig. 1 that

$$r = r_0 + Y \cos \phi \quad (21)$$

Dividing equation (21) by  $r_0$  and using the definition  $t = \frac{r}{r_0}$  gives

$$t = 1 + \frac{Y}{r_0} \cos \phi \quad (22)$$

For a given value of  $X$ , the derivative of  $t$  is

$$dt = \left( \frac{\cos \phi}{r_0} \right) dY \quad (23)$$

Solving equation (23) for  $dY$  and substituting the value into equation (7) yields



$$t dt = \frac{L_R (2\xi) \cos \phi}{\rho_e u_e r_o^2} \left( \frac{\rho_e}{\bar{\rho}} \right) d\eta \quad (24)$$

When equation (24) is integrated from the surface outward in the normal direction, it yields

$$t^2 = 1 + \frac{2 L_R (2\xi)^{1/2}}{\rho_e u_e r_o^2} \cos \phi \int_0^\eta \frac{\rho_e}{\bar{\rho}} d\eta \quad (25)$$

Using equations (5) and (17), the expression for  $t$  in the transformed coordinate plane is

$$t = \left[ 1 + \frac{2 L_R (2\xi)^{1/2}}{\rho_e u_e r_o^2} \cos \phi \int_0^\eta \theta d\eta \right]^{1/2} \quad (26)$$

As equation (22) indicates,  $t = 1$  is a good approximation for most axisymmetric boundary layer flows. The numerical solution procedure was, therefore, designed such that the transverse curvature correction could be retained or dropped from the solution of the boundary layer equations.

#### Method of Modelling Body Radius

The geometry of an axisymmetric body is determined in the new solution procedure by fitting a quadratic curve of the form

$$r_o(z) = A_i + B_i z + C_i z^2 \quad (27)$$

through a series of surface coordinates as shown in Fig. 2 .

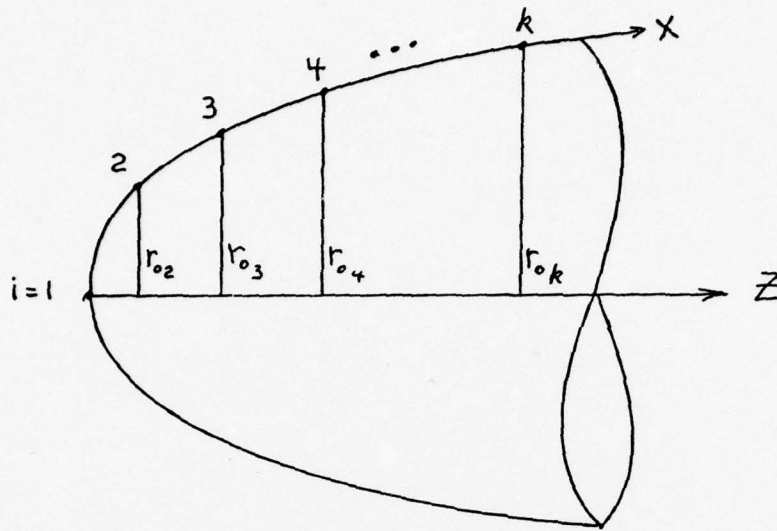


Fig. 2. Radius Curve Fitting

Since the existing computer solution procedure required the input of surface pressure at a finite number of surface locations, the coordinates  $r_o, Z$  of these locations are input and used in the new solution procedure to determine  $r_o(Z)$ . The coefficients  $A_i, B_i,$  and  $C_i$  are then determined by fitting equation (27) through three consecutive surface locations starting with location  $i$ . In using equation (27) to determine  $r_o$ , the first set of coefficients  $A_i, B_i,$  and  $C_i$  is used until the second surface location is reached and then the second set of coefficients would be used until the third surface location is reached. This technique is continued for increasing values of  $X$  until the last surface location ( $i = k$ ) is reached. Since the changeover in coefficients is made at points for which  $r_o$  is known exactly, errors in determining  $r_o$  do not propagate.

The angle  $\phi$  between the centerline axis and the tangent to the surface is required in order to determine the transverse curvature parameter  $t$  in equation (26). This angle is observed from Fig. 1 to be

$$\phi = \tan^{-1} \left( \frac{dr_o}{dz} \right) \quad (28)$$

where  $\frac{dr_o}{dz}$  determined from equation (27) is

$$\frac{dr_o}{dz} = B_i + 2 C_i Z \quad (29)$$

Since the numerical marching technique used to solve equations (11), (12), and (13) proceeds stepwise along the surface of the body, distance along the surface is related to centerline distance by (See Fig. 1)

$$\frac{dZ}{dX} = \cos \phi \quad (30)$$

#### Representation of Turbulence Produced Terms

Closure of the turbulence correlations in the boundary layer equations is effected by the eddy viscosity terms  $\bar{\epsilon}$  and  $\hat{\epsilon}$  (See Appendix A), where

$$\bar{\epsilon} = 1 + \frac{\epsilon}{\mu} \quad (31)$$

$$\hat{\epsilon} = 1 + \frac{\epsilon}{\mu} \frac{P_r}{P_{rt}} \quad (32)$$



The actual eddy viscosity  $\epsilon$  used in the solution procedure is a two layered model in which two separate formulas are used for the inner and outer region of the boundary layer.

The inner region model is based on Prandtl's mixing length theory (Ref 13: 548).

$$\left(\frac{\epsilon}{\mu}\right)_i = \frac{\rho l_m}{\mu} \left| \frac{\partial u}{\partial y} \right| \quad (33)$$

This expression after being fitted with the experimentally determined mixing length  $l_m$  of Van Driest (Ref 15: 1009) is

$$\left(\frac{\epsilon}{\mu}\right)_i = \frac{K_1 y^2}{\mu} \left\{ 1 - \exp \left[ -\frac{y \rho}{26 \mu} \left( \frac{\tau_w}{\rho} \right)^{\frac{1}{2}} \right] \right\} \left| \frac{\partial u}{\partial y} \right| \quad (34)$$

The value of  $K_1$  used in this report is 0.4 as given by Van Driest and validated by Cebeci (Ref 4: 23). The wall shear stress  $\tau_w$  is given as

$$\tau_w = \mu_w \left( \frac{\partial u}{\partial y} \right)_w \quad (35)$$

The eddy viscosity model used for the outer region of the boundary layer (Ref 3: 526) is

$$\left(\frac{\epsilon}{\mu}\right)_o = K_2 \frac{\rho}{\mu} \int_0^{\infty} (u_e - u) dy \quad (36)$$

where the value given for  $K_2$  is 0.0168.

Changeover from the inner region model to the outer

region model is made when the value of  $\left(\frac{\epsilon}{\mu}\right)_i$  is equal to  $\left(\frac{\epsilon}{\mu}\right)_0$ .

Since the transformed boundary layer equations (11), (12), and (13) are solved in the  $\xi, \eta$  plane, it is necessary to transform equations (34) and (36) into this coordinate plane. These equations after being transformed by use of the transformation equations (9) and (10) are

$$\left(\frac{\epsilon}{\mu}\right)_i = \frac{P_1 K_1}{\lambda} \left[ 1 - \exp\left(\frac{-\sqrt{P_1 P_2}}{26l}\right) \right]^2 \left| \frac{\partial F}{\partial \eta} \right|_w \quad (37)$$

$$\left(\frac{\epsilon}{\mu}\right)_0 = \frac{K_2 \sqrt{2\xi}}{\theta^2 \mu_e r_o^3 l} \int_0^\eta (1-F) \frac{\theta}{t^j} d\eta \quad (38)$$

where

$$P_1 = \frac{\rho_e^2 u_e \left[ \frac{r_o}{\cos \phi} (t-1) \right]^2 r_o t^j}{\mu_e (2\xi)^{1/2} \theta^3} \quad (39)$$

$$P_2 = l_w \left( \frac{\partial F}{\partial \eta} \right)_w \quad (40)$$

The turbulent Prandtl number  $P_{rt}$  appearing in equation (32) is determined from experimental data, and the value used in this report is 0.9 as suggested by Cebeci (Ref 2:260) for air. With this value of  $P_{rt}$  and equations (35) and (36),  $\bar{\epsilon}$  and  $\hat{\epsilon}$  are determined since the static Prandtl number  $P_r$  is known for air.

For cases of transition from laminar to turbulent flow, a transition model developed by Harris (Ref 4:29) is used in the solution procedure. The model introduces a transition

factor  $I$  which is multiplied by the eddy viscosity  $\epsilon$  such that equations (31) and (32) become

$$\bar{\epsilon} = 1 + \left( \frac{\epsilon}{\mu} \right) I \quad (41)$$

$$\hat{\epsilon} = 1 + \left( \frac{\epsilon}{\mu} \right) \left( \frac{p_r}{p_{r_t}} \right) I \quad (42)$$

The transition factor  $I$  is given by

$$I = 1 - \exp \left[ -0.412 \left( \frac{x - x_t}{.5 x_t} \right)^2 \right] \quad (43)$$

where  $x_t$  is the surface location at which the transition from laminar to turbulent flow begins. With this model, it can be seen that  $I$  would have a value of approximately zero prior to the transition point and then asymptotically approach unity beyond the transition point.

#### Boundary Conditions

The transformed boundary layer equations (11), (12), and (13) are solved by a method in which these equations are linearized to a first order set of equations in  $F, \theta$ , and  $V$ . This set of equations is then solved subject to boundary conditions on  $F, \theta$ , and  $V$  at both the wall and the outer edge of the boundary layer.

The boundary conditions at the wall or surface of the body necessary to satisfy the conditions of no slip at the wall, no mass transfer, and a constant body temperature are



$$\bar{u}(x, 0) = 0 \quad (44)$$

$$\tilde{v}(x, 0) = 0 \quad (45)$$

$$\bar{T}(x, 0) = 0 \quad (46)$$

The boundary conditions at the outer edge of the boundary layer, which are determined by external flow properties, are

$$\bar{u}(x, y_e) = u_e(x) \quad (47)$$

$$\bar{T}(x, y_e) = \bar{T}_e(x) \quad (48)$$

In terms of the transformed variables, these boundary conditions are

$$F(\xi, 0) = 0 \quad (49)$$

$$V(\xi, 0) = 0 \quad (50)$$

$$\Theta(\xi, 0) = T_w/T_e \quad (51)$$

$$F(\xi, \eta_e) = 1 \quad (52)$$

$$\Theta(\xi, \eta_e) = 1 \quad (53)$$

Although there is no physical boundary condition for  $\tilde{v}(x, y_e)$ , a mathematical boundary condition on  $V(\xi, \eta_e)$  is required in the numerical solution. Since the numerical solution

technique uses an iterative type solution at each step along the surface to obtain a solution to the transformed boundary layer equations, the value used for a boundary condition on  $V(\xi, \eta_e)$  is the last calculated value of  $V(\xi, \eta_e)$ .

$$V(\xi, \eta_e)_i = V(\xi, \eta_e)_{i-1} \quad (54)$$

### III. Solution Technique

#### Grid Generation in the Transformed Plane

The transformed boundary layer equations (11), (12), and (13) are solved by a numerical marching procedure. This procedure obtains a solution at each step along the surface moving downstream in the flow field.

In order to implement this method of solution, a grid is generated in the transformed plane in such a way that the ratio of any two successive spacings in the  $\eta$  direction is a constant. Spacing of steps in the  $\xi$  direction is variable in the sense that it can be doubled at any point along the surface. The grid is generated by the following formula.

$$\Delta\eta_{n-1} = (K)^{n-2} \Delta\eta_1, \quad n = 2, N \quad (55)$$

$K$  is the ratio of any two successive spacings in the  $\eta$  direction and  $\Delta\eta_1$  is the assigned value of the first grid spacing as shown in Fig. 3. This grid allows for short steps near the wall where velocity and temperature gradients are normally greatest and larger steps as the edge of the boundary layer is approached. The values of  $K$ ,  $N$ , and  $\Delta\eta_1$  are chosen such that a minimum number of points have to be used in order to obtain a solution for any given problem. Typical values of  $K$ ,  $N$ , and  $\Delta\eta_1$  used in this study were 1.1, 100, and .0005 respectively. A typical starting value for  $\Delta X$  was .001 which was then doubled at several points along the surface.



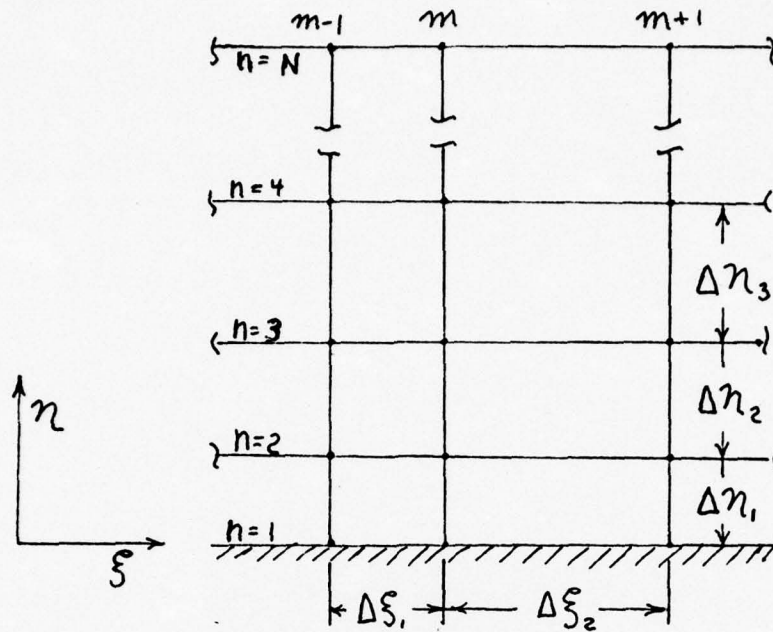


Fig.3. Grid in Transformed Plane

At each  $\xi$  station, when a solution to the boundary layer equations is obtained, the convergence of both  $F$  and  $\Theta$  is checked at the  $(N - 15)$  grid point in the  $\eta$  direction. This is accomplished by using the following two relations.

$$F(N-16) - F(N-15) \geq 0.0001 \quad (56)$$

$$\Theta(N-16) - \Theta(N-15) \geq 0.0001 \quad (57)$$

This convergence check is based on the fact that  $F$  and  $\Theta$  approach unity as the boundary layer edge is approached. If either of equations (56) or (57) is true, another grid point is added in the  $\eta$  direction. This solution procedure is then capable to some extent to correct for a value of  $N$

that is too small as the numerical solution steps along the surface.

### Finite Difference Approximations

The partial derivatives in the transformed boundary layer equations (11), (12), and (13) are approximated by a three point finite difference scheme. The derivative of a variable with respect to  $\xi$  is approximated by a forward difference method in which the value of a derivative at any  $\xi$  station is a function of values of the variable at the preceding two  $\xi$  stations and the present  $\xi$  station. The derivatives with respect to  $\eta$  are approximated by a central difference method in which the value of a derivative at any grid point is a function of values of the dependent variable above, below, and at the grid point of interest. The derivation of these finite difference expressions is given in Appendix B.

By substituting these finite difference expressions into the transformed boundary layer equations, a linearized set of algebraic equations was obtained. If a grid point  $m+1, n$  is the point for which the boundary layer equations are being evaluated, these linearized boundary layer equations (See Appendix B) are

$$\begin{aligned} &A_{11n} F_{m+1, n-1} + A_{12n} F_{m+1, n} + A_{13n} F_{m+1, n+1} + B_{11n} \theta_{m+1, n-1} \\ &+ B_{12n} \theta_{m+1, n} + B_{13n} \theta_{m+1, n+1} + C_{11n} V_{m+1, n-1} + C_{12n} V_{m+1, n} \\ &+ C_{13n} V_{m+1, n+1} = D_{1n} \end{aligned} \quad (58)$$

$$\begin{aligned}
& A_{21_n} F_{m+1, n-1} + A_{22_n} F_{m+1, n} + A_{23_n} F_{m+1, n+1} + B_{21_n} \Theta_{m+1, n-1} \\
& + B_{22_n} \Theta_{m+1, n} + B_{23_n} \Theta_{m+1, n+1} + C_{21_n} V_{m+1, n-1} + C_{22_n} V_{m+1, n} \\
& + C_{23_n} V_{m+1, n+1} = D_{2_n}
\end{aligned} \tag{59}$$

$$\begin{aligned}
& A_{31_n} F_{m+1, n-1} + A_{32_n} F_{m+1, n} + A_{33_n} F_{m+1, n+1} + B_{31_n} \Theta_{m+1, n-1} \\
& + B_{32_n} \Theta_{m+1, n} + B_{33_n} \Theta_{m+1, n+1} + C_{31_n} V_{m+1, n-1} + C_{32_n} V_{m+1, n} \\
& + C_{33_n} V_{m+1, n+1} = D_{3_n}
\end{aligned} \tag{60}$$

The subscripts of  $F$ ,  $\Theta$ , and  $V$  indicate the grid points at which the variables are evaluated. The subscripted coefficients  $A, B, C$  and  $D$  are evaluated from known values of the boundary layer properties at  $\xi$  stations  $m-1$  and  $m$  as shown in Appendix B.

#### Matrix Method of Solution

The linearized boundary layer equations given in equations (58), (59), and (60) were developed for the grid point  $m+1, n$  of Fig.3. If these linearized equations are written for all grid points of  $\xi$  station  $m+1$  with  $N = 6$ , the matrix equation (61) results. This equation has been written for an unrealistic case of six grid points in the direction but serves to illustrate the matrix equation that results regardless of the value of  $N$ . The linearized boundary layer equations have fewer terms when written at either grid point  $m+1, 2$  or  $m+1, N-1$ . This is due to the boundary conditions which are used to specify values of  $F, \Theta$ ,



$$\begin{bmatrix}
 A_{12}_2 B_{12}_2 C_{12}_2 A_{13}_2 B_{13}_2 C_{13}_2 \\
 A_{22}_2 B_{22}_2 C_{22}_2 A_{23}_2 B_{23}_2 C_{23}_2 \\
 A_{32}_2 B_{32}_2 C_{32}_2 A_{33}_2 B_{33}_2 C_{33}_2 \\
 A_{11}_3 B_{11}_3 C_{11}_3 A_{12}_3 B_{12}_3 C_{12}_3 A_{13}_3 B_{13}_3 C_{13}_3 \\
 A_{21}_3 B_{21}_3 C_{21}_3 A_{22}_3 B_{22}_3 C_{22}_3 A_{23}_3 B_{23}_3 C_{23}_3 \\
 A_{31}_3 B_{31}_3 C_{31}_3 A_{32}_3 B_{32}_3 C_{32}_3 A_{33}_3 B_{33}_3 C_{33}_3 \\
 A_{11}_4 B_{11}_4 C_{11}_4 A_{12}_4 B_{12}_4 C_{12}_4 A_{13}_4 B_{13}_4 C_{13}_4 \\
 A_{21}_4 B_{21}_4 C_{21}_4 A_{22}_4 B_{22}_4 C_{22}_4 A_{23}_4 B_{23}_4 C_{23}_4 \\
 A_{31}_4 B_{31}_4 C_{31}_4 A_{32}_4 B_{32}_4 C_{32}_4 A_{33}_4 B_{33}_4 C_{33}_4 \\
 A_{11}_5 B_{11}_5 C_{11}_5 A_{12}_5 B_{12}_5 C_{12}_5 \\
 A_{21}_5 B_{21}_5 C_{21}_5 A_{22}_5 B_{22}_5 C_{22}_5 \\
 A_{31}_5 B_{31}_5 C_{31}_5 A_{32}_5 B_{32}_5 C_{32}_5
 \end{bmatrix}
 =
 \begin{bmatrix}
 F_{m+1,2} \\
 \Theta_{m+1,2} \\
 V_{m+1,2} \\
 F_{m+1,3} \\
 \Theta_{m+1,3} \\
 V_{m+1,3} \\
 F_{m+1,4} \\
 \Theta_{m+1,4} \\
 V_{m+1,4} \\
 F_{m+1,5} \\
 \Theta_{m+1,5} \\
 V_{m+1,5}
 \end{bmatrix}
 =
 \begin{bmatrix}
 D_{12}_2 \\
 D_{22}_2 \\
 D_{32}_2 \\
 D_{13}_3 \\
 D_{23}_3 \\
 D_{33}_3 \\
 D_{14}_4 \\
 D_{24}_4 \\
 D_{34}_4 \\
 D_{15}_5 \\
 D_{25}_5 \\
 D_{35}_5
 \end{bmatrix}$$

(61)

and  $V$  at grid points  $m+1, 1$  and  $m+1, N$ .

Matrix equation (61) is then a system of  $3 \times (N-2)$  linear equations in  $3 \times (N-2)$  unknowns. Equation (61) is solved for  $F$ ,  $\Theta$ , and  $V$  by use of a Gaussian elimination method (Ref 6:301).

Once the solution is obtained, it is checked for convergence by computing

$$\frac{F_{m+1,2} - F_{m+1,1}}{\Delta \eta_1} = F_{\text{CONV}} \quad (62)$$

each time equation (61) is solved. The present value and the last computed value of  $F_{\text{CONV}}$  are retained so that the following comparison can be made.

$$F_{\text{CONV}} \Big|_{\text{NEW}} - F_{\text{CONV}} \Big|_{\text{OLD}} \geq \text{ERROR} \quad (63)$$

The value of ERROR used in this study was .0005. If equation (63) is not true then the solution of equation (61) is accepted as the solution of the transformed boundary layer equations. If equation (63) is true then the subscripted coefficients  $A$ ,  $B$ ,  $C$ , and  $D$  are updated using the values of  $F$ ,  $\Theta$ , and  $V$  just obtained from the solution of equation (61). With these new values of  $A$ ,  $B$ ,  $C$ , and  $D$  the solution of equation (61) is undertaken again. This procedure of updating  $A$ ,  $B$ ,  $C$ , and  $D$  is explained in detail in Appendix B. This iterative type procedure is continued until the convergence criteria of equation (63) is satisfied or 100 attempted solutions of equation (61)

have been made.

#### Logic of the Numerical Solution Procedure

This numerical solution procedure as implemented into a computer program requires certain inputs describing the problem in order to obtain a solution to the boundary layer equations. The free stream quantities required to be input to the computer program are the Mach number  $M_\infty$ , temperature  $T_\infty$ , and Reynolds number  $Re_\infty$ . The pressure  $P_c$  at a finite number of surface locations and the surface temperature  $T_w$ , which is assumed constant, are also required inputs to the computer program. It is also necessary to know whether the flow is laminar or turbulent, and if the flow transitions from laminar to turbulent flow, the transition point  $X_t$  must also be known. These quantities necessary to describe the physical problem are depicted in Fig. 4.

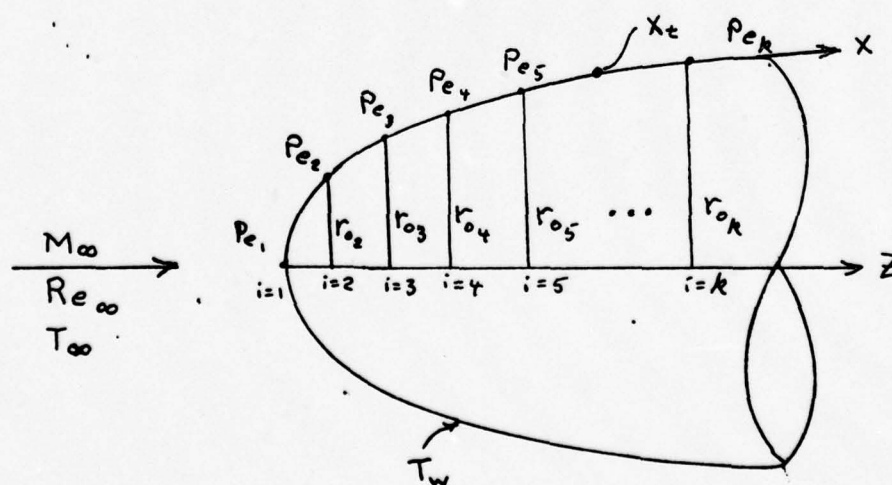


Fig. 4. Physical Quantities Describing the Problem



With these quantities describing the problem, the curve fitting procedure to determine a continuous function for  $r_0$  is then accomplished. For portions of the surface where the radius is changing rapidly, the number of surface pressure entries should be greater than on portions of the surface where the radius is slowly varying. This improves the accuracy of the radius modelling since the curve fitting procedure uses the coordinates of the surface pressure entries to determine  $r_0$  as a function of  $z$ .

In order to make the transformation of independent variable from physical coordinates  $x, y$  to transformed coordinates  $\xi, \eta$  it is also necessary to know the local boundary layer edge properties of  $\rho_e, \mu_e$ , and  $u_e$ . These properties are determined as in the existing solution by first determining  $\frac{dP}{dx}$  at each of the surface pressure points. The pressure gradient at each of the surface pressure points is approximated by a central finite difference method as developed in Appendix B. This approximation for  $\frac{dP}{dx}$  is

$$\left. \frac{dP}{dx} \right|_i = \frac{(x_i - x_{i-1}) P_{i+1}}{(x_{i+1} - x_i)(x_{i+1} - x_{i-1})} - \frac{(2x_i - x_{i-1} - x_{i+1}) P_i}{(x_{i+1} - x_i)(x_i - x_{i-1})} - \frac{(x_{i+1} - x_i) P_{i-1}}{(x_{i+1} - x_{i-1})(x_i - x_{i-1})} \quad (64)$$

where the subscripts refer to the surface points of Fig. 4. The pressure gradient  $\frac{dP}{dx}$  was then made a continuous function of distance along the surface by a curve fitting procedure similar to that used for the radius  $r_0$ . The local

edge pressure can then be determined at any point on the surface by integrating this continuous function  $\frac{dp}{dx}$  forward from the last known value of the pressure  $P_e$ . This integration is accomplished in the computer program by use of a trapezoidal rule for integration. The boundary layer edge temperature was then computed by assuming that temperature could be related to pressure by the isentropic relation

$$\frac{T_e}{T_o} = \left( \frac{P_e}{P_o} \right)^{\frac{\gamma}{1-\gamma}} \quad (65)$$

(Ref 9:53) where  $T_o$  and  $P_o$  are stagnation values of  $T$  and  $P$ . With these quantities known,  $M_e$  is calculated from equation (6). The local edge velocity is determined by using the energy equation for an inviscid perfect gas (Ref 9:53) which is given by

$$\frac{u_e^2}{2} = C_p T_o - C_p T_e \quad (66)$$

From the perfect gas equation,  $\rho_e$  is determined. All quantities required for the transformation equation (7) are now known.

The first step  $\Delta x$  along the surface is now taken and transformed into  $\Delta \xi$  by equation (7). The grid in the  $\eta$  direction is also generated at this point.

In order to start the solution, the transformed boundary layer equations are solved by a similar solution technique at the first three  $\xi$  stations. This technique assumes arbitrary, but identical, profiles for  $F$ ,  $\Theta$ , and  $V$  at the

first two  $\xi$  stations. Values of  $\bar{e}$ ,  $\hat{e}$ , and  $t$  are set equal to unity for this similar solution. With these assumptions and using  $\Delta\xi_1 = \Delta\xi_2$ , all the coefficients  $A$ ,  $B$ ,  $C$ , and  $D$  of the linearized boundary layer equations (58), (59), and (60) can be determined. The matrix equation (61) can then be solved for  $F$ ,  $\Theta$ , and  $V$  at  $\xi$  station 3 of Fig. 5. When this solution is obtained, the values of  $F$ ,  $\Theta$ , and  $V$  at  $\xi$  stations 1 and 2 are set equal to the solved values at  $\xi$  station 3. The coefficients  $A$ ,  $B$ ,  $C$ , and  $D$  can now be updated and a new solution for  $F$ ,  $\Theta$ , and  $V$  obtained at  $\xi$  station 3. This procedure is repeated until the solved values of  $F$ ,  $\Theta$ , and  $V$  converge. After establishing these initial profiles by similar solution, the solution of the boundary layer equations can proceed as described in the

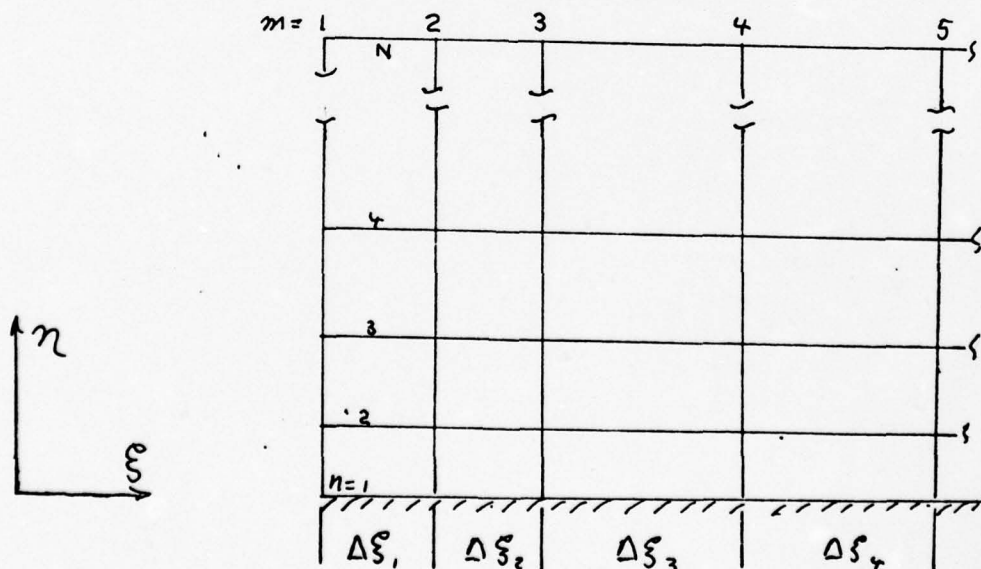


Fig. 5. Grid for Starting Solution



last section. Several surface steps must be taken before the effect of starting the procedure by similar solutions is purged from the solution of the boundary layer equations. From comparison with experimental data, this effect appears to have vanished within the first twenty steps along the surface.

Once a solution to the transformed boundary layer equations is obtained at an  $\xi$  station, values are assigned to  $F$ ,  $\Theta$ , and  $V$  at five points exterior to the grid used in the solution. These extra values of  $F$ ,  $\Theta$ , and  $V$  allow for grid expansion in the  $\eta$  direction, if necessary, later. The value assigned to  $F$  and  $\Theta$  at these extra points is unity. The value assigned to  $V$  at these extra points is determined from an expansion of  $V$  given by

$$V_{m+1, k} = V_{m+1, N-1} + \left. \frac{\partial V}{\partial \eta} \right)_{m+1, N-1} \sum_{N-1}^k \Delta \eta_k \quad (67)$$

$$k = N, N+5$$

where  $\left. \frac{\partial V}{\partial \eta} \right)_{m+1, N-1}$  can be determined from equation (B-39), and  $\Delta \eta_k$  can be determined from equation (55). It is necessary to calculate values of  $F$ ,  $\Theta$ , and  $V$  at five extra points to ensure continuity in the finite difference scheme used to approximate derivatives in  $\xi$ .

Having solved the transformed boundary layer equations at any  $\xi$  station, the boundary layer thickness  $\delta$ , displacement thickness  $\delta_1$ , and momentum thickness  $\delta_2$  can be determined. The boundary layer thickness is taken as the



value of  $\eta$  for which the value of  $F$  is approximately .995. The boundary layer thickness in physical coordinates  $x, y$  is determined by using the inverse transformation of equation (8) which is

$$y = \frac{\sqrt{2\xi}}{\rho_e u_e(r_{e/LR})} \int_0^\eta \frac{\theta}{\tau} d\eta \quad (68)$$

The integral in the above equation is evaluated by a trapezoidal integration from the surface out to the value of  $\eta$  for which  $F$  is approximately .995. The value of  $y$  determined is the boundary layer thickness  $\delta$ . The displacement thickness and momentum thickness are calculated in a similar manner.

The eddy viscosity terms  $\bar{\epsilon}$  and  $\hat{\epsilon}$  are now calculated at all grid points of the  $\xi$  station for which the solution of the transformed boundary layer equations was determined. These values of  $\bar{\epsilon}$  and  $\hat{\epsilon}$  will be used in the solution of the transformed boundary layer equations at the next  $\xi$  station.

At this point,  $F$  and  $\Theta$  are checked by equations (56) and (57) to determine if they are approaching the outer edge boundary conditions. If necessary, another grid point is added to the outer edge of the grid.

Next the non-dimensional heat transfer rate and skin friction are calculated in terms of a Stanton number and coefficient of friction. The Stanton number (Ref 16:526) is

$$St_{\infty} = \frac{h_c}{C_p \rho_{\infty} u_{\infty}} \quad (69)$$

where the heat transfer coefficient  $h_c$  is given by

$$h_c = \frac{\mu_w C_p}{P_r (T_o - T_w)} \left( \frac{\partial T}{\partial y} \right)_w \quad (70)$$

The coefficient of skin friction (Ref 13:128) is

$$C_{f_{\infty}} = \frac{\tau_w}{\frac{1}{2} \rho_{\infty} u_{\infty}^2} \quad (71)$$

where the wall shear stress  $\tau_w$  is given by

$$\tau_w = \mu_w \left( \frac{\partial u}{\partial y} \right)_w \quad (72)$$

A local Stanton number  $St_e$  and a local coefficient of skin friction  $C_{f_e}$  are also calculated using equations (69) and (71) with  $\rho_{\infty}$  and  $u_{\infty}$  replaced by  $\rho_e$  and  $u_e$  respectively. The wall derivatives  $\left( \frac{\partial T}{\partial y} \right)_w$  and  $\left( \frac{\partial u}{\partial y} \right)_w$ , appearing in equations (70) and (72) are transformed into the  $\xi, \eta$  coordinate plane and evaluated by a four point finite difference scheme developed in Appendix C.

At this point, another step along the surface could be taken and the procedure for solution of the boundary layer equations repeated. Several other parameters are calculated in the computer program; however, the logic presented in this section covers the main points of the program. A flow diagram is given in Fig. 6 showing the

logic and sequence of events in the computer program. This flow diagram is not intended to be a detailed break-down of the computer program, but is intended to show the sequence of events discussed in this report.

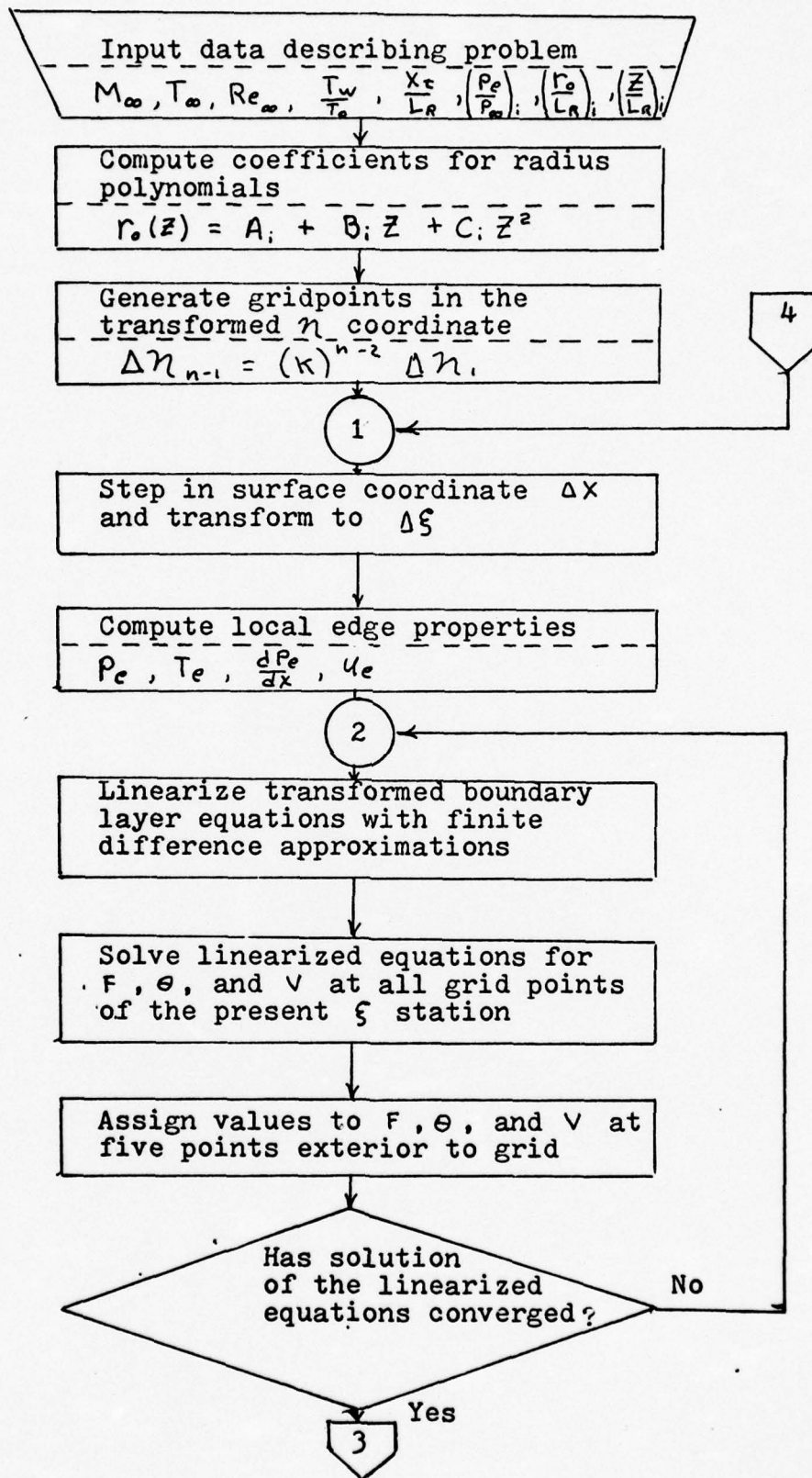


Fig. 6. Flow Diagram of Computer Program



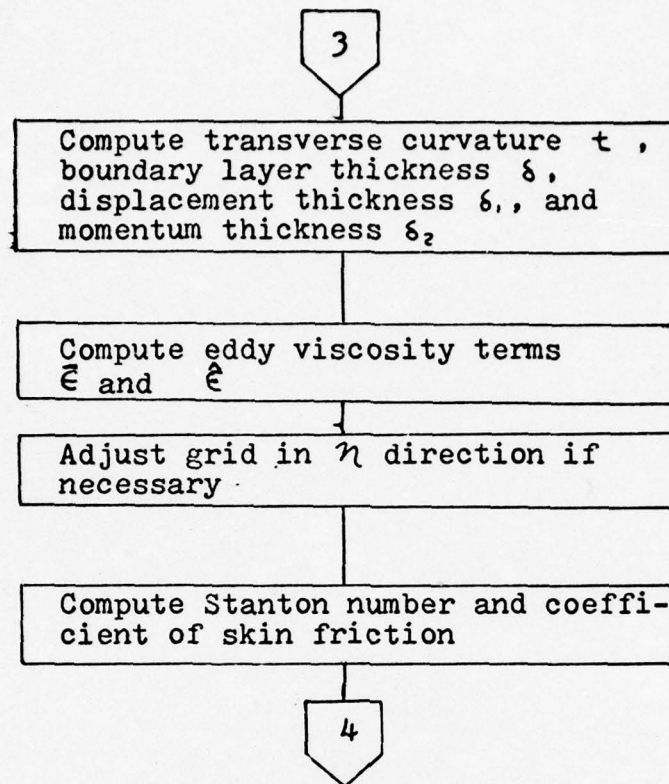


Fig. 6. Flow Diagram of Computer Program (cont.)

#### IV. Validation of New Solution

##### Comparison with Experimental Results

The two cases against which computed solutions were compared with experimental results are turbulent flow over a pointed, waisted body of revolution and laminar flow over a spherically blunted body of revolution. These two cases test the new solution in distinctly different types of flows.

Turbulent Flow Over a Waisted Body of Revolution. The experimental data, upon which this comparison was made, was obtained by Winter et al. (Ref 16:939) in 1965. The experiment provided boundary layer data for turbulent flow over an axisymmetric body in the presence of a streamwise pressure gradient. The data was reduced by Winter to obtain velocity profiles, skin friction coefficient, momentum thickness, and Mach number variation at the boundary layer edge. The accuracy of the skin friction coefficients obtained in the experiment was estimated by Winter to be about  $\pm .02$  per-cent. This was the only mention of accuracy given in Ref. 16 for the experiment.

The geometry of the test body of revolution is shown in Fig. 7. Boundary layer data was experimentally determined for several different free stream Mach number flows over this body. A comparison of computed boundary layer parameters with experimentally determined determined boundary layer parameters was made for Mach numbers of 1.398 and 1.70. The test conditions associated with these two Mach

numbers were

	Case 1	Case 2
$M_\infty =$	1.398	1.7
$Re_\infty =$	$10.1 \times 10^6$	$10.0 \times 10^6$
$T_\infty =$	$385.4^\circ R$	$388.9^\circ R$
$\frac{T_w}{T_\infty} =$	.976	.971

Since the actual pressure data obtained by Winter et al. was not available, the pressure data along the surface of the body was obtained from the Mach number distribution determined in the experiment. This Mach number distribution at the boundary layer edge is shown in Fig. 8. The pressure distribution was found from this Mach number distribution by using the following perfect gas relation (Ref 9:53):

$$\frac{P_e}{P_o} = \left( 1 + \frac{\gamma-1}{2} M_e^2 \right)^{-\gamma/(\gamma-1)} \quad (73)$$

The input to the computer program required the pressure data to be input in the non-dimensional form  $\frac{P_e}{P_\infty}$ ; therefore equation (73) was multiplied by  $\frac{P_o}{P_\infty}$  to obtain the proper pressure input. The pressure data  $\frac{P_e}{P_\infty}$ , along with corresponding values of  $\frac{r_o}{L_R}$  and  $\frac{z}{L_R}$ , was input to the computer program at twenty-seven surface locations. The reference length  $L_R$  was chosen to be the centerline length of the axisymmetric body.

Comparisons of computed and experimentally determined distributions of momentum thickness and skin friction



coefficient are given in figures 9 through 12. Since the axisymmetric test body was relatively slender, computed results with and without transverse curvature correction are given in figures 9 through 12. A comparison of computed and experimentally determined velocity profiles is given in figures 13 through 15.

These comparisons show the computed boundary layer parameters to agree well with the experimentally determined parameters. From figures 9 through 12, the computed solution is seen to be improved when corrected for transverse curvature.

Laminar Flow Over a Spherically Blunted Cone. The experimental results, upon which this comparison was made, were obtained by Bushnell (Ref 1:18) in 1968. This experiment provided heat transfer data for laminar flow over a spherically blunted cone. The heat transfer data obtained in this experiment was a ratio of heat transfer coefficients  $\frac{h_c}{h_{c_0}}$  where  $h_{c_0}$  is the heat transfer coefficient at the stagnation point. The heat transfer data was obtained by thermocouples and an automatic data reduction system. The estimated accuracy of the resultant heat transfer-coefficient data given in Ref 1 was 15 per-cent.

The blunted cone is shown in Fig. 14. The test conditions for the experiment were

$$M_\infty = 7.95$$

$$Re_\infty = 1.65 \times 10^6$$

$$T_\infty = 103.4^\circ R$$

$$T_w/T_0 = .38$$



The pressure data obtained in the experiment was given in the non-dimensional form  $\frac{P_e}{P_o}$ . This experimental pressure data was not given for the spherically blunted portion of the cone; therefore, a Newtonian pressure distribution (Ref 10:366) was used for this portion of the test body. This combination of experimental and theoretical pressure distribution is given in Fig. 17. This pressure distribution is put into the form  $\frac{P_e}{P_o}$  and input to the computer program at fourteen surface locations. The corresponding values of  $\frac{r_o}{L_R}$  and  $\frac{z}{L_R}$  are also input. The reference length used was the diameter at the base of the body.

Since the heat transfer output of the computer program was in the form of a Stanton number, it could be compared with the experimental data by use of the following equality:

$$\frac{h_c}{h_{c_o}} = \frac{St_{\infty}}{St_{\infty_o}} \quad (74)$$

The stagnation Stanton number was in error due to the similar solution method used to start the numerical solution; therefore, the  $St_{\infty_o}$  used in equation (74) was found by a formula given by Van Driest (Ref 10:366). The computed value of  $\frac{h_c}{h_{c_o}}$  determined by equation (74) is compared with the experimentally determined value of  $\frac{h_c}{h_{c_o}}$  in Fig. 18.

The computed results agree very well with the experimental results over the entire surface of the blunted cone.

### Comparison of Accuracy With Other Computer Solutions

Since reference to several different axisymmetric boundary layer programs can be found in the literature, a comparison was made with two of these computer solutions to determine the relative accuracy of the solution developed in this report. The two computer solutions compared were those of Cebeci (Ref 2:370), 1974, and Harris (Ref 4:54-55), 1971. Both of these solution methods had been applied to waisted body data of Winter et al. The computed momentum thickness and computed skin friction coefficient for the  $M_\infty = 1.398$  case were used as the basis of comparison.

Cebeci's method of solution is considerably different from the solution developed in this report. A different method of linearizing the boundary layer equations is used in Cebeci's method. Also in this method, the momentum and energy equations are solved separately, and an iterative procedure is used to obtain convergence of the solutions of these two equations.

The solution method of Harris differs from the solution developed in this report mainly in the method of solving the boundary layer equations. Harris's method solves the momentum and energy equations simultaneously and uses these results to integrate the continuity equation.

The results of these two solution methods are compared with the results of the solution developed in this report in Fig. 18 and Fig. 19. Since Cebeci's solution was started using an experimentally determined velocity profile at

$z/L_r = .4$ , the comparisons with both solution methods was made starting at this point. From these comparisons, the solution developed in this report appears to have approximately the same accuracy as Harris's solution and slightly better accuracy than Cebeci's solution.

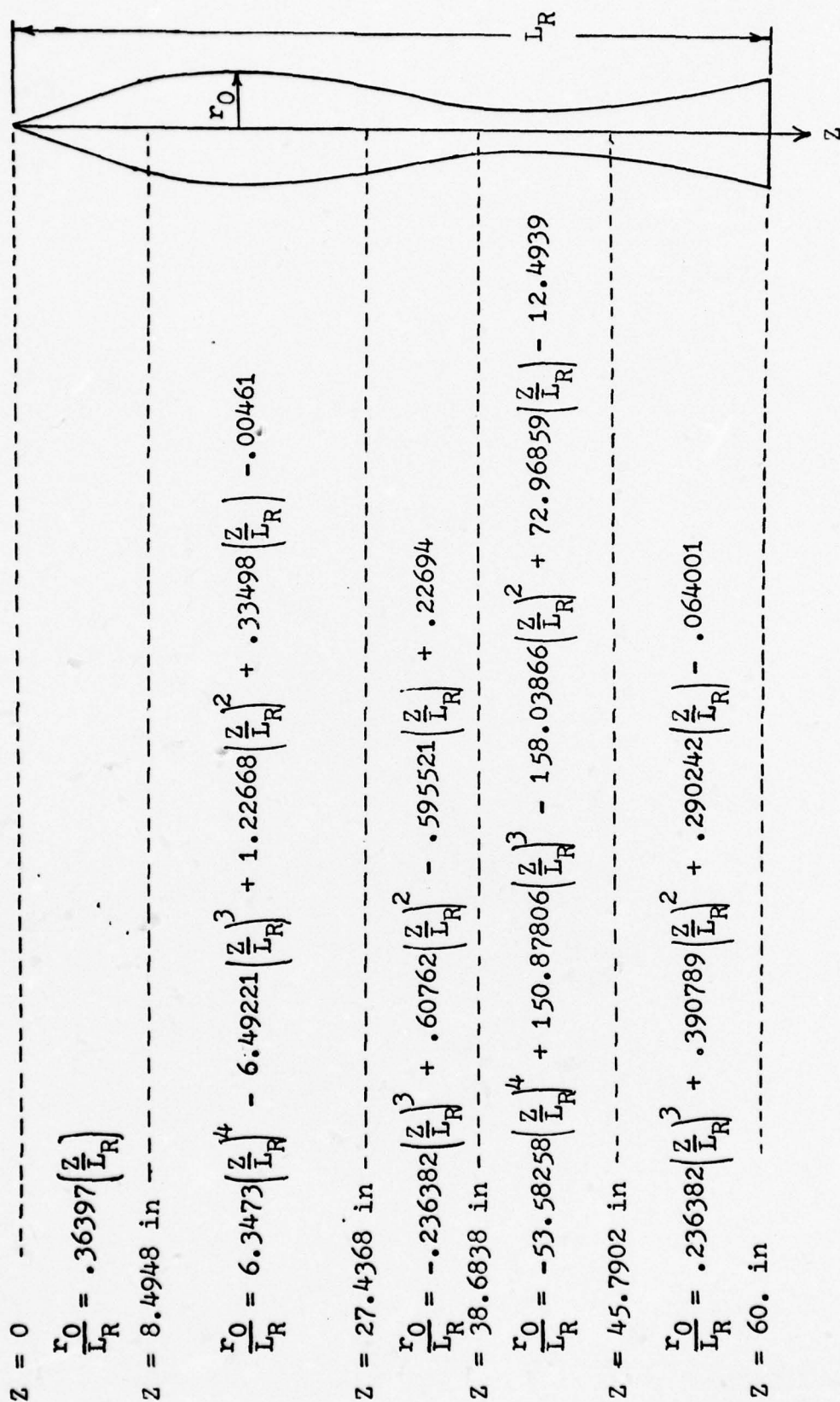


Fig. 7. Geometry of Axisymmetric Waisted Body



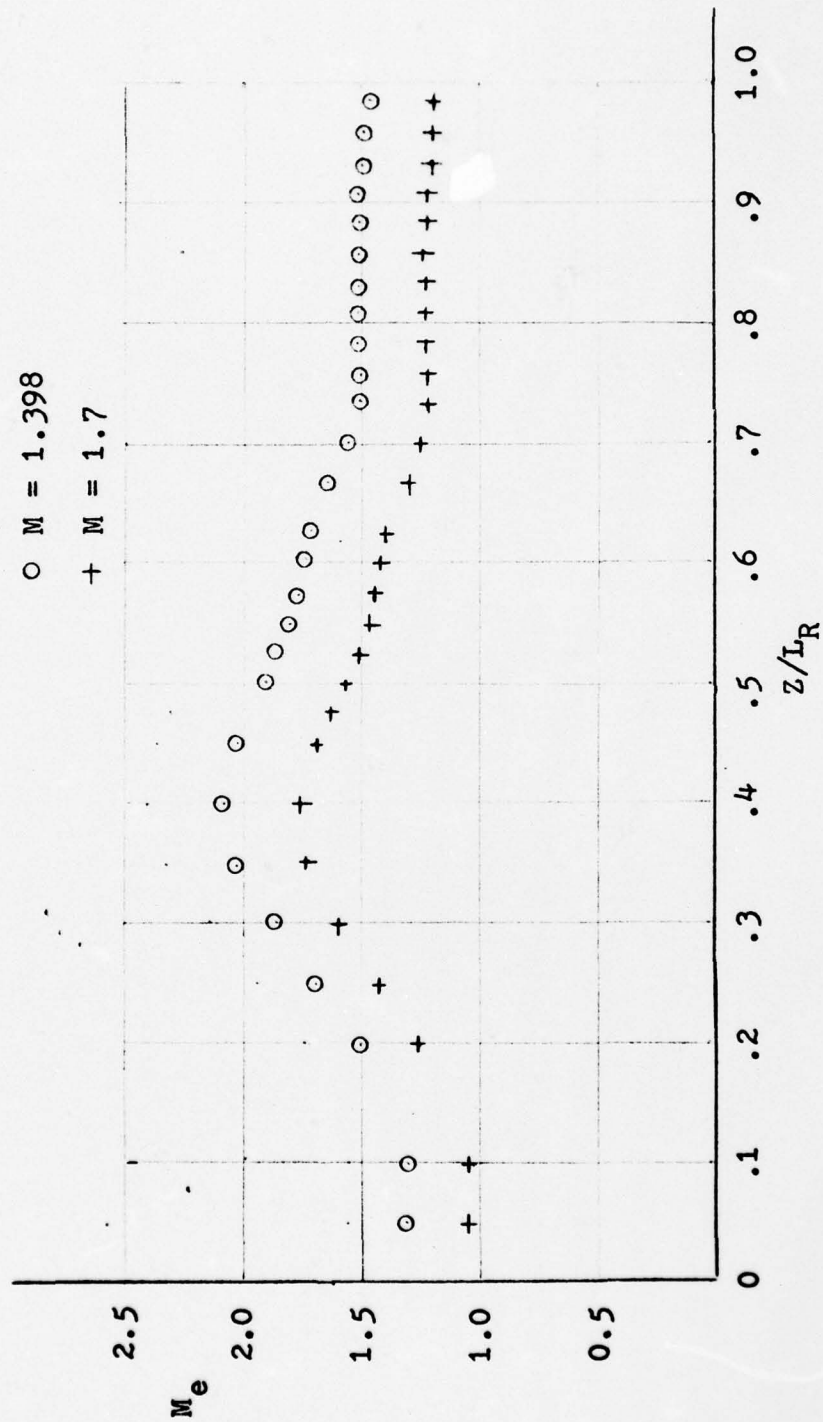


Fig. 8. Mach Number Distribution on Waisted Body

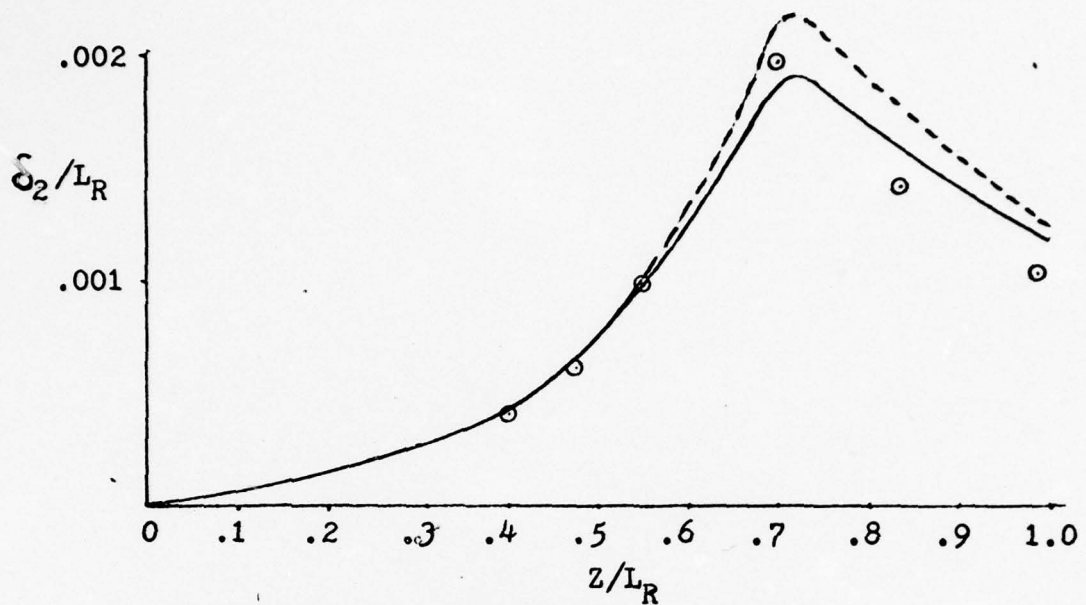


Fig. 9. Momentum Thickness for  $M_\infty = 1.398$

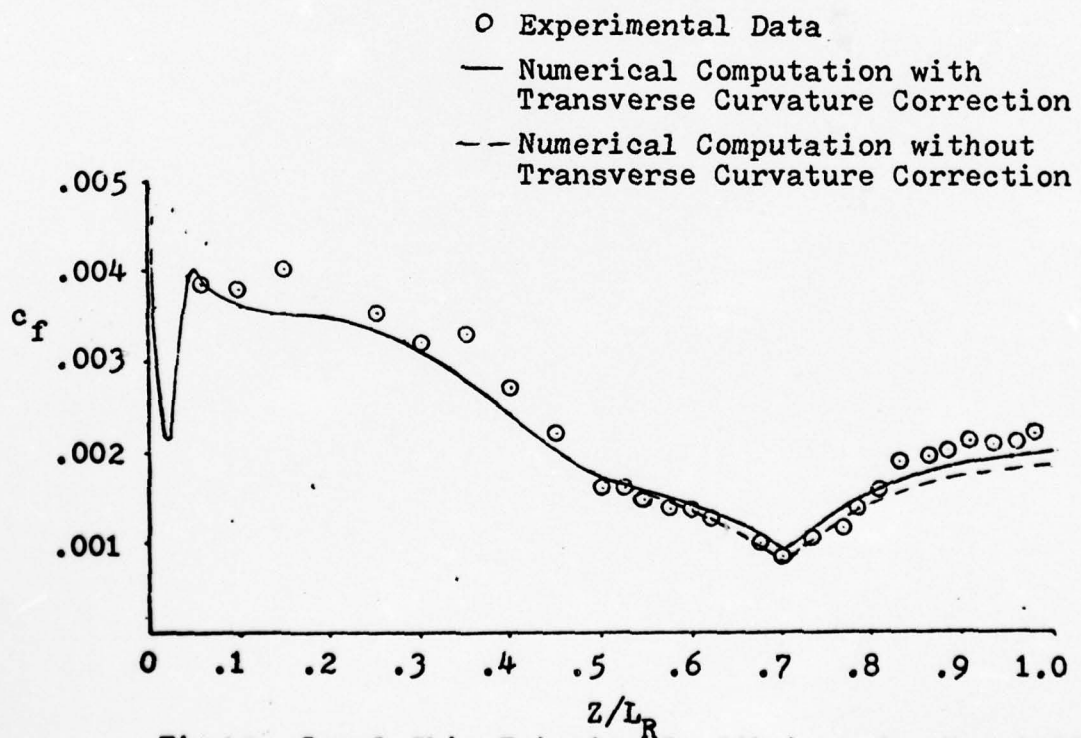


Fig. 10. Local Skin Friction Coefficient for  $M_\infty = 1.398$

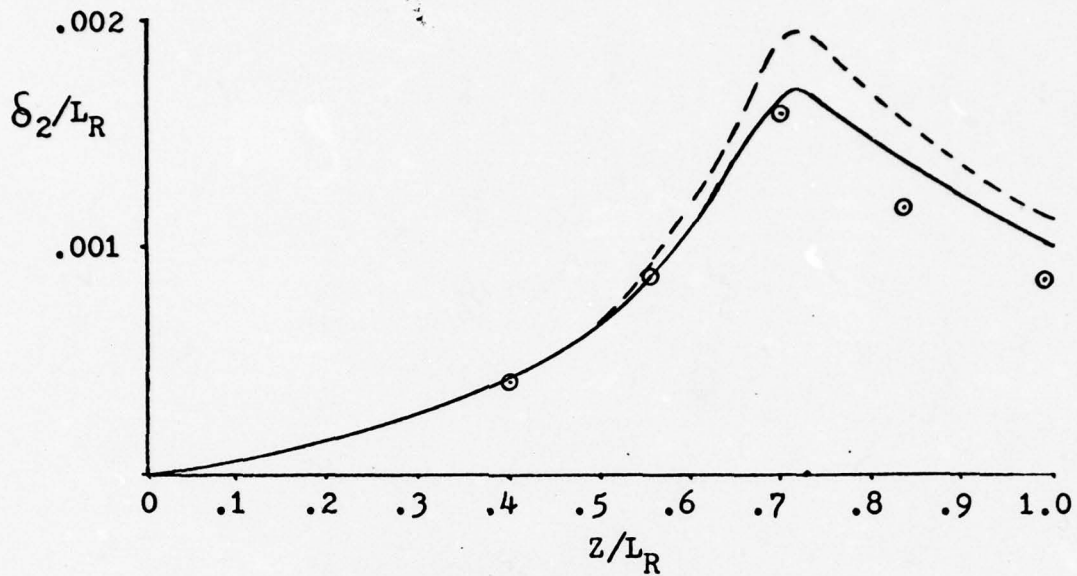


Fig. 11. Momentum Thickness for  $M_\infty = 1.7$

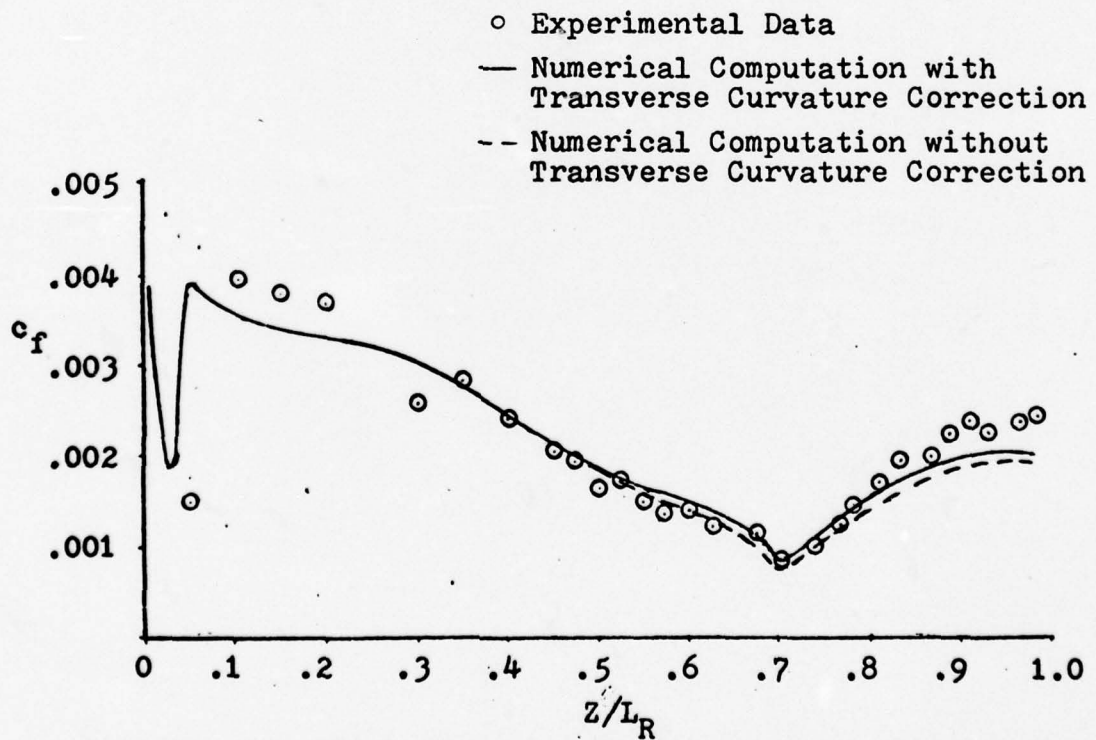


Fig. 12. Local Skin Friction Coefficient for  $M_\infty = 1.7$

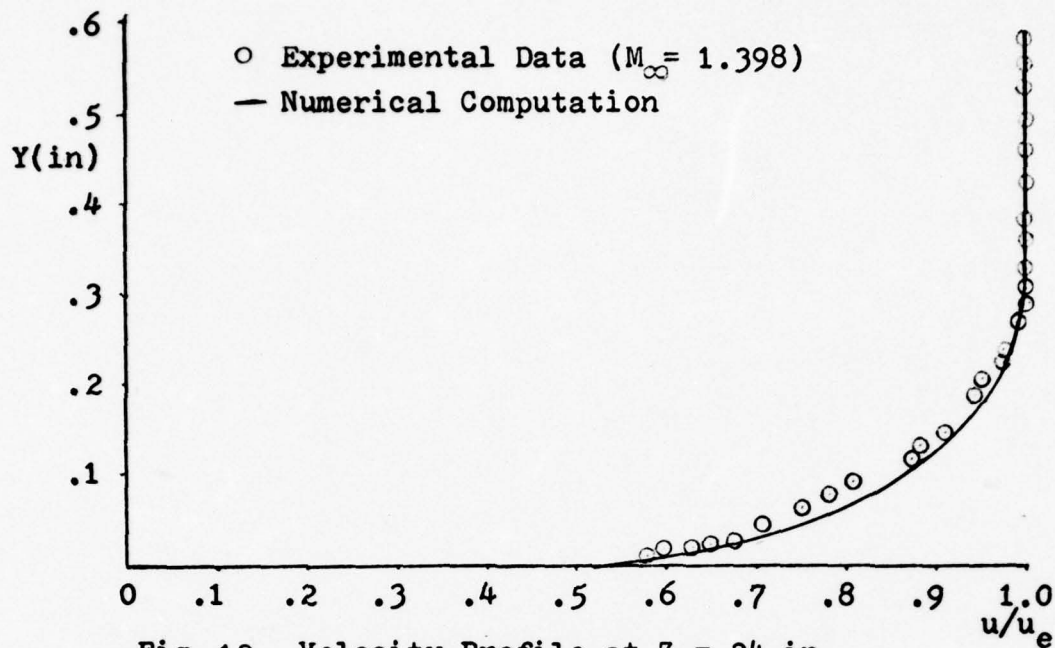


Fig. 13. Velocity Profile at  $Z = 24$  in.

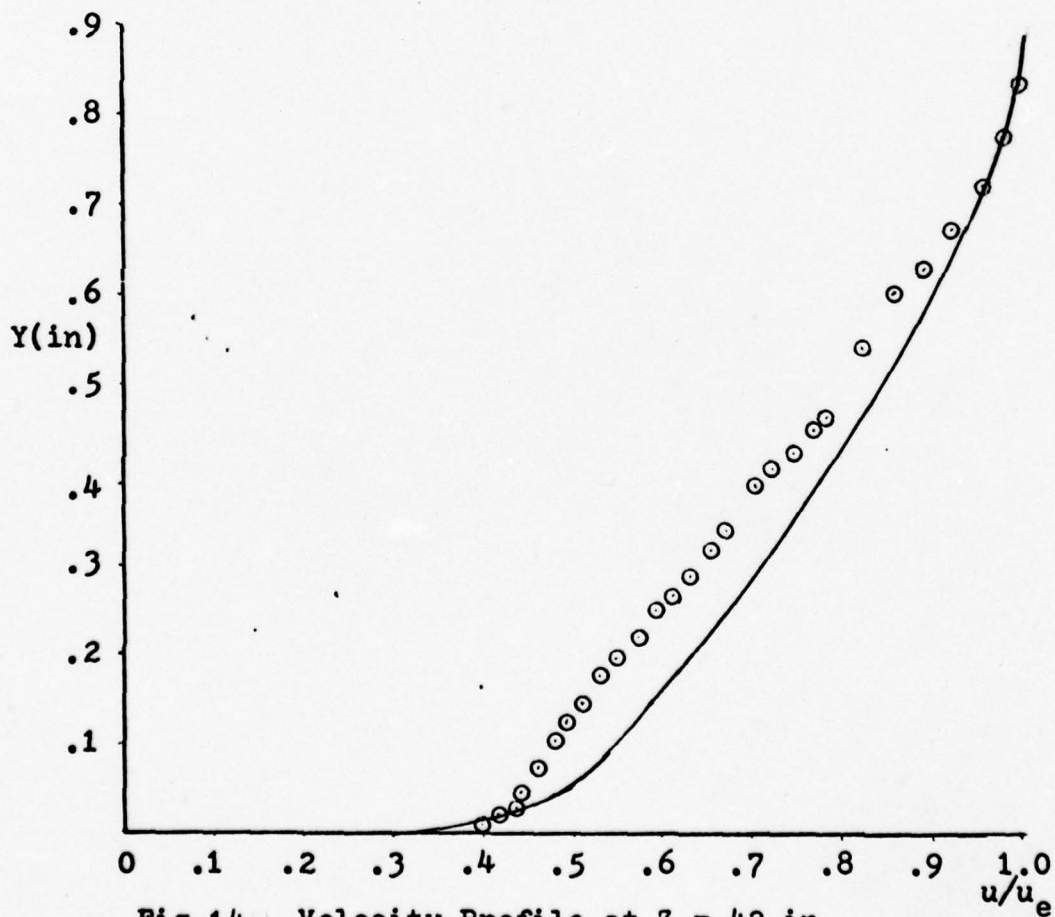


Fig. 14. Velocity Profile at  $Z = 42$  in.



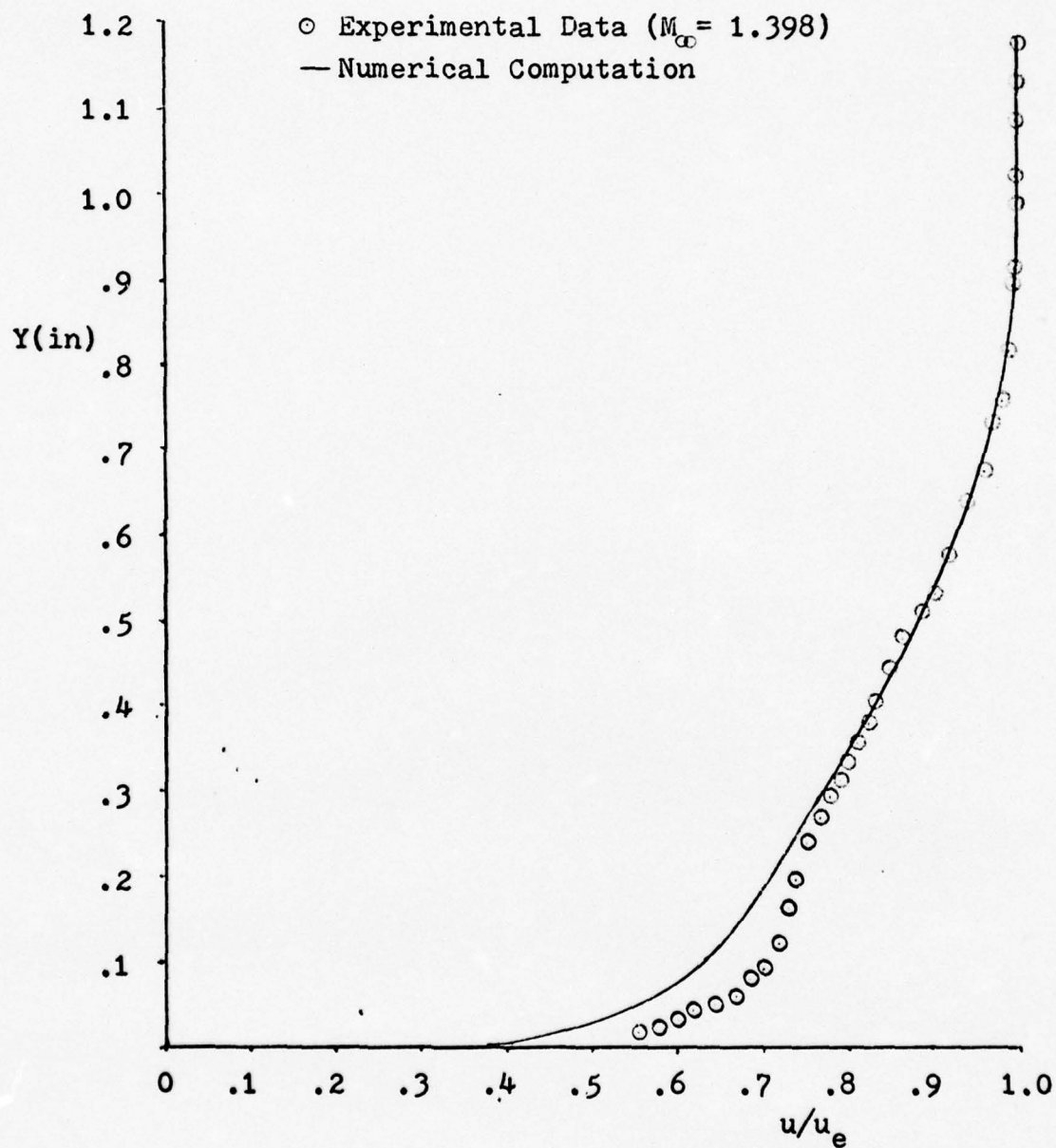


Fig. 15. Velocity Profile at  $Z = 50$  in.

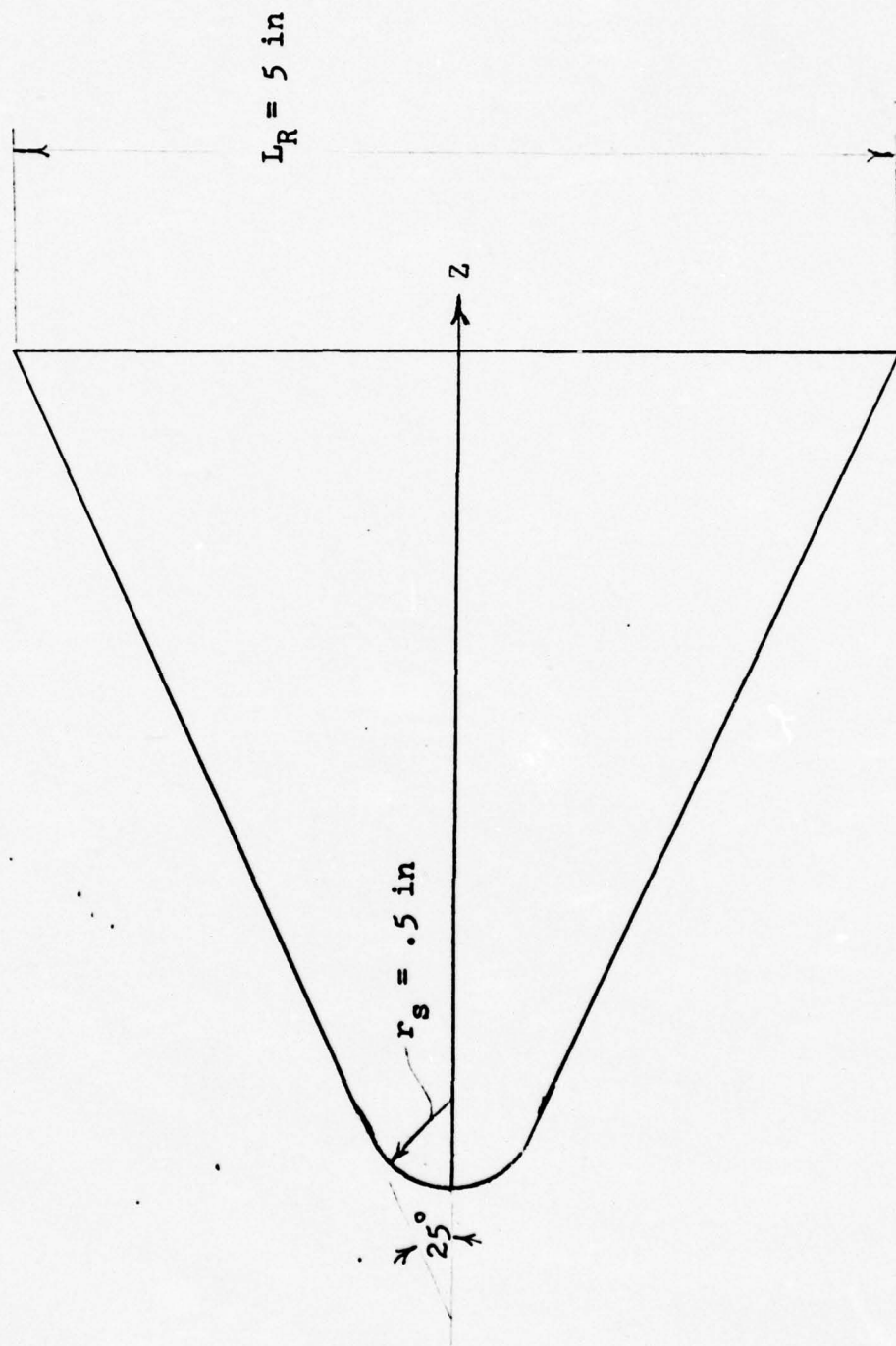


Fig. 16 Geometry of Spherically Blunted Cone

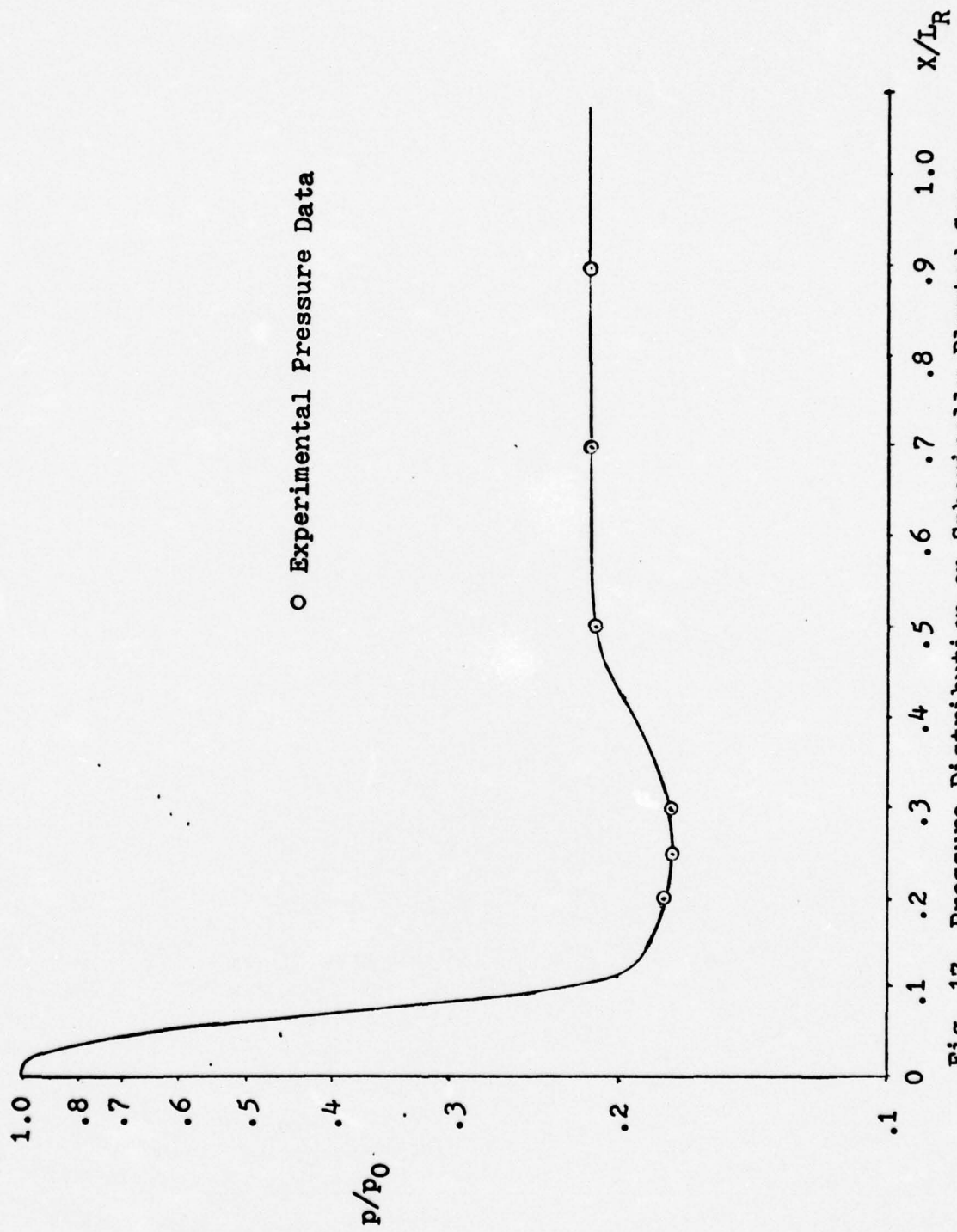


Fig. 17. Pressure Distribution on Spherically Blunted Cone

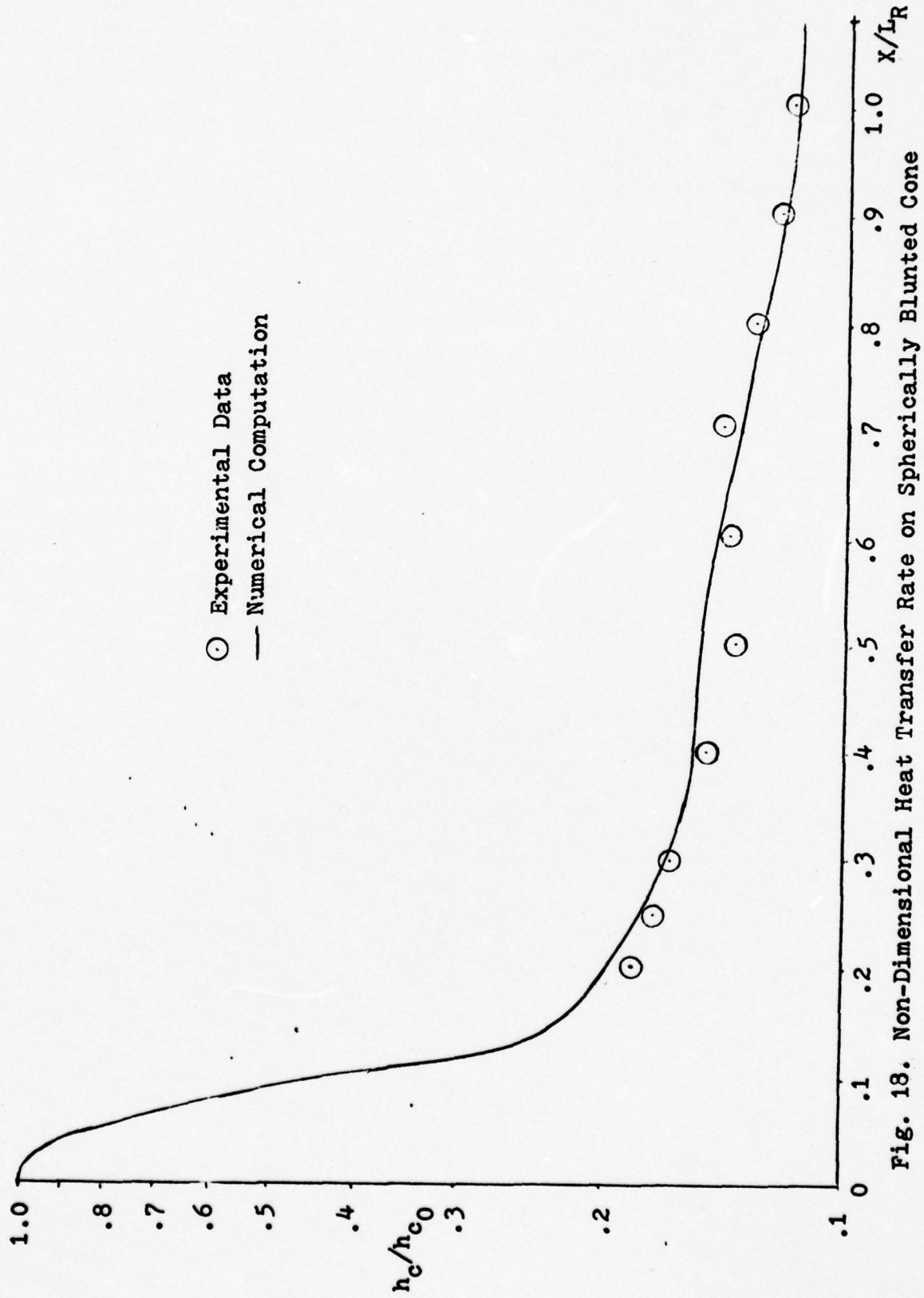


Fig. 18. Non-Dimensional Heat Transfer Rate on Spherically Blunted Cone



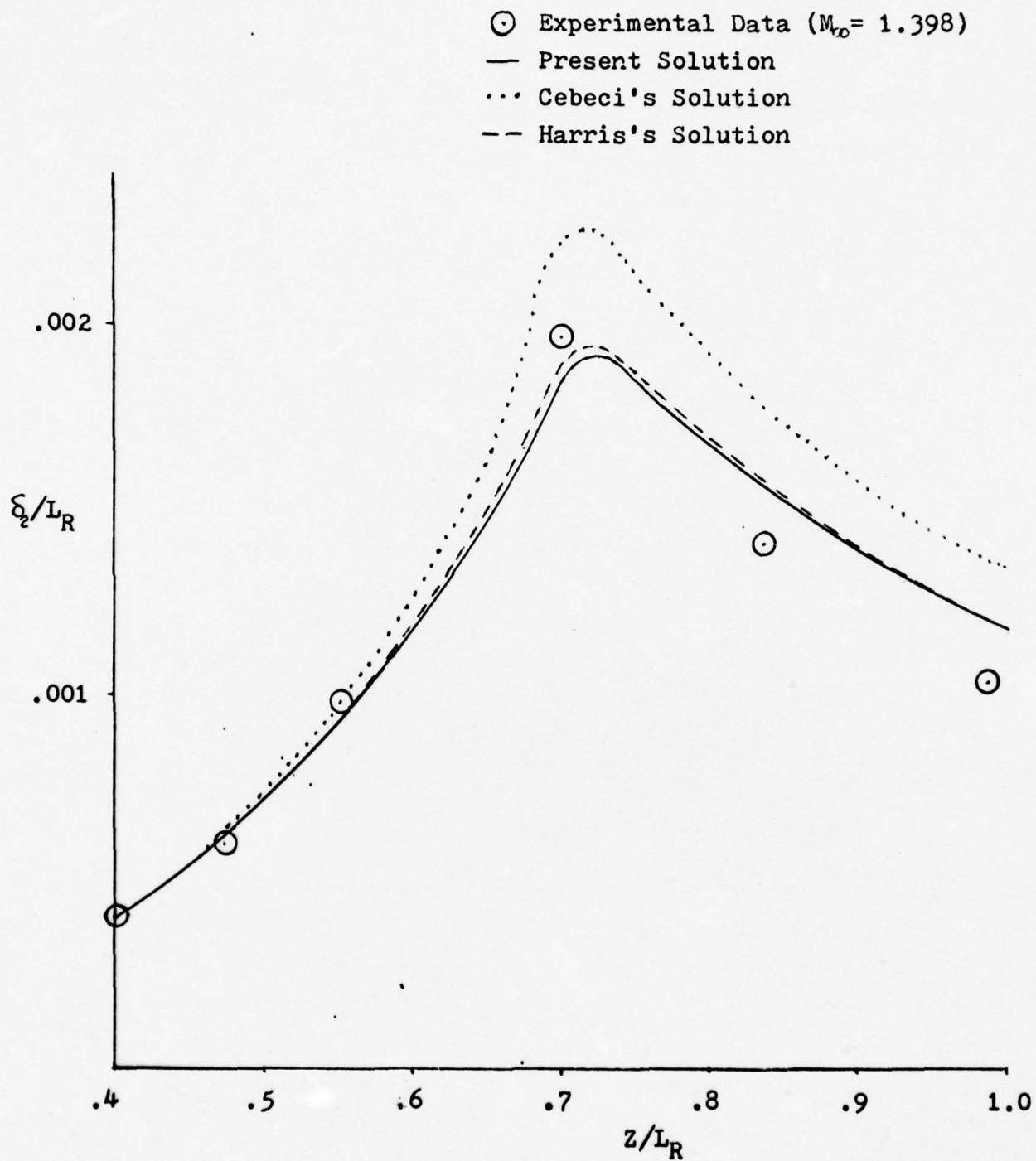


Fig. 19. Comparison of Momentum Thickness for Different Methods of Solution

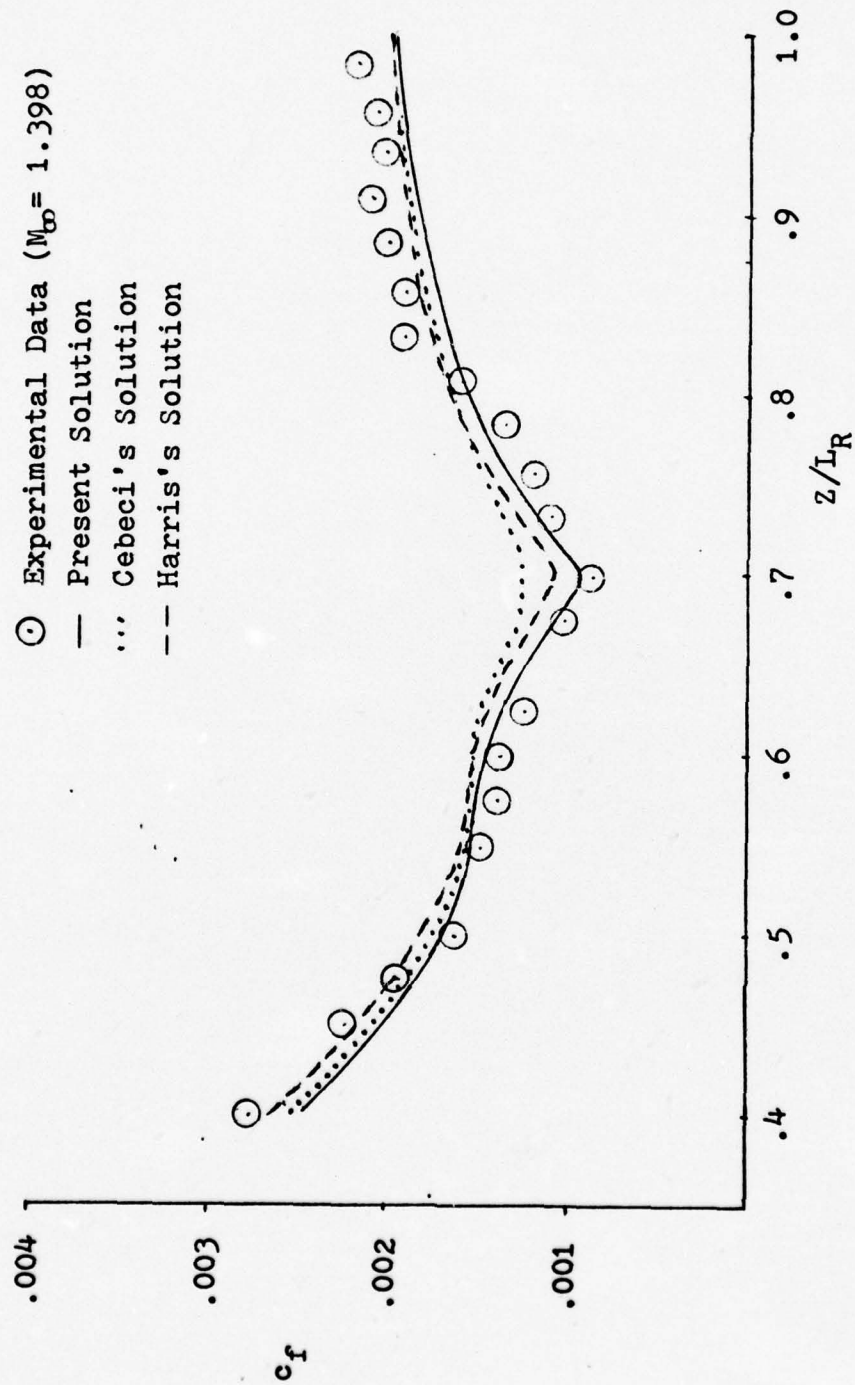


Fig. 20. Comparison of Skin Friction Coefficient for Different Methods of Solution

## V. Conclusions

The numerical solution of boundary layer flows as developed by Dr. Shang has now been expanded to include flows over arbitrary shaped axisymmetric bodies. The new solution was validated by testing it against two different sets of experimental data. The experimental data of Winter et al. (Ref 16:939) tested the computed values of momentum thickness, skin friction coefficient, and velocity profiles for turbulent flow over a slender pointed body of revolution. The data of Bushnell (Ref 1:18) was used to test the computed heat transfer rate for laminar flow over a spherically blunted cone. The comparison of these computed boundary layer parameters with the experimentally determined parameters show the new solution to be very accurate.

The accuracy of the solution procedure developed in this report was compared with two other recent computer solutions using the data of Winter et al. The solution developed in this report was determined to have approximately the same accuracy as Harris's method of solution (Ref 4:54) and slightly better accuracy than Cebeci's method (Ref 2:370).

The solution procedure developed in this report can, therefore, be used to accurately determine boundary layer parameters for either laminar or turbulent flow over either a two-dimensional or axisymmetric surface.



## Bibliography

1. Bushnell, D. M., et al. Heat Transfer and Pressure Distribution on a Spherically Blunted 25 Half Angle Cone at Mach 8 and Angles of Attack up to 90. NASA Technical Note D-4792. Washington: National Aeronautics and Space Administration, October 1968.
2. Cebeci, C. and A.M.O. Smith. Analysis of Turbulent Boundary Layers. New York: Academic Press, 1974.
3. Cebeci, C. and A.M.O. Smith. "A Finite Difference Method for Calculating Compressible Laminar and Turbulent Boundary Layers." Journal of Basic Engineering, September 1970.
4. Harris, J. E. Numerical Solution of the Equations for Compressible Laminar, Transitional, and Turbulent Boundary Layers and Comparisons with Experimental Data. NASA Technical Report R-368. Washington: National Aeronautic and Space Administration, August 1971.
5. Hilderbrand, F. B. Advanced Calculus for Applications. Englewood Cliff, New Jersey: Prentice Hall, Inc., 1962.
6. Hornbeck, R. W. Numerical Marching Techniques for Fluid Flows with Heat Transfer. NASA Special Publication SP-297. Washington: National Aeronautics and Space Administration, 1973.
7. Karamcheti, K. Principles of Ideal Fluid Aerodynamics. New York: John Wiley and Sons, Inc., 1966.
8. Kreith, F. Principles of Heat Transfer. Scranton, Pennsylvania: International Textbook Company, 1967.
9. Liepmann, H. W. and A. Roshko. Elements of Gasdynamics. New York: John Wiley and Sons, Inc., 1967.
10. Lin, C. C. Turbulent Flows and Heat Transfer in Gases. Princeton, New Jersey: Princeton University Press, 1959.
11. Moore, F. K. Theory of Laminar Flows. Princeton, New Jersey: Princeton University Press, 1964.
12. Rouse, H. Advanced Mechanics of Fluids. New York: John Wiley and Sons, Inc., 1959.
13. Schlichting, H. Boundary Layer Theory. New York: McGraw-Hill Book Company, 1968.



14. Shepherd, D. G. Elements of Fluid Mechanics. New York: Harcourt, Brace and World, Inc., 1965.
15. Van Driest, E. R. "On Turbulent Flow Near A Wall." Journal of the Aeronautical Sciences, November 1956.
16. Winter, K. G., et al. "Turbulent Boundary Layer Studies on a Waisted Body of Revolution in Subsonic and Supersonic Flow." Recent Developments in Boundary Layer Research, AGARDograph 97, May 1965.
17. Ames Research Staff. Equations, Tables, and Charts for Compressible Flow. NACA Technical Report R-1135. Washington: National Advisory Committee for Aeronautics, 1953.

## Appendix A

### Development of Two-Dimensional and Axisymmetric Boundary Layer Equations

The boundary layer equations are obtained from equations describing the conservation of mass, momentum, and energy within a moving fluid. These conservation equations can be obtained by examining the rate of change of mass, momentum, and energy within a finite region  $R$  of space enclosed by a surface  $S$  fixed in the flowing fluid. Using Fig. 21 in which  $\hat{n}$  is a unit vector normal to the surface  $S$ , the integral equations for time rate of change of mass, momentum, and energy (Ref 11:26-27) are respectively

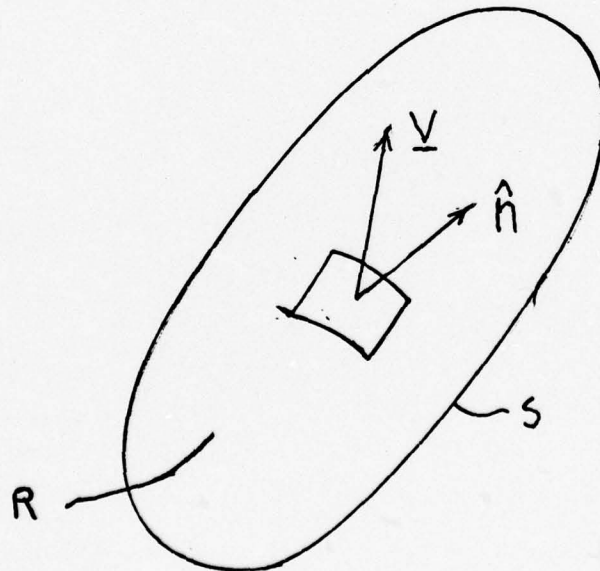


Fig. 21. Finite Region of Flow Field

$$\frac{\partial}{\partial t} \iiint_R \rho d\tau = - \oint \rho \underline{v} \cdot \hat{n} dS \quad (A-1)$$

$$\begin{aligned} \frac{\partial}{\partial t} \iiint_R \rho \underline{v} d\tau = & - \oint \underline{v} (\rho \underline{v} \cdot \hat{n}) dS \\ & + \oint \underline{\sigma} \cdot \hat{n} dS \end{aligned} \quad (A-2)$$

$$\begin{aligned} \frac{\partial}{\partial t} \iiint_R \rho (e + \frac{v^2}{2}) d\tau = & - \oint \rho (e + \frac{v^2}{2}) \underline{v} \cdot \hat{n} dS \\ & + \oint (\underline{\sigma} \cdot \underline{v}) \cdot \hat{n} dS - \oint k \nabla T \cdot \hat{n} dS \end{aligned} \quad (A-3)$$

Equations (A-1), (A-2), and (A-3) are valid for compressible, viscous, heat conducting fluids. The vector  $k \nabla T$  is the heat flux vector and  $\underline{\sigma}$  is the stress tensor (Ref 11:35) given by

$$\underline{\sigma} = -p \underline{I}_0 + (\lambda \nabla \cdot \underline{v}) \underline{I}_0 + \mu (\nabla \underline{v} + \nabla \underline{v}^*) \quad (A-4)$$

The value of  $\lambda$  in equation (A-4) as determined by Stokes (Ref 13:57) is  $-\frac{2}{3}\mu$ .

By use of the divergence theorem (Ref 5:292) as given in equation (A-5), the surface integrals in equations (A-1), (A-2), and (A-3) can be changed to volume integrals.

$$\oint \underline{A} \cdot \hat{n} dS = \iiint_R \nabla \cdot \underline{A} d\tau \quad (A-5)$$

Since  $R$  is a fixed volume, the partial derivative  $\frac{\partial}{\partial t}$  can be taken inside the integral sign of equations (A-1), (A-2), and (A-3). By combining terms, each of these equations could

be expressed as one volume integral. By taking the limit as  $R$  tends to zero, the differential form of these conservation equations is

$$\frac{\partial \rho}{\partial t} + \nabla \cdot \rho \underline{V} = 0 \quad (\text{A-6})$$

$$\frac{\partial}{\partial t}(\rho \underline{V}) + \nabla \cdot (\rho \underline{V} \underline{V} - \underline{\underline{\sigma}}) = 0 \quad (\text{A-7})$$

$$\begin{aligned} \frac{\partial}{\partial t} \left[ \rho \left( e + \frac{\underline{V}^2}{2} \right) \right] &= -\nabla \cdot \rho \left( e + \frac{\underline{V}^2}{2} \right) \underline{V} \\ &+ \nabla \cdot kT + \nabla \cdot (\underline{\underline{\sigma}} \cdot \underline{V}) \end{aligned} \quad (\text{A-8})$$

In order to further simplify equations (A-6), (A-7), and (A-8), the assumption of steady flow is made. Also the equation for mechanical energy, obtained by forming the scalar product of equation (A-7) with the velocity vector  $\underline{V}$ , is subtracted from equation (A-8). With these simplifications, equations (A-6), (A-7), and (A-8) become

$$\nabla \cdot \rho \underline{V} = 0 \quad (\text{A-9})$$

$$\nabla \cdot (\rho \underline{V} \underline{V} - \underline{\underline{\sigma}}) = 0 \quad (\text{A-10})$$

$$\nabla \cdot \rho h \underline{V} = \underline{V} \cdot \nabla \rho + \nabla \cdot k \nabla T + \underline{\underline{\tau}} \cdot \nabla \underline{V} \quad (\text{A-11})$$

The definitions of enthalpy ( $h = e + \frac{p}{\rho}$ ) and rate of strain tensor ( $\underline{\underline{\tau}} = \underline{\underline{\sigma}} - p \underline{\underline{I}}$ ) have been used in equation (A-11).

In order to obtain boundary layer equations from equations (A-9), (A-10), and (A-11), it is necessary to express



these equations in a surface oriented coordinate system. The coordinate system to be used for an axisymmetric surface is shown in Fig. 22. This orthogonal curvilinear coordinate system is oriented such that, for any point on the surface, the  $X$  axis is parallel to the surface and the  $Y$  axis is perpendicular to the surface. The third orthogonal coordinate  $\omega$  is taken as the azimuth angle within the meridian plane of the axisymmetric body. The quantity  $K_c$  is the curvature in the  $r_0, z$  plane and  $1/K_c$  is the radius of curvature within this plane. The curvature  $K_c$  is defined to be  $\frac{d\theta}{dx}$ . The scale factors (Ref 12:220) necessary to

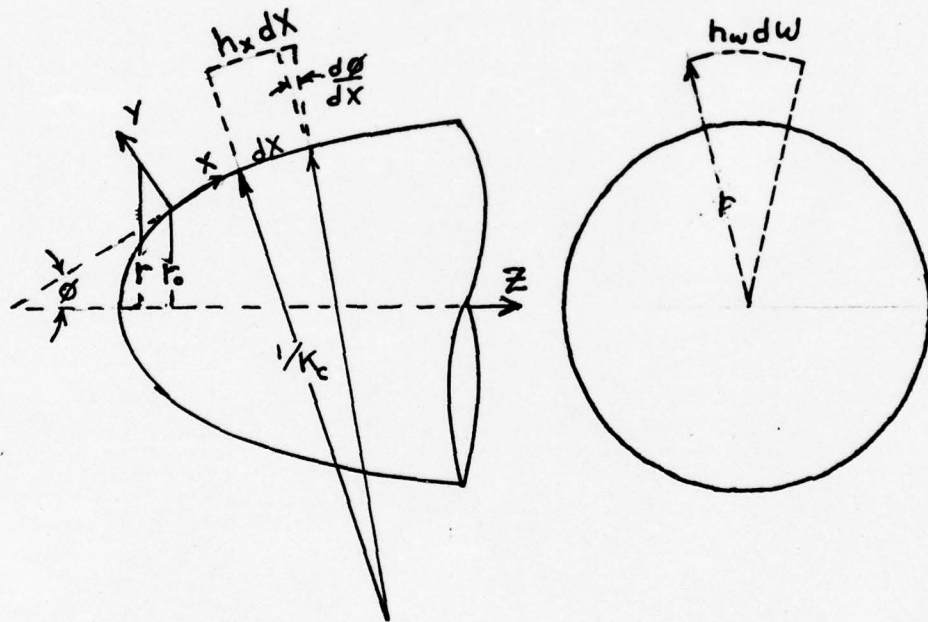


Fig. 22. Orthogonal Curvilinear Coordinates for an Axisymmetric Body

define differential arc lengths along any one of the  $x$ ,  $y$ , or  $w$  surfaces while holding the other two coordinates constant are given by  $h_x$ ,  $h_y$ , and  $h_w$  of the following three relations:

$$h_x dX = (1 + K_c Y) dX \quad (A-12)$$

$$h_y dY = dY \quad (A-13)$$

$$h_w d\omega = r d\omega \quad (A-14)$$

With these values of  $h_x = (1 + K_c Y)$ ,  $h_y = 1$ , and  $h_w = r$ , the vector operators in the surface oriented coordinate system can be obtained by using the general form of these operators (Ref 5:302-303) which are

$$\nabla \cdot \underline{A} = \frac{1}{h_1 h_2 h_3} \left[ \frac{\partial}{\partial X_1} (h_1 h_2 A_1) + \frac{\partial}{\partial X_2} (h_1 h_3 A_2) + \frac{\partial}{\partial X_3} (h_1 h_2 A_3) \right] \quad (A-15)$$

$$\nabla \psi = \frac{1}{h_1} \frac{\partial \psi}{\partial X_1} \hat{i} + \frac{1}{h_2} \frac{\partial \psi}{\partial X_2} \hat{j} + \frac{1}{h_3} \frac{\partial \psi}{\partial X_3} \hat{k} \quad (A-16)$$

$$\nabla \times \underline{A} = \frac{1}{h_1 h_2 h_3} \begin{vmatrix} h_1 \hat{i} & h_2 \hat{j} & h_3 \hat{k} \\ \frac{\partial}{\partial X_1} & \frac{\partial}{\partial X_2} & \frac{\partial}{\partial X_3} \\ h_1 A_1 & h_2 A_2 & h_3 A_3 \end{vmatrix} \quad (A-17)$$

In the above three equations,  $X_1$ ,  $X_2$ , and  $X_3$  are the orthogonal curvilinear coordinates along which the unit vectors  $\hat{i}$ ,  $\hat{j}$ , and  $\hat{k}$  are respectively aligned.

Before using equations (A-15), (A-16), and (A-17) to form vector operator for the orthogonal curvilinear coordinates of Fig. 22, the following approximation is made.

$$1 + K_c \gamma \approx 1 \quad (\text{A-18})$$

This is a valid approximation since the maximum value of  $\gamma$  will be the boundary layer thickness and the magnitude of  $K_c$  is small everywhere on an axisymmetric body except at a sharply pointed tip. However, the value of  $\gamma$  is approximately zero at the tip since the boundary layer thickness is very small in this region. With this assumption, the vector operators for the orthogonal curvilinear coordinates of Fig. 22 are

$$\nabla \cdot \underline{A} = \frac{1}{r} \left[ \frac{\partial}{\partial x} (r A_x) + \frac{\partial}{\partial y} (r A_y) + \frac{\partial}{\partial w} (A_w) \right] \quad (\text{A-19})$$

$$\nabla \psi = \frac{\partial \psi}{\partial x} \hat{i} + \frac{\partial \psi}{\partial y} \hat{j} + \frac{1}{r} \frac{\partial \psi}{\partial w} \hat{k} \quad (\text{A-20})$$

$$\nabla \times \underline{A} = \frac{1}{r} \begin{vmatrix} \hat{i} & \hat{j} & r \hat{k} \\ \frac{\partial}{\partial x} & \frac{\partial}{\partial y} & \frac{\partial}{\partial z} \\ A_x & A_y & A_w \end{vmatrix} \quad (\text{A-21})$$

These vector operators are used in equations (A-9), (A-10), and (A-11) to express the conservation equations in a surface oriented coordinate system.

Boundary layer equations applicable to turbulent flows over axisymmetric surfaces can be obtained by the following steps:

1. Apply the vector operators of equations (A-19), (A-20), and (A-21) to the conservation equations (A-9), (A-10), and (A-11)
2. Assume no swirl effect ( $\frac{\partial}{\partial \omega} = 0$ )
3. Represent the fluid properties as the sum of a mean flow property and a fluctuating property (Ref 13:526)
4. Time average the resulting equations and retain only the significant correlations (Ref 4:13) which are  $\overline{\rho'v'}$ ,  $\overline{u'v'}$ , and  $\overline{v'T'}$
5. Perform an order of magnitude analysis using the thin boundary layer assumption (Ref 13:118).

The boundary layer equations for conservation of mass, momentum, and energy which result from this procedure are respectively

$$\frac{\partial}{\partial x} [r \bar{\rho} \bar{u}] + \frac{\partial}{\partial y} \left[ r \bar{\rho} \left( \bar{v} + \frac{\overline{\rho'v'}}{\bar{\rho}} \right) \right] = 0 \quad (A-22)$$

$$\begin{aligned} \bar{\rho} \bar{u} \frac{\partial \bar{u}}{\partial x} + \bar{\rho} \left( \bar{v} + \frac{\overline{\rho'v'}}{\bar{\rho}} \right) \frac{\partial \bar{u}}{\partial y} = & - \frac{\partial \bar{p}}{\partial x} \\ & + \frac{1}{r} \frac{\partial}{\partial y} \left[ r \left( \mu \frac{\partial \bar{u}}{\partial y} + \bar{\rho} \overline{u'v'} \right) \right] \end{aligned} \quad (A-23)$$



$$\begin{aligned}
\bar{\rho} \bar{u} \frac{\partial \bar{h}}{\partial x} + \bar{\rho} \left( \bar{v} + \frac{\overline{\rho'v'}}{\bar{\rho}} \right) \frac{\partial \bar{h}}{\partial y} &= \bar{u} \frac{\partial \bar{\rho}}{\partial x} + \mu \left( \frac{\partial \bar{u}}{\partial y} \right)^2 \\
- \bar{\rho} \overline{u'v'} \frac{\partial \bar{u}}{\partial y} + \frac{1}{r} \frac{\partial}{\partial y} \left( \frac{rk}{c_p} \frac{\partial \bar{h}}{\partial y} \right) &- \bar{\rho} \overline{u'v'} \frac{\partial \bar{u}}{\partial y} \\
- \frac{1}{r} \frac{\partial}{\partial y} \left( \frac{rk}{c_p} \frac{\partial \bar{h}}{\partial y} \right) - \frac{1}{r} \frac{\partial}{\partial y} (r c_p \bar{\rho} \overline{v'T'}) & \quad (A-24)
\end{aligned}$$

The radius  $r$  entered into equations (A-22), (A-23), and (A-24) by the scale factor  $h_w = r$ . For a two-dimensional surface, the values of  $h_x$  and  $h_y$  would be unity, and the value of  $h_w$  would be zero. The result of deriving boundary layer equations for the two-dimensional case would be equations (A-22), (A-23), and (A-24) with  $r$  replaced by unity. In order to use the same set of equations for either two-dimensional or axisymmetric surfaces,  $r$  is replaced by  $r^j$  where  $j=0$  for two-dimensional surfaces and  $j=1$  for axisymmetric surfaces.

In order to have a solvable set of boundary layer equations,  $\frac{\overline{\rho'v'}}{\bar{\rho}}$  is grouped together with  $\bar{v}$ , and the turbulent transport quantities  $\bar{\rho} \overline{u'v'}$  and  $c_p \bar{\rho} \overline{v'T'}$  are represented by an eddy viscosity and eddy conductivity respectively. This method of handling the turbulence produced correlations is introduced into equations (A-22), (A-23), and (A-24) by use of the following definitions:

$$\tilde{v} = \bar{v} + \frac{\overline{\rho'v'}}{\bar{\rho}} \quad (\text{Normal velocity}) \quad (A-25)$$

$$\epsilon = \frac{\bar{\rho} \overline{u'v'}}{\frac{\partial \bar{u}}{\partial y}} \quad (\text{Eddy viscosity}) \quad (A-26)$$

$$K_t = -C_p \frac{\bar{\rho} \overline{v' T'}}{\frac{\partial \bar{u}}{\partial y}} \quad (\text{Eddy conductivity}) \quad (\text{A-27})$$

$$Pr_t = \frac{C_p \epsilon}{K_t} \quad (\text{Turbulent Prandtl number}) \quad (\text{A-28})$$

$$\bar{\epsilon} = 1 + \frac{\epsilon}{\mu} \quad (\text{A-29})$$

$$\hat{\epsilon} = 1 + \frac{\epsilon}{\mu} \frac{Pr_t}{Pr} \quad (\text{Associated eddy viscosity terms}) \quad (\text{A-30})$$

After replacing  $r$  by  $r^j$  and using the above definitions, equations (A-22), (A-23), and (A-24) are

$$\frac{\partial}{\partial x} (r^j \bar{\rho} \bar{u}) + \frac{\partial}{\partial y} (r^j \bar{\rho} \tilde{v}) = 0 \quad (\text{A-31})$$

$$\bar{\rho} \bar{u} \frac{\partial \bar{u}}{\partial x} + \bar{\rho} \tilde{v} \frac{\partial \bar{u}}{\partial y} = -\frac{\partial \bar{p}}{\partial x} + \frac{1}{r^j} \frac{\partial}{\partial y} (r^j \mu \bar{\epsilon} \frac{\partial \bar{u}}{\partial y}) \quad (\text{A-32})$$

$$\begin{aligned} \bar{\rho} \bar{u} \frac{\partial}{\partial x} (C_p \bar{T}) + \bar{\rho} \tilde{v} \frac{\partial}{\partial y} (C_p \bar{T}) &= \bar{u} \frac{\partial \bar{p}}{\partial x} + \mu \bar{\epsilon} \left( \frac{\partial \bar{u}}{\partial y} \right)^2 \\ &+ \frac{1}{r^j} \frac{\partial}{\partial y} \left( \frac{r^j \mu \hat{\epsilon}}{Pr} \frac{\partial}{\partial y} (C_p \bar{T}) \right) \end{aligned} \quad (\text{A-33})$$

This set of boundary layer equations (A-31), (A-32), and (A-33) is valid for compressible heat conducting boundary layers over either two-dimensional or axisymmetric surfaces depending upon the choice of  $j$ . These equations are also valid for either laminar or turbulent flows depending upon the value given  $\bar{\epsilon}$  and  $\hat{\epsilon}$ .

## Appendix B

### Three Point Finite Difference Approximations and Linearization of the Transformed Boundary Layer Equations

The foundation of finite difference methods is the Taylor series. Both the forward difference method used to approximate derivatives in  $\xi$  and the central difference method used to approximate derivatives in  $\eta$  are obtained by manipulation of a Taylor series. These approximations for derivatives are used to linearize the transformed boundary layer equations. The finite difference approximations are to be determined for a grid point  $m+1, n$  of Fig. 3.

The forward difference method is obtained from the following two truncated Taylor series expansions of a variable  $H$  about the grid point  $m+1, n$ .

$$H_{m,n} = H_{m+1,n} - \Delta\xi_2 \left. \frac{\partial H}{\partial \xi} \right|_{m+1,n} + \frac{\Delta\xi_2^2}{2} \left. \frac{\partial^2 H}{\partial \xi^2} \right|_{m+1,n} \quad (B-1)$$

$$H_{m-1,n} = H_{m+1,n} - (\Delta\xi_1 + \Delta\xi_2) \left. \frac{\partial H}{\partial \xi} \right|_{m+1,n} + \frac{(\Delta\xi_1 + \Delta\xi_2)^2}{2} \left. \frac{\partial^2 H}{\partial \xi^2} \right|_{m+1,n} \quad (B-2)$$

Solving equation (B-1) for  $\left. \frac{\partial^2 H}{\partial \xi^2} \right|_{m+1,n}$  and substituting the value into equation (B-2) yields



$$\begin{aligned} \frac{\partial H}{\partial \xi} \Big|_{m+1,n} = & \left[ \frac{\Delta \xi_1 + 2\Delta \xi_2}{\Delta \xi_2 (\Delta \xi_1 + \Delta \xi_2)} \right] H_{m+1,n} - \left[ \frac{\Delta \xi_1 + \Delta \xi_2}{\Delta \xi_1 \Delta \xi_2} \right] H_{m,n} \\ & + \left[ \frac{\Delta \xi_2}{\Delta \xi_1 (\Delta \xi_1 + \Delta \xi_2)} \right] H_{m-1,n} \end{aligned} \quad (B-3)$$

The central difference method, used to approximate derivatives in  $\eta$ , is obtained from the following two truncated Taylor series expansions about a grid point  $m+1, n$ .

$$H_{m+1,n+1} = H_{m+1,n} + \frac{\partial H}{\partial \eta} \Big|_{m+1,n} \Delta \eta_n + \frac{1}{2} \frac{\partial^2 H}{\partial \eta^2} \Big|_{m+1,n} \Delta \eta_n^2 \quad (B-4)$$

$$H_{m+1,n-1} = H_{m+1,n} - \frac{\partial H}{\partial \eta} \Big|_{m+1,n} \Delta \eta_{n-1} + \frac{1}{2} \frac{\partial^2 H}{\partial \eta^2} \Big|_{m+1,n} \Delta \eta_n^2 \quad (B-5)$$

Solving equation (B-4) for  $\frac{\partial^2 H}{\partial \eta^2}$  and substituting the value into equation (B-3) gives

$$\begin{aligned} \frac{\partial H}{\partial \eta} \Big|_{m+1,n} = & \left[ \frac{\Delta \eta_{n-1}}{\Delta \eta_n (\Delta \eta_{n-1} + \Delta \eta_n)} \right] H_{m+1,n+1} - \left[ \frac{\Delta \eta_{n-1} - \Delta \eta_n}{\Delta \eta_n \Delta \eta_{n-1}} \right] H_{m+1,n} \\ & - \left[ \frac{\Delta \eta_n}{\Delta \eta_{n-1} (\Delta \eta_{n-1} + \Delta \eta_n)} \right] H_{m+1,n-1} \end{aligned} \quad (B-6)$$

Since the transformed boundary layer equations contain second derivatives in  $\eta$ , the approximation for  $\frac{\partial^2 H}{\partial \eta^2}$  is found by eliminating  $\frac{\partial H}{\partial \eta}$  between equations (B-4) and (B-5).



$$\left. \frac{\partial^2 H}{\partial \eta^2} \right|_{m+1,n} = \left[ \frac{2}{\Delta \eta_n (\Delta \eta_n + \Delta \eta_{n-1})} \right] H_{m+1,n+1} - \left[ \frac{2}{\Delta \eta_n \Delta \eta_{n-1}} \right] H_{m+1,n} + \left[ \frac{2}{\Delta \eta_n (\Delta \eta_n + \Delta \eta_{n-1})} \right] H_{m+1,n-1} \quad (B-7)$$

In order to linearize products of variables ( $G_{m+1,n} H_{m+1,n}$ ) it is first necessary to find expressions for both  $H$  and  $G$  at station  $m+1$  as functions of the known values at  $\xi$  stations  $m-1$  and  $m$ . The desired expression for  $H_{m+1,n}$  is found by eliminating  $\frac{\partial H}{\partial \xi}$  between equations (B-1) and (B-2). After truncating second order terms, the expression for  $H_{m+1,n}$  is

$$H_{m+1,n} = \left[ \frac{\Delta \xi_1 + \Delta \xi_2}{\Delta \xi_1} \right] H_{m,n} - \left[ \frac{\Delta \xi_2}{\Delta \xi_1} \right] H_{m-1,n} \quad (B-8)$$

Replacing  $H$  by  $G$  in equation (B-8) gives the desired expression for  $G_{m+1,n}$ . When equation (B-8) is used to evaluate  $H_{m+1,n}$  and  $G_{m+1,n}$ , the values will be given by  $H_{m+1}$  and  $G_{m+1}$  respectively. The following equality is now used in the linearization process.

$$H_{m+1,n} G_{m+1,n} = H_{m+1,n} G_{m+1,n} + H_{m+1,n} G_{m+1,n} - H_{m+1,n} G_{m+1,n} \quad (B-9)$$

By replacing terms in equation (B-9) with values determined from equation (B-9), the following expression linear in  $H_{m+1,n}$  and  $G_{m+1,n}$  is obtained.

$$H_{m+1,n} G_{m+1,n} = H_{m+1,n} \cdot G_{m+1,n} + G_{m+1,n} (H_{m+1,n} - H_{m+1,n} \cdot G_{m+1,n}) \quad (B-10)$$

Products of variables and derivatives  $(G \frac{\partial H}{\partial \xi})_{m+1,n}$  or  $G \frac{\partial H}{\partial \eta}|_{m+1,n}$  can now be put into linear form. Using equation (B-3), the product  $G \frac{\partial H}{\partial \xi}|_{m+1,n}$  is

$$G \frac{\partial H}{\partial \xi}|_{m+1,n} = G_{m+1,n} \left\{ \left[ \frac{\Delta \xi_1 + 2 \Delta \xi_2}{\Delta \xi_2 (\Delta \xi_1 + \Delta \xi_2)} \right] H_{m+1,n} - \left[ \frac{\Delta \xi_1 + \Delta \xi_2}{\Delta \xi_1 \Delta \xi_2} \right] H_{m,n} + \left[ \frac{\Delta \xi_2}{\Delta \xi_1 (\Delta \xi_1 + \Delta \xi_2)} \right] H_{m-1,n} \right\} \quad (B-11)$$

Equation (B-10) is used to replace the product  $G_{m+1,n} H_{m+1,n}$  in equation (B-11), which makes the equation linear in  $G_{m+1,n}$  and  $H_{m+1,n}$ . If the evaluation of  $\frac{\partial H}{\partial \eta}|_{m,n}$  is given by  $HY$ , the linear approximation for  $G \frac{\partial H}{\partial \eta}$  is

$$G \frac{\partial H}{\partial \eta}|_{m+1,n} = G_{m+1,n} \cdot HY + G_{m+1,n} \left( \frac{\partial H}{\partial \eta} \right)_{m+1,n} - G_{m+1,n} \cdot HY \quad (B-12)$$

A product of derivatives in  $\eta$  is linearized by

$$\left( \frac{\partial G}{\partial \eta} \right) \left( \frac{\partial H}{\partial \eta} \right) \Big|_{m+1,n} = G_Y \left( \frac{\partial H}{\partial \eta} \right)_{m+1,n} + HY \left( \frac{\partial G}{\partial \eta} \right)_{m+1,n} - G_Y \cdot HY \quad (B-13)$$

where  $G_Y$  is the evaluation of  $\frac{\partial G}{\partial \eta}|_{m,n}$ .

Before using these approximations for derivatives and product terms to linearize the transformed boundary layer equations, the following definitions are introduced to simplify the finite difference expressions.

$$Y_1 = \frac{2 (\Delta \xi_1 + 2 \Delta \xi_2)}{\Delta \xi_1 + \Delta \xi_2} \quad (B-14)$$

$$Y_2 = \frac{2 (\Delta \xi_1 + \Delta \xi_2)}{\Delta \xi_1} \quad (B-15)$$

$$Y_3 = \frac{2 \Delta \xi_2^2}{\Delta \xi_1 (\Delta \xi_1 + \Delta \xi_2)} \quad (B-16)$$

$$Y_4 = \frac{\Delta \xi_1 + \Delta \xi_2}{\Delta \xi_1} \quad (B-17)$$

$$Y_5 = \frac{\Delta \xi_2}{\Delta \xi_1} \quad (B-18)$$

$$Y_7 = \frac{\Delta \eta_n}{\Delta \eta_{n-1}} \quad (B-19)$$

$$Y_8 = \frac{2 \Delta \eta_n^2}{\Delta \eta_{n-1} (\Delta \eta_n + \Delta \eta_{n-1})} \quad (B-20)$$

$$Y_9 = \frac{2 \Delta \eta_{n-1}}{\Delta \eta_{n-1} + \Delta \eta_n} \quad (B-21)$$

$$Y_{10} = \frac{\Delta \eta_{n-1} - \Delta \eta_n}{\Delta \eta_{n-1}} \quad (B-22)$$

$$XL = \frac{\Delta \xi_2}{2 \Delta \eta_n} \quad (B-23)$$

$$FM1 = Y_4 F_{m,n} - Y_5 F_{m-1,n} \quad (B-24)$$

$$FM2 = Y_2 F_{m,n} - Y_3 F_{m-1,n} \quad (B-25)$$

$$FY = \left. \frac{\partial F}{\partial \eta} \right|_{m,n} \quad (B-26)$$

$$TM1 = \gamma_4 \theta_{m,n} - \gamma_5 \theta_{m-1,n} \quad (B-27)$$

$$TM2 = \gamma_2 \theta_{m,n} - \gamma_3 \theta_{m-1,n} \quad (B-28)$$

$$TY = \left. \frac{\partial \theta}{\partial \eta} \right|_{m,n} \quad (B-29)$$

$$VM1 = \gamma_4 V_{m,n} - \gamma_5 V_{m-1,n} \quad (B-30)$$

$$VM2 = \gamma_2 V_{m,n} - \gamma_3 V_{m-1,n} \quad (B-31)$$

$$VY = \left. \frac{\partial V}{\partial \eta} \right|_{m,n} \quad (B-32)$$

The transformed boundary layer equations (11), (12), and (13) with derivatives expanded are

$$F + 2\xi \frac{\partial F}{\partial \xi} + \frac{\partial V}{\partial \eta} = 0 \quad (B-33)$$

$$\begin{aligned} & \ell \bar{\epsilon} t^{2j} \frac{\partial^2 F}{\partial \eta^2} + \ell \bar{\epsilon} \frac{\partial F}{\partial \eta} \frac{\partial (t^{2j})}{\partial \eta^2} + \ell t^{2j} \frac{\partial F}{\partial \eta} \frac{\partial \bar{\epsilon}}{\partial \eta} \\ & + \bar{\epsilon} t^{2j} \frac{\partial \ell}{\partial \theta} \frac{\partial F}{\partial \eta} \frac{\partial \theta}{\partial \eta} - V \frac{\partial F}{\partial \eta} + \beta \theta - \beta F^2 = 2\xi F \frac{\partial F}{\partial \xi} \end{aligned} \quad (B-34)$$

$$\begin{aligned} & \frac{\ell}{P_r} \hat{\epsilon} t^{2j} \frac{\partial^2 \theta}{\partial \eta^2} + \frac{\ell}{P_r} \hat{\epsilon} \frac{\partial (t^{2j})}{\partial \eta} \frac{\partial \theta}{\partial \eta} + \frac{\ell}{P_r} \frac{\partial \hat{\epsilon}}{\partial \eta} t^{2j} \frac{\partial \theta}{\partial \eta} \\ & + \frac{\ell}{P_r} \frac{\partial \ell}{\partial \theta} \left( \frac{\partial \theta}{\partial \eta} \right)^2 \hat{\epsilon} t^{2j} - V \frac{\partial \theta}{\partial \eta} + \ell \bar{\epsilon} t^{2j} \alpha \left( \frac{\partial F}{\partial \eta} \right)^2 \\ & = 2\xi F \frac{\partial \theta}{\partial \xi} \end{aligned} \quad (B-35)$$



Using the development for linearizing terms in the variables  $G$  and  $H$ , the transformed boundary layer equations can now be linearized in  $F$ ,  $\theta$ , and  $V$ . At the grid point  $m+1, n$ , the linearization is accomplished by substituting the following expressions into equations (B-33), (B-34), and (B-35).

$$\left. \frac{\partial F}{\partial \xi} \right|_{m+1, n} = \frac{Y_1 F_{m+1, n} - Y_2 F_{m, n} + Y_3 F_{m-1, n}}{2 \Delta \xi_2} \quad (B-36)$$

$$\left. \frac{\partial F}{\partial \eta} \right|_{m+1, n} = \frac{-Y_8 F_{m+1, n-1}}{2 \Delta \eta_n} - \frac{Y_{10} F_{m+1, n}}{\Delta \eta_n} + \frac{Y_9 F_{m+1, n+1}}{2 \Delta \eta_n} \quad (B-37)$$

$$\left. \frac{\partial \theta}{\partial \eta} \right|_{m+1, n} = \frac{-Y_8 \theta_{m+1, n-1}}{2 \Delta \eta_n} - \frac{Y_{10} \theta_{m+1, n}}{\Delta \eta_n} + \frac{Y_9 \theta_{m+1, n+1}}{2 \Delta \eta_n} \quad (B-38)$$

$$\left. \frac{\partial V}{\partial \eta} \right|_{m+1, n} = \frac{-Y_8 V_{m+1, n-1}}{2 \Delta \eta_n} - \frac{Y_{10} V_{m+1, n}}{\Delta \eta_n} + \frac{Y_9 V_{m+1, n+1}}{2 \Delta \eta_n} \quad (B-39)$$

$$\left. \frac{\partial^2 F}{\partial \eta^2} \right|_{m+1, n} = \frac{Y_8 F_{m+1, n-1} - 2 Y_7 F_{m+1, n} + Y_6 F_{m+1, n+1}}{\Delta \eta_n^2} \quad (B-40)$$

$$\left. \frac{\partial^2 \theta}{\partial \eta^2} \right|_{m+1, n} = \frac{Y_8 \theta_{m+1, n-1} - 2 Y_7 \theta_{m+1, n} + Y_6 \theta_{m+1, n+1}}{\Delta \eta_n^2} \quad (B-41)$$

$$\left. \left( \frac{\partial F}{\partial \eta} \right) \left( \frac{\partial \theta}{\partial \eta} \right) \right|_{m+1, n} = F Y \left( \frac{\partial \theta}{\partial \eta} \right)_{m+1, n} + T Y \left( \frac{\partial F}{\partial \eta} \right)_{m+1, n} - F Y \cdot G Y \quad (B-42)$$

$$\left. \left( \frac{\partial F}{\partial \eta} \right)^2 \right|_{m+1, n} = 2 F Y \left( \frac{\partial F}{\partial \eta} \right)_{m+1, n} - F Y^2 \quad (B-43)$$

$$\left. \left( \frac{\partial \theta}{\partial \eta} \right)^2 \right|_{m+1, n} = 2 T Y \left( \frac{\partial \theta}{\partial \eta} \right)_{m+1, n} - T Y^2 \quad (B-44)$$

$$F \left. \frac{\partial F}{\partial \xi} \right|_{m+1, n} = \frac{(2 \cdot Y_1 F_{m1} - F_{m2}) F_{m+1, n} - F_{m1}^2 \cdot Y_1}{2 \Delta \xi_2} \quad (B-45)$$

$$F \frac{\partial \theta}{\partial \xi} \Big|_{m+1, n} = \frac{(Y_1 \cdot TM1 - TM2) F_{m+1, n} + Y_1 \cdot \theta_{m+1, n}}{2 \Delta \xi_2} - \frac{Y_1 \cdot TM1 \cdot FMI}{2 \Delta \xi_2} \quad (B-46)$$

$$V \frac{\partial F}{\partial \eta} \Big|_{m+1, n} = V_{m+1, n} \cdot FY + VMI \cdot \left( \frac{\partial F}{\partial \eta} \right)_{m+1, n} - VMI \cdot FY \quad (B-47)$$

$$V \frac{\partial \theta}{\partial \eta} \Big|_{m+1, n} = V_{m+1, n} \cdot TY + VMI \cdot \left( \frac{\partial \theta}{\partial \eta} \right)_{m+1, n} - VMI \cdot TY \quad (B-48)$$

$$F^2 \Big|_{m+1, n} = 2 \cdot FMI \cdot F_{m+1, n} - FMI^2 \quad (B-49)$$

After collecting terms, the result of substituting equations (B-36) through (B-49) into the transformed boundary layer equations (B-33), (B-34), and (B-35) is the following three equations.

$$F_{m+1, n} \left[ \Delta \xi_2 + \xi \cdot Y1 \right] + V_{m+1, n-1} \left[ -Y_8 \cdot XL \right] + V_{m+1, n} \left[ -2Y_{10} \cdot XL \right] + V_{m+1, n+1} \left[ Y_9 \cdot XL \right] = \xi \cdot FM2 \quad (B-50)$$

$$F_{m+1, n-1} \left[ Y_8 \cdot XL \left( 2\bar{l} \bar{E} t^{2j} - \bar{l} \bar{E} \frac{\partial t^{2j}}{\partial \eta} - \bar{l} t^{2j} \right. \right. \\ \left. \left. + VMI - \bar{E} t^{2j} \frac{\partial \bar{l}}{\partial \theta} TY \right) \right]$$

$$+ F_{m+1, n} \left[ -4Y_7 \cdot XL \cdot \bar{l} \bar{E} t^{2j} - 2Y_{10} \cdot XL \left( \bar{l} \bar{E} \frac{\partial t^{2j}}{\partial \eta} \right. \right. \\ \left. \left. + \bar{l} t^{2j} \frac{\partial \bar{E}}{\partial \eta} - VMI + \bar{E} t^{2j} \cdot \frac{\partial \bar{l}}{\partial \theta} \cdot TY - 2\Delta \xi_2 \cdot \beta \cdot FMI \right. \right. \\ \left. \left. - 2\Delta \xi_2 \cdot \beta \cdot FMI - \xi (2Y_1 \cdot FMI - FM2) \right) \right]$$

$$+ F_{m+1, n+1} \left[ \frac{2Y_6 \cdot XL \cdot \bar{l} \bar{E} t^{2j}}{\Delta \eta_n} + Y_9 \cdot XL \left( \bar{E} \bar{l} \frac{\partial t^{2j}}{\partial \eta} + \bar{l} t^{2j} \frac{\partial \bar{E}}{\partial \eta} \right. \right. \\ \left. \left. - VMI + \bar{E} t^{2j} \cdot \frac{\partial \bar{l}}{\partial \theta} \cdot TY \right) \right]$$

$$+ \Theta_{m+1, n} \left[ -2Y_{10} \cdot XL \cdot \bar{E} t^{2j} \cdot \frac{\partial \bar{l}}{\partial \theta} \cdot FY + \beta \cdot \Delta \xi_2 \right]$$

$$+ \Theta_{m+1, n-1} \left[ -Y_8 \cdot XL \cdot \bar{E} t^{2j} \cdot \frac{\partial \bar{l}}{\partial \theta} \cdot FY \right]$$

$$+ \Theta_{m+1, n+1} \left[ Y_9 \cdot XL \cdot \bar{E} t^{2j} \cdot \frac{\partial \bar{l}}{\partial \theta} \cdot FY \right]$$

$$+ V_{m+1, n} \left[ -FY \cdot \Delta \xi_2 \right] = \left[ FY \cdot \Delta \xi_2 \left( \bar{E} t^{2j} \frac{\partial \bar{l}}{\partial \theta} TY - VMI \right) \right.$$

$$\left. - FMI^2 (\Delta \xi_2 \cdot \beta + Y_1 \cdot \xi) \right] \quad (B-51)$$

$$\begin{aligned}
& F_{m+1, n-1} \left[ -2 Y_8 \cdot F Y \cdot X L \cdot \ell \bar{E} t^{2j} \alpha \right] \\
& + F_{m+1, n} \left[ -4 Y_{10} F Y \cdot X L \cdot \ell \bar{E} t^{2j} \alpha - \xi (Y_i \cdot T M 1 - T M 2) \right] \\
& + F_{m+1, n+1} \left[ 2 Y_9 \cdot F Y \cdot X L \cdot \ell \bar{E} t^{2j} \alpha \right] \\
& + \Theta_{m+1, n-1} \left[ \frac{Y_8 \cdot X L}{P_r} \left( \frac{2 \ell \hat{E} t^{2j}}{\Delta \eta_n} - \ell \hat{E} \frac{\partial t^{2j}}{\partial \eta} - \ell \cdot \frac{\partial \hat{E}}{\partial \eta} \cdot t^{2j} \right. \right. \\
& \quad \left. \left. + P_r \cdot V M 1 - 2 T Y \frac{\partial \ell}{\partial \theta} \hat{E} t^{2j} \right) \right] \\
& + \Theta_{m+1, n} \left[ -\frac{4 Y_7 \cdot X L \cdot \ell \hat{E} t^{2j}}{\Delta \eta_n \cdot P_r} - \frac{2 Y_{10} (X L)}{P_r} \left( \ell \hat{E} \frac{\partial t^{2j}}{\partial \eta} \right. \right. \\
& \quad \left. \left. + \ell \cdot \frac{\partial \hat{E}}{\partial \eta} \cdot t^{2j} - P_r \cdot V M 1 + 2 T Y \frac{\partial \ell}{\partial \theta} \hat{E} t^{2j} \right) \right] \\
& + \Theta_{m+1, n+1} \left[ \frac{X L}{P_r} \left\{ \frac{2 Y_6 \ell \hat{E} t^{2j}}{\Delta \eta_n} + Y_9 \left( \ell \hat{E} \frac{\partial t^{2j}}{\partial \eta} + \ell \frac{\partial \hat{E}}{\partial \eta} t^{2j} \right. \right. \right. \\
& \quad \left. \left. \left. - P_r \cdot V M 1 + 2 T Y \frac{\partial \ell}{\partial \theta} \hat{E} t^{2j} \right) \right\} \right] \\
& + V_{m+1, n} \left[ \Delta \xi_2 \cdot T Y \right] = \left[ \frac{\Delta \xi_2 \cdot T Y}{P_r} \left( \frac{\partial \ell}{\partial \theta} \hat{E} t^{2j} T Y \right. \right. \\
& \quad \left. \left. - P_r \cdot V M 1 \right) + \Delta \xi_2 \ell \bar{E} t^{2j} \alpha \cdot F Y^2 - \xi \cdot Y_i \cdot T M 1 \cdot F M 1 \right] \quad (B-52)
\end{aligned}$$

The derivatives in  $\eta$ , contained in the brackets [ ] of equations (B-50), (B-51), and (B-52), are evaluated using known values at  $\xi$  station  $m$ . The derivative  $\frac{\partial \ell}{\partial \theta}$  is found



by explicitly taking the derivative of equation (20) and evaluating the result at  $\xi$  station  $m$ .

The values of  $t^{2j}$ ,  $\ell$ ,  $\bar{\epsilon}$ , and  $\hat{\epsilon}$  within the brackets are determined from known values at  $\xi$  stations  $m-1$  and  $m$  by use of the relation given in equation (B-8). All other quantities in the brackets can be explicitly determined at the grid point  $m+1, n$ . Equations (B-50), (B-51), and (B-52) are then, at a given  $\xi$  station, a constant coefficient set of linear algebraic equations.

The solution method for these equations uses an iterative method, if required, to achieve the convergence criteria of equation (63). If iterations are required, the values of  $FMI$ ,  $TMI$ ,  $VMI$ ,  $FY$ ,  $TY$ , and  $VY$  are updated after the initial solution of equations (B-50), (B-51), and (B-52) at a given  $\xi$  station. The values of  $FMI$ ,  $TMI$ , and  $VMI$  are replaced by the values of  $F$ ,  $\theta$ , and  $V$  determined in the previous iteration. With these values of  $F$ ,  $\theta$ , and  $V$ , the derivatives  $\frac{\partial F}{\partial \eta}$ ,  $\frac{\partial \theta}{\partial \eta}$ , and  $\frac{\partial V}{\partial \eta}$  can be determined.  $FY$ ,  $TY$ , and  $VY$  are then replaced by  $\frac{\partial F}{\partial \eta}$ ,  $\frac{\partial \theta}{\partial \eta}$ , and  $\frac{\partial V}{\partial \eta}$ .

Equations (B-50), (B-51), and (B-52) are now written in a simplified form for reference purposes. Equations (B-50), (B-51), and (B-52) are given by equations (B-53), (B-54), and (B-55) respectively.

$$\begin{aligned}
& A_{11_n} F_{m+1, n-1} + A_{12_n} F_{m+1, n} + A_{13_n} F_{m+1, n+1} + B_{11_n} \Theta_{m+1, n-1} \\
& + B_{12_n} \Theta_{m+1, n} + B_{13_n} \Theta_{m+1, n+1} + C_{11_n} V_{m+1, n-1} + C_{12_n} V_{m+1, n} \\
& + C_{13_n} V_{m+1, n+1} = D_{1_n}
\end{aligned} \tag{B-53}$$

$$\begin{aligned}
& A_{21_n} F_{m+1, n-1} + A_{22_n} F_{m+1, n} + A_{23_n} F_{m+1, n+1} + B_{21_n} \Theta_{m+1, n-1} \\
& + B_{22_n} \Theta_{m+1, n} + B_{23_n} \Theta_{m+1, n+1} + C_{21_n} V_{m+1, n-1} + C_{22_n} V_{m+1, n} \\
& + C_{23_n} V_{m+1, n+1} = D_{2_n}
\end{aligned} \tag{B-54}$$

$$\begin{aligned}
& A_{31_n} F_{m+1, n-1} + A_{32_n} F_{m+1, n} + A_{33_n} F_{m+1, n+1} + B_{31_n} \Theta_{m+1, n-1} \\
& + B_{32_n} \Theta_{m+1, n} + B_{33_n} \Theta_{m+1, n+1} + C_{31_n} V_{m+1, n-1} + C_{32_n} V_{m+1, n} \\
& + C_{33_n} V_{m+1, n+1} = D_{3_n}
\end{aligned} \tag{B-55}$$

The subscripted coefficients  $A, B, C$ , and  $D$  are defined by the bracketted terms of equations (B-50), (B-51), and (B-52).

## Appendix C

### Four Point Finite Difference Approximations For Evaluating Wall Derivatives

The wall derivatives, required to evaluate the heat transfer rate and skin friction coefficient, are evaluated by use of a four point finite difference scheme. The four point finite difference approximation for the derivative of a variable  $H$  with respect to the transformed coordinate  $\eta$  is found in a similar manner to that used in the three point finite difference method. However, the four point finite difference method is more accurate since the truncated Taylor series, used in the development, retain third order terms. To find the four point finite difference expression for  $\frac{\partial H}{\partial \eta} \Big|_w$  at  $\xi$  station  $m$  of the grid in Fig. 3, the following three truncated Taylor series expansions are used.

$$H_{m,2} = H_{m,1} + \frac{\partial H}{\partial \eta} \Big|_{m,1} \Delta \eta_1 + \frac{1}{2} \frac{\partial^2 H}{\partial \eta^2} \Big|_{m,1} \Delta \eta_1^2 + \frac{1}{9} \frac{\partial^3 H}{\partial \eta^3} \Big|_{m,1} \Delta \eta_1^3 \quad (C-1)$$

$$\begin{aligned} H_{m,3} = H_{m,1} + \frac{\partial H}{\partial \eta} \Big|_{m,1} (\Delta \eta_1 + \Delta \eta_2) + \frac{1}{2} \frac{\partial^2 H}{\partial \eta^2} \Big|_{m,1} (\Delta \eta_1 + \Delta \eta_2)^2 \\ + \frac{1}{9} \frac{\partial^3 H}{\partial \eta^3} \Big|_{m,1} (\Delta \eta_1 + \Delta \eta_2)^3 \end{aligned} \quad (C-2)$$

$$\begin{aligned} H_{m,4} = H_{m,1} + \frac{\partial H}{\partial \eta} \Big|_{m,1} (\Delta \eta_1 + \Delta \eta_2 + \Delta \eta_3) + \frac{1}{2} \frac{\partial^2 H}{\partial \eta^2} \Big|_{m,1} (\Delta \eta_1 + \Delta \eta_2 + \Delta \eta_3)^2 \\ + \frac{1}{9} \frac{\partial^3 H}{\partial \eta^3} \Big|_{m,1} (\Delta \eta_1 + \Delta \eta_2 + \Delta \eta_3)^3 \end{aligned} \quad (C-3)$$



By introducing the definition of  $\Delta \eta$ , given by equation (54) and substituting the value of  $\frac{\partial^3 H}{\partial \eta^3}$  from equation (C-1) into equations (C-2) and (C-3), the following two expressions are obtained.

$$H_{m,2} - H_{m,1} - \frac{H_{m,3} - H_{m,1}}{(1+\kappa)^3} = \frac{\partial H}{\partial \eta} \Big|_{m,1} \left( 1 - \frac{1}{(1+\kappa)^2} \right) \Delta \eta_1 + \frac{1}{2} \frac{\partial^2 H}{\partial \eta^2} \Big|_{m,1} \left( 1 - \frac{1}{(1+\kappa)} \right) \Delta \eta_1^2 \quad (C-4)$$

$$H_{m,2} - H_{m,1} - \frac{(H_{m,4} - H_{m,1})}{(1+\kappa+\kappa^2)^3} = \frac{\partial H}{\partial \eta} \Big|_{m,1} \left( 1 - \frac{1}{(1+\kappa+\kappa^2)^2} \right) \Delta \eta_1 + \frac{1}{2} \frac{\partial^2 H}{\partial \eta^2} \Big|_{m,1} \left( 1 - \frac{1}{(1+\kappa+\kappa^2)} \right) \Delta \eta_1^2 \quad (C-5)$$

Eliminating  $\frac{\partial^2 H}{\partial \eta^2}$  between equations (C-4) and (C-5), the expression for  $\frac{\partial H}{\partial \eta} \Big|_{m,1}$  is then found to be

$$\begin{aligned} \frac{\partial H}{\partial \eta} \Big|_{m,1} = & H_{m,1} \left[ \frac{-(1+\kappa+\kappa^2)^2 (\kappa^2+\kappa-1) - (1+\kappa)}{(1+\kappa)(1+\kappa+\kappa^2) \kappa^3} \right] \\ & + H_{m,2} \left[ \frac{1+\kappa+\kappa^2}{\kappa^2} \right] + H_{m,3} \left[ \frac{-(1+\kappa+\kappa^2)}{(1+\kappa) \kappa^3} \right] \\ & + H_{m,4} \left[ \frac{1}{(1+\kappa+\kappa^2) \kappa^3} \right] \end{aligned} \quad (C-6)$$

Equation (C-6) is the four point finite difference expression used to evaluate wall derivatives.



Appendix D

Computer Program Listing

[illegible]

**C**

C

C

**C**

C

C  
C

C

C

CC

C

C

**C**

**C**

CC

```

C      PRT=TURBULENT PRANDTL NUMBER
C      XINTER=INTERMITTENCY FACTOR
C      DYW=MINIMUM STEP SIZE FOR NORMAL COORDINATE IN TRANSFORMED PLANE
C      IEDGE=TOTAL NUMBER OF POINTS IN NORMAL COORDINATE DIRECTION
C      IDIFF=0 (FOR THREE POINT FINITE DIFFERENCE SCHEME)
C           1 (FOR TWO POINT FINITE DIFFERENCE SCHEME)
C      IEND1=TOTAL NUMBER OF INTEGRATION STEPS IN STREAMWISE DIRECTION
C      MSP=DESIRED INTERVAL IN NUMBER OF STEPS IN STREAMWISE DIRECTION
C      J2DA=0 (TWO DIMENSIONAL SURFACE)
C           1 (AXISYMMETRIC BODY)
C      INUM=NUMBER OF PRESSURE DATA POINTS ENTERED
C      IPRES=0 (FOR NO PRESSURE GRADIENT)
C           1 (IF PRESSURE GRADIENT EXISTS)
C      ITRAN=0 (FOR NO TRANSVERSE CURVATURE EFFECT)
C           1 (FOR TRANSVERSE CURVATURE EFFECTS)
C      ICON=0 (IF BODY GEOMETRY IS TO BE COMPUTED FROM PRESSURE DATA
C              LOCATIONS)
C           1 (IF BODY GEOMETRY IS COMPUTED FROM SURFACE EQUATIONS)
C      ICHS=STATION NUMBER WHERE STREAMWISE STEP SIZE IS TO BE DOUBLED
C      IPRN=NUMBER OF STEPS WHERE DESIRED WHERE DETAILED PRINTOUTS OF
C           PROFILES IS DESIRED
C      Z=CENTERLINE LOCATION OF PRESSURE OF PRESSURE DATA ENTRIES
C      R=RADIUS OF PRESSURE DATA ENTRIES
C      CP=SURFACE PRESSURE DIVIDED BY FREE STREAM PRESSURE
C      R,BTRX,AND Z ARE SCALED BY SAME LENGTH AS USED IN REY
C      P1P2=RATIO OF TOTAL PRESSURE IN FRONT OF SHOCK TO TOTAL PRESSURE
C           BEHIND SHOCK (IF FREE STREAM CONDITIONS ARE INPUT AS THOSE
C           BEHIND SHOCK THEN P1P2=1 )
C
C *****
C      READ(5,8002) G, PR, XMINF, REY, TA
C      READ(5,8002) DS, SI, OMEGA, ERROR, XX<
C      READ(5,8002) B0,BTRX, PRT, XINTER, DYW
C      READ(5,8003) IEDGE,INTACT,IDIFF,IEND1,MSP,J2DA,INUM,IPRES,ITRAN,
1      ICON
C      READ(5,8003) (ICHS(I), I = 1, 8)
C      READ(5,8003) (IPRN(I), I = 1, 9)
C      XLAM=.5*BTRX
C      IF(IPRES.EQ.0) GO TO 79
C      IF(INUM.EQ.0) GO TO 20
C      READ(5,8002) DPMAX,P1P2
C      READ(5,8002) (CP(IJ),IJ=1,INUM)
79  CONTINUE
C      IF(INUM.EQ.0) GO TO 20
C      IF(ICON.EQ.1) GO TO 4
C      READ(5,8002) (R(IJ),IJ=1,INUM)
4  CONTINUE
C      READ(5,8002) (Z(IJ),IJ=1,INUM)
C      WRITE(5,7111) INUM
7111 FORMAT(10X,"ALL ",I2," DATA PTS ENTERED")
C      IF(J2DA.EQ.0) GO TO 81
C *****
C

```



```

C
C   THIS SUBROUTINE COMPUTES BODY GEOMETRY FROM A FINITE NUMBER OF
C   LOCATIONS
C
C   CALL CONST(ICON,IREF)
C
C *****
C 81 CONTINUE
C   IF(J2DA.EQ.1) GO TO 85
C   DO 83 KT=1,INUM
C   XP(KT)=Z(KT)
C 83 CONTINUE
C 86 CONTINUE
C   IF(IPRES.EQ.0) GO TO 20
C   WRITE(6,1100)
C   XMSQ=XMINF*XMINF
C *****
C
C   THIS SUBROUTINE COMPUTES LEADING AND TRAILING EDGE PRESSURE
C   GRADIENTS
C
C   CALL SMTHPR(BTRX,DPMAX,G,XMSQ)
C
C *****
C   COMPUTE NONDIMENSIONALIZING QUANTITIES
C
C 20   Z1= 1. + (G - 1.)/2.*XMINF**2
C      P10 = (1./(G*XMINF**2))*(Z1**(G/(G-1.)))
C      T10 = (1./((G - 1.)*XMINF**2))*Z1
C      R10 = G*P10/(T10*(G - 1.))
C      TINF = T10/Z1
C      TW = 80*T10
C      IF(OMEGA.EQ. 0.) GO TO 101
C      VIS10 = T10**OMEGA
C      EPS = (((G - 1.)*XMINF**2)**(OMEGA/2.))/SQRT(REY)
C      VISINF = TINF**OMEGA
C      GO TO 102
C 101  TC=198.6/((G-1.)*XMINF**2*TA)
C      VIS10 = (T10**1.5)*(1. + TC)/(T10+TC)
C      EPS = (((1.+(198.6/TA))*(((G - 1.)*XMINF**2)**1.5)))/(((G - 1.)*X
C 1MINF**2)+(198.6/TA))/REY)**.5
C      VISINF = (TINF**1.5)*(1. + TC)/(TINF+TC)
C 102  SU=198.6
C
C   OUTPUT INITIAL CONDITIONS
C
C   WRITE(6,9002)
C   WRITE(6,9003) G, PR, XMINF, REY, TA, 30, EPS
C   WRITE(6,9004) P10, R10, T10, VIS10, SI
C   WRITE(6,9005) OMEGA,PRT,BTRX
C   IF(XINTER.EQ.1.) WRITE(6,9019)
C   IF(XINTER.EQ.1.) WRITE(6,9019)
C   IF(XINTER.EQ.0.) WRITE(6,9020)
C   IF(J2DA.EQ.0) WRITE(6,9021)
C   IF(J2DA.NE.0) WRITE(6,9022)
C   IF(ITRAN.EQ.0) WRITE(6,9086)
C   IF(ITRAN.EQ.1) WRITE(6,9087)

```



```

C
C      INPUT INITIAL PROFILE
C
12  MSTART=2
C      INITIALIZE THE STREAMWISE LOCATION
      S=SI
      IF(J2DA,EQ.1) S=0.0
      DS2=DS1=DS
      DX2DS=DX1DS=DXDS=0.
      SEPO=1.
C      INITIALIZE THE STREAMWISE LOCATION
      Y(1)=0.0
      DO 201 LL=2,200
      DY=XXK**(LL-2)*DYW
201  Y(LL)=Y(LL-1)+DY
      DO 700 LL = 1, 200
      D1(LL)=D2(LL)=D3(LL)=XNV(LL)=0.
      VP(LL)=VN(LL)=VO(LL)=-Y(LL)
      FP(LL)=FO(LL)=FN(LL)=TP(LL)=TN(LL)=TO(LL)=EP(LL)=EO(LL)=EN(LL)=
1  ETP(LL)=ETO(LL)=ETN(LL)=1.0
      T2JP(LL)=T2JO(LL)=T2JN(LL)=1.0
700  CONTINUE
      DO 701 J = 1, 200
      DO 701 I = 1, 3
701  A1(J,I)=A2(J,I)=A3(J,I)=B1(J,I)=B2(J,I)=B3(J,I)=C1(J,I)
1  =C2(J,I)=C3(J,I)=0.
      PREF=G*XMINF**2
      TRFF = (G - 1.)*XMINF**2
      RCON=0.0
      ZCON=0.0
C
C      INITIALIZE COUNTERS
C
      NC=1
      KEND=INUM-2
      IF(ICON,EQ.1) KEND=IREF
      ICOUN=MSTART
      IQ=IEDGE
      IG=1
      IP=1
      INDOCH=0
      ITCNT1 = 1
      IIN=0
C
C      *** BEGIN FIRST-ORDER-TRIDIAGONAL MATRIX SOLUTION ***
C
      DO 115 M=MSTART,IEND1
      IF(J2DA,EQ.0) GO TO 48
46  CONTINUE
      IF(NC,EQ.KEND) GO TO 47
      IF(ICON,EQ.0) ZREF=Z(NC+1)
      IF(ICON,EQ.1) ZREF=F(NC)
      IF(ZCON,GE.ZREF) NC=NC+1
C      DRDZ=SLOPE OF TANGENT TO SURFACE OF BODY
C      ALPHA=ANGLE BETWEEN TANGENT TO SURFACE AND CENTERLINE

```

```

C      RCON=RADIUS OF AXISYMMETRIC BODY
C      ZCON=CENTERLINE DISTANCE
C      S=SURFACE COORDINATE IN STREAMWISE DIRECTION
47  DRDZ=R(NC)+2.*C(NC)*ZCON+3.*D(NC)*ZCON**2+4.*E(NC)*ZCON**3
      ALPHA=ATAN(DRDZ)
      IF(S.LT.SI) DZ=(DS2/10.)*COS(ALPHA)
      IF(S.LT.SI) ZCON=ZCON+DZ
      IF(S.LT.SI) RCON=A(NC)+3(NC)*ZCON+C(NC)*ZCON**2+7(NC)*ZCON**3+E(NC
1) *ZCON**4
      IF(S.LT.SI) S=S+DS2/10.
      IF(S.LT.SI) GO TO 46
      D7=DS2*COS(ALPHA)
      ZCON=ZCON+DZ
      RCON=A(NC)+8(NC)*ZCON+C(NC)*ZCON**2+D(NC)*ZCON**3+E(NC)*ZCON**4
48  CONTINUE
      IF(M.EQ.MSTART) MP=MSTART
      IF(M.EQ.TEND1) MP=M
      IF(M.EQ.(M/MSP)*MSP) MP=M
      S=S+DS2
      DX2DS = DX1DS
      DX1DS = DXDS
C*****
C
C      THIS SUBROUTINE COMPUTES LOCAL PRESSURE,PRESSURE GRADIENT,
C      AND TEMPERATURE
C
C      CALL PRESS4(S,XMINF,G,PBG1,DPBG1,TETNF,XME,IPRES,P1P2)
C
C*****
      PE = PBG1/PREF
      PP = DPBG1/PREF
      TE = TETNF/TREF
      UE = SQRT(2.*(T10 - TE))
      RE=G*PE/((G-1.0)*TE)
      TR=SU/(TETNF*TA)
      IF (OMEGA) 642,676,642
642  XNUE=TE**OMEGA
      GOTO688
676  XNUE=TE**1.5*(1.+198.6/(TA*TREF))/(TE+198.6/(TA*TREF))
688  CONTINUE
C
C      COMPUTE LOCAL XI AND STEP LENGTHS
C
C      DXDS=DERIVATIVE OF TRANSFORMED SURFACE COORDINATE WRT
C      SURFACE COORDINATE
C
      DXDS=RE*UE*XNUE
      IF(J2DA.NE.0) DXDS=DXDS*RCON**2
      IF(M.EQ.2) DX1DS=DX2DS=DXDS
      DX2=.5*DS2*((1.+DS2/DS1)*DX1DS+DS1*DXDS/(DS1+DS2)-DS2*DS2*DX2DS/
1 (DS1*(DS1+DS2)))
      REYNDE=PE*UE*S/XNUE
      REYEXT=REY*VISINF*REYNDE
      IF(M.EQ.2) DX1=DX2

```

```

C
C      X=TRANSFORMED STREAMWISE COORDINATE
C
C      IF(M.EQ.2) X=DXDS*SI
C      X=X+DX2
C      COMPUTE STEP LENGTH FUNCTIONS
C
C      Y1=2.*(DX1+2.*DX2)/(DX1+DX2)
C      IF(I0IFF.EQ.1) Y1 = 2.
C      Y2=((DX1+DX2)/DX1)*2.0
C      Y3=(DX2*DX2/(DX1*(DX1+DX2)))*2.0
C      Y4=(DX1+DX2)/DX1
C      Y5=DX2/DX1
C      TWTE = TW/TE
C
C      COMPUTE ALPHA, BETA, AND LAMBDA
C
C      DUEOX=-PP/(RE*UE*DXDS)
C      XAL=UE*HF/TE
C      XRE=2.0*X*DUEOX/UE
C
C      6998 LENGTH=TEDGE
C      *****
C
C      ASSIGN THE MATRIX ELEMENTS FOR THE FINITE DIFFERENCE EQUATIONS
C
C      CALL ELMATX( M,DX2,X,XAL,XBE,TR,IDIFF,Y1,Y2,Y3,Y4,Y5,TWTE,ITCNT1,
C      1 ITRAN,A1,A2,A3,B1,B2,B3,C1,C2,C3)
C
C      *****
C
C      *****
C
C      MATRIX INVERSION, SOLVE FOR F, THETA AND V
C
C      CALL MATEQN3(FP,TP,VP,D1,D2,D3,A1,B1,C1,A2,B2,C2,A3,B3,C3,3,LENGTH
C      1 ,200)
C
C      *****
C      ITCNT1=ITCNT1+1
C      N=IEDGE+1
C      DY=DYW*XXX**(TEDGE-2)
C      VK=(VP(TEDGE)/(XXX*(1.+1./XXX))-VP(IEDGE-1)*(1.-1./XXX)*XXX-
C      1 VP(IEDGE-2)*XXX/(1.+1./XXX))/DY
C      DY=DYW*XXX**(IEDGE-1)
C      KON=N+5
C      D065IQ=N,KOV
C      DY=DYW*XXX**(N-1)+DY
C      FP(IQ)=TP(IQ)=1.0
C      65 VP(IQ)=VP(IEDGE-1)+VK*DY
C      INITIATION OF SIMILAR SOLUTIONS
C      IF(M.EQ.2) GO TO 8020
C      GO TO 8013

```

AD-A034 943

AIR FORCE INST OF TECH WRIGHT-PATTERSON AFB OHIO SCH--ETC F/G 20/4  
NUMERICAL SOLUTION OF THE COMPRESSIBLE BOUNDARY LAYER EQUATIONS--ETC(U)  
DEC 76 C R BLAKE  
GA/MC/76D-4

UNCLASSIFIED

NL

2 OF 2

ADAO34943



END

DATE  
FILMED  
3 - 77



```

8020 DO 8019 I=1,KON
      VO(I)=VN(I)=VP(I)
      FO(I)=FN(I)=FP(I)
8019 TO(I)=TV(I)=TP(I)
C      INITIATION OF SIMILAR SOLUTIONS
8018 IO=IEDG+1
C
C      U AND THETA PROFILES ITERATIONS
      TAU2=(FP(2)-FP(1))/DYW
      IF(ITCNT1.EQ.2) TAU1=10.*TAU2
      RT12=TAJ1/TAU2-1.
      TAU1=TAU2
      IF(ITCNT1.LE.100) GO TO 7005
      WRITE(6,2003) M
      CALL EXIT
7005 IF(ABS(RT12).GT.ERROR) GO TO 6998
C      U AND THETA PROFILES ITERATIONS
C
C
C      COMPUTE BLT, ROT(DELTA STAR) AND BMT(THETA)
55  CO=TP(1)
      TPI=0.
      BLT=BLDT=BLMT=0.
      XNN(1)=0.
      DO 57 N=2,KON
        DY=DYW*XXX**(N-2)
        CX=TP(N)
        TPI=TPI+.5*DY*(CO+CX)
        CO=CX
C
C      XNN=COORDINATE NORMAL TO SURFACE
C
      XNN(N)=EPS*TPI*SQR(2.*X)/(RE*UE)
      IF(J2DA.NE.0) XNN(N)=XNV(N)/RCON
      IF(J2DA.EQ.1) T2JP(N)=1.+2.*SQR(2.*X)*EPS*COS(ALPHA)*TPI/(RE*UE
1 *RCON**2)
      IF(ITRAN.NE.0) XNN(N)=(PCON/COS(ALPHA))*(SQR(T2JP(N))-1.)
      BLDT=BLDT+(2.-FP(N)/TP(N)-FP(N-1)/TP(N-1))*(XNN(N)-XNN(N-1))/2.
      BLMT=BLMT+(FP(N)*(1.-FP(N))/TP(N)+FP(N-1)*(1.-FP(N-1))/TP(N-1))
1 *(XNN(N)-XNN(N-1))/2.
      IF(BLT.GT.0.) GO TO 57
      IF(FP(N).GE.0.995) BLT=XNN(N)-(FP(N)-.995)*(XNV(N)-XNN(N-1))
1 /(FP(N)-FP(N-1))
57  CONTINUE
C      COMPUTE BLT, ROT(DELTA STAR) AND BMT(THETA)
C
C      COMPUTE THE EDDY VISCOSITY COEFFICIENT
      IF(S.LE.BTRX) GO TO 58
C*****
C
C      THIS SUBROUTINE COMPUTES EDDY VISCOSITIES
C
      CALL REYSTR (KON,TR,X,TREF,XNUE,XBE,S,ITCNT1,
1 RCON,ALPHA,ITRAN)

```

```

C
C*****
58  ITCNT1=1
C
C  ASSESMENT OF GRID PONITS IN ETA
C
  IF(INDCH) 71, 71, 732
71  CONTINUE
  IF(M - 20) 732, 732, 72
72  IF(ABS(FP(IEDGE-15)-FP(IEDGE-16))-0.0001) 73,73,74
73  IF(ABS(TP(IEDGE-15) - TP(IEDGE-16)) - .0001) 732, 732, 74
74  IEDGE=IEDGE+1
  IQ=IQ+1
  DY=DYW*XXK**(IEDGE-2)
  Y(IEDGE) = Y(IEDGE-1) + DY
732 IQ = IQ - 1
  ASSESMENT OF GRID PONITS IN ETA
C
C
C*****
C  THIS SUBROUTINE COMPUTES WALL STRESS AND HEAT TRANSFER RATES
C
  CALL CFSTNO (TR,XNUE,X,S,XBE,M,BLDT,BLMT,BLT,PBG1,JPBG1,REYEXT,
1 XME,MP,ROCN,ITRAN,ZCON)
C
C*****
C
C  SHIFT PROFILES BACK ONE XI STATION
C
  NN = IQ + 5
  DO 118 N=1,NN
  FN(N)=FO(N)
  FO(N)=FP(N)
  TN(N)=TO(N)
  TO(N)=TP(N)
  VN(N)=VO(N)
  VO(N)=VP(N)
  ETN(N)=ETO(N)
  ETO(N)=ETP(N)
  FN(N)=EO(N)
  EO(N)=EP(N)
  T2JN(N)=T2JO(N)
  T2JO(N)=T2JP(N)
118 CONTINUE
  DX1=DX2
  DS1=DS2
  IF(M+1-ICHS(IG)) 114,113,114
113 DS2=2.0*DS1
  IG = IG+1
  INDCH = 1
  IF (M.EQ.IEND1) GO TO 237
  GO TO 111
114 DS2=DS1
  INDCH = 0

```

```

      IF (M.EQ.IEND1) GO TO 237
      GO TO 111
237 IIN = 1
C*****
C
C      THIS SUBROUTINE ALONG WITH SUBROUTINE CFSTNO IS USED TO OUTPUT
C      ALL DATA
C
111 CALL PRNCHS      (ICOUN,IP,IG,IQ,MSTART,IIN,M,S,Y,RLT)
C
C*****
115 CONTINUE
      END
C
C
C
C
C
C ///////////////////////////////////////////////////////////////////
C
      SUBROUTINE PRESSM(S,X4,G,P,DPOX,T,Y4,IPRES,P122)
C
C ///////////////////////////////////////////////////////////////////
      COMMON/CONST/ R(30),Z(30),XP(30),A(30),B(30),C(30),D(30),E(30),
1F(30),CP(30),DP(30),INUM
100  FORMAT( 5X,*WARNING....CALCULATION IS OUTSIDE OF THE PRESCRIBED PR
      ESSURE DATA, S IS LESS THAN XP(1)*)
200  FORMAT( 5X,*WARNING....CALCULATION IS OUTSIDE OF THE PRESCRIBED PR
      ESSURE DATA, S IS GREATER THAN XP(END)*)
300  FORMAT(1X,5E15.9)
      IR=0
      IPM1=INUM-1
      IF(IPRES.EQ.0) GO TO 40
      DO 20 I=1,INUM
      IF(S.LT.XP(1)) WRITE(5,100)
      IF(S.GT.XP(INUM)) WRITE(5,200)
      IF(S.LE.XP(1)) IR=1
      IF(IR.NE.0) GO TO 30
      IF(S.GE.XP(IPM1)) IR=INUM
      IF(IR.NE.0) GO TO 30
      IF((S.GE.XP(I)).AND.(S.LT.XP(I+1))) IR=I
      IF(IR.EQ.0) GO TO 20
C      SEEKING THE BEST FIT
      RS=(S-XP(I))/(XP(I+1)-XP(I))
      IF(RS.GT.0.5) IP=I+1
C      SEEKING THE BEST FIT
      IF(IR.NE.0) GO TO 30
20  CONTINUE
30  IF(IR.GT.IPM1) IR=IPM1
      IRP=IR+1
      IRM=IR-1
      IF(IR.EQ.1) IPM=IR+2
C      COMPUTE THE CUBIC SPLINE COEFFICIENTS
      X1=(XP(IRP)+XP(IRM)-2.0*XP(IR))*(XP(IRP)-XP(IRM))

```



```

      X2=(XP(IRM)-XP(IR))*(XP(IRM)-XP(IR))
      X3=(XP(IRP)-XP(IR))*(XP(IRP)-XP(IR))
      X4=XP(IPM)-XP(IR)
      X5=XP(IPM)-XP(IR)
      X6=XP(IRP)-XP(IR)
      DETS=X5*X6*X4
      C2=(DP(IR)*X1+DP(IRP)*X2-DP(IRM)*X3)/DETS
      C3=(DP(IR)*X4-DP(IRP)*X5+DP(IRM)*X6)/DETS
C     COMPUTE THE CUBIC SPLINE COEFFICIENTS
      DXP=S-XP(IR)
      DXP2=DXP**2
      DXPF=DXP/20.
      DPOX1=DP(IR)
      P=CP(IR)
      DO 10 I=1,20
      X=I*DXPF
      X2=X*X
      DPOX2=DP(IR)+C2*X+C3*X2
      P=P+0.5*(DPOX1+DPOX2)*DXPF
10    DPOX1=DPOX2
      DPOX=DP(IR)+C2*DXP+C3*DXP2
      T=(P*P1P2)**((G-1.0)/G)
      YM=SQRT(2.0*((2.0+(G-1.0)*XM*XM)/(2.0*T)-1.0)/(G-1.0))
      WRITE(6,300) S,P,DPOX,T,YM
      GO TO 50
40    P=1.0
      DPOX=0.
      T=(P*P1P2)**((G-1.0)/G)
      YM=SQRT(2.0*((2.0+(G-1.0)*XM*XM)/(2.0*T)-1.0)/(G-1.0))
50    RETURN
      END
C ///////////////////////////////////////////////////////////////////
C
      SUBROUTINE SMTHPR(BTRX,DPMAX,G,XMSQ)
C
C ///////////////////////////////////////////////////////////////////
      COMMON/CONST/ R(30),Z(30),XP(30),A(30),B(30),C(30),J(30),E(30),
1F(30),CP(30),DP(30),INUM
100  FORMAT(1X,*FIRST CP DATA POINT YIELDS ADVERSE PRESSURE GRADIENT TO
10  STEEP FOR CALCULATION TO CONTINUE*)
200  FORMAT(1H0,11X,3HS/L,15X,2HCP,11X,6HP/PINF,14X,4HDPDX)
300  FORMAT(1X,4(4X,E15.9))
      DPTOL=DPMAX*1.01
C     COMPUTE THE TRAILING EDGE DPOX
      IPM1=INUM-1
      IPM2=INUM-2
      DX1=XP(IPM1)-XP(INUM)
      DX2=XP(IPM2)-XP(INUM)
      DX12=DX1*DX1
      DX22=DX2*DX2
      DP(INUM)=(CP(IPM2)*DX12-CP(IPM1)*DX22-CP(INUM)*(DX12-DX22))/
1  (DX1*DX2*(DX1-DX2))
C     COMPUTE THE TRAILING EDGE DPOX
10    IMAX=0

```



```

C      COMPUTE THE LEADING EDGE DPOX
      DX1=XP(2)-XP(1)
      DX2=XP(3)-XP(1)
      DX12=DX1*DX1
      DX22=DX2*DX2
      DP(1)=(CP(3)*DX12-CP(2)*DX22-CP(1)*(DX12-DX22))/(DX1*DX2*(DX1-
1 DX2))
      IF(DP(1).GT.DPMAX) WRITE(6,100)
      IF(DP(1).GT.DPMAX) CALL EXIT
C      COMPUTE THE LEADING EDGE DPOX
      DO 20 I=2,IPM1
      IM1=I-1
      IP1=I+1
      DX1=XP(IM1)-XP(I)
      DX2=XP(IP1)-XP(I)
      DX12=DX1*DX1
      DX22=DX2*DX2
      DP(I)=(CP(IP1)*DX12-CP(IM1)*DX22-CP(I)*(DX12-DX22))/(DX1*DX2*
1 (DX1-DX2))
20      IF((DP(I).GT.DPTOL).AND.(XP(I).LE.BTRX)) IMAX=I
      IF(IMAX.EQ.0) GO TO 50
C      SMOOTHING THE CP DATA IN THE LEADING EDGE REGION
      IMM1=IMAX-1
      IMP1=IMAX+1
      DX1=XP(IMM1)-XP(IMAX)
      DX2=XP(IMP1)-XP(IMAX)
      DX12=DX1*DX1
      DX22=DX2*DX2
      CP(IMM1)=(CP(IMP1)*DX12-CP(IMAX)*(DX12-DX22)-DX1*DX2*(DX1-DX2)
1 *DPMAX)/DX22
      GO TO 10
C      SMOOTHING THE CP DATA IN THE LEADING EDGE REGION
50      WRITE(6,200)
      DO 30 I=1,INUM
      PC=2.0*(CP(I)-1.0)/(G*XMSQ)
30      WRITE(6,300) XP(I),PC,CP(I),DP(I)
      RETURN
      END
C //////////////////////////////////////
C
      SUBROUTINE CFSTNO (TR,XNUE,X,S,XBE,1,9LDT,BLMT,BLT,PBG1,DPBG1,
1 REYEXT,XME,MP,RCON,ITRAN,ZCON)
C
C //////////////////////////////////////
      COMMON C, PR, REY, XMINF, OMEGA, BD, TW, P10, T10, R10, VIS10, TE,
1 PE,RE,UE,VISINF,SU,EPS,DS,OYW,SI,ERROR,TC,TA,TEGE,IEND1,INTACT,
2 PRT,XYK,STRX,XLAM,VARPRT,XINTER,SEPO,ICHS(8),IPRN(9),EO(200),
3 EN(200),EP(200),ETO(200),ETN(200),ETP(200),FO(200),FN(200),J2DA,
4 FP(200),TN(200),TO(200),XNN(200),VN(200),VO(200),VP(200),TP(200),
5 O1(200),O2(200),O3(200),T2JP(200),T2JO(200),T2JN(200)
2999 FORMAT(1H0,10X,5HS/L =,E15.8,10X,6H Z/L =,E15.8,10X,5HR/L =,E15.8)
2000 FORMAT(1H0,10X,5HS/L =,E15.8)
2001 FORMAT(2X,7HXME =,E15.8,2X,7HPE =,E15.8,2X,7HDPINF=,E15.8,
1 2X,7HXB =,E15.8,2X,7HTW/TE =,E15.8)

```

```

2002 FORMAT(2X,7HBLT   =,E15.8,2X,7HBLMT  =,E15.8,2X,7HBLDT  =,E15.8,
1 2X,7HREYMT =,E15.8,2X,7HREYDT =,E15.8)
2003 FORMAT(2X,7HCFNO  =,E15.8,2X,7HCFEND =,E15.8,2X,7HSTNO  =,E15.8,
1 2X,7HSTENO  =,E15.8,2X,7HREYEXT=,E15.8)
  TWTE=TP(1)
  IF(OMEGA.EQ.0.) GO TO 855
  IF(OMEGA .EQ. 1.) GO TO 8551
  XLM1 = 1./(TWTE**(1. - OMEGA))
  GO TO 855
855 XLM1 = (1.0+TR)*SQRT(TWTE)/(TWTE+TR)
  GO TO 855
8551 XLM1 = 1.
856 CONTINUE
  Y11=((2.+XXK)*(1.+XXK+XXK**2)+1.+XXK)/((1.+XXK)*(1.+XXK+XXK**2))
  Y12=(1.+XXK+XXK**2)/XXK**2
  Y13=(1.+XXK+XXK**2)/(XXK**3*(1.+XXK))
  Y14=1./(XXK**3*(1.+XXK+XXK**2))
  TAU=XLM1*RE*XNUE*UE*UE*(-Y11*FP(1)+Y12*FP(2)-Y13*FP(3)+Y14*FP(4))
1 / (DYW*SQRT(2.*X))
  QS = XLM1*RE*XNUE*UE*TE*(Y11*TP(1)-Y12*TP(2)+Y13*TP(3)-Y14*TP(4))
1 / (DYW*SQRT(2.*X)*PR)
  IF(J2DA.NE.0) TAU=TAU*RCON
  IF(J2DA.NE.0) QS=QS*RCON
  STNO = 0.
  IF(BO .NE. 1.) STNO = EPS*QS/((1. - BO)*(TE + .5*UE**2))
  STENO = STNO/(RE*UE)
  CFNO = 2.*EPS*TAU
  CFENO = CFNO/(RE*UE*UE)
  REYDT=REYEXT*BLDT
  REYMT=REYEXT*BLMT
C
C  SELECTION OF THE OUTPJT
C  IF(M.NE.MD) GO TO 1000
C  SELECTION OF THE OUTPJT
C
C  OUTPUT STATION DATA
C
  IF(J2DA.EQ.1) GO TO 457
  WRITE(6,2000) S
457 CONTINUE
  IF(J2DA.EQ.0) GO TO 456
  WRITE(6,2999) S,ZCON,RCON
456 CONTINUE
  WRITE(6,2001) XME,PBG1,DPBG1,XRE,TWTE
  WRITE(6,2002) BLT,BLMT,BLDT,REYMT,REYDT
  WRITE(6,2003) CFNO,CFENO,STNO,STENO,REYEXT
1000 RETURN
  END
C ///////////////////////////////////////////////////////////////////
C
  SUBROUTINE ELMATX( M,DX2,X,XAL,XBE,TR,IDIFF,Y1,Y2,Y3,Y4,Y5,TWTE,
1  ITCNT1,ITRAN,A1,A2,A3,I1,B2,B3,C1,C2,C3)
C
C ///////////////////////////////////////////////////////////////////

```

```

COMMON C, PR, REY, XMINF, OMEGA, BO, TW, P10, T10, R10, VIS10, TE,
1 PE,RE,UE,VISINF,SU,EPS,DS,DYW,SI,ERROR,TC,TA,IEDGE,IEND1,INFACT,
2 PRT,XXK,BTRX,XLAM,VARPRT,XINTER,SEPO,ICHS(8),IPRN(3),EO(200),
3 FN(200),EP(200),ETO(200),ETN(200),ETP(200),FO(200),FN(200),J2DA,
4 EP(200),TH(200),TO(200),XNN(200),VY(200),VO(200),VP(200),TP(200),
501(200),O2(200),O3(200),T2JP(200),T2JJ(200),T2JN(200)
DIMENSION A1(200,3),A2(200,3),A3(200,3),B1(200,3),B2(200,3),
1 B3(200,3),C1(200,3),C2(200,3),C3(200,3)

```

```

C
C THE INNER EDGE BOUNDARY CONDITION
C

```

```

DO 8011 I=1,3
8011 A1(1,I)=A2(1,I)=A3(1,I)=B1(1,I)=B2(1,I)=B3(1,I)=C1(1,I)=C3(1,I)
1 =C3(1,I)=0.
A1(1,1)=1.0
B2(1,1)=1.0
D1(1)=0.
D2(1)=TWTF
IF(SEPO.EQ.0.) GO TO 8012
C3(1,1)=1.0
D3(1)=0.
GO TO 8013
8012 XL=DX2/(2.0*DYW)
A3(1,1)=DX2+X*Y1
C3(1,1)=-2.*XL*(2.+XXK)/(1.+XXK)
C3(1,2)=2.*XL*(1.+XXK)/XXK
C3(1,3)=-2.*XL/(XXK*(1.+XXK))
D3(1)=0.

```

```

C
C THE INNER EDGE BOUNDARY CONDITION
C

```

```

C THE FIELD POINTS EVALUATION
C

```

```

8013 NM1=IEDGE-1
DO 8014 N=2,NM1
DY=XXK*(N-1)*DYW
DYM1=DY/XXK
XL=DX2/(2.0*DY)
Y6=2./(1.+DYM1/DY)
Y7=DY/DYM1
Y8=2./((DYM1/DY)*(1.+DYM1/DY))
Y9=2./(1.+DY/DYM1)
Y10=1.-DY/DYM1
SEP=1.0
IF(FO(N).LE.0.) SEP=0.
IF(ITCNT1 .GT. 1) GO TO 7000
IF(INIF= .EQ. 1) GO TO 7501
FM1=Y4*FO(N)-Y5*FN(N)
TM1=Y4*TO(N)-Y5*TN(N)
VM1=Y4*VO(N)-Y5*VN(N)
IF(SEPO.EQ.0.) VM1=VO(N)
EM1 =(Y4*(EO(N-1)+EO(N)+EO(N+1))-Y5*(EN(N-1)+EN(N)+EN(N+1)))/3.
ETM1 =(Y4*(ETO(N-1)+ETO(N)+ETO(N+1))-Y5*(ETN(N-1)+ETN(N)+ETN(N+1)
1 ))/3.

```



```

T2J=Y4*T2JO(N)-Y5*T2JN(N)
GO TO 7001
7501 FM1 = F0(N)
TM1 = T0(N)
VM1 = V0(N)
EM1=(E0(N-1)+E0(N)+E0(N+1))/3.
ETM1=(ET0(N-1)+ET0(N)+ET0(N+1))/3.
T2J=T2JO(N)
GO TO 7001
7000 FM1 = FP(N)
TM1 = TP(N)
VM1 = VP(N)
EM1=(EP(N-1)+EP(N)+EP(N+1))/3.
ETM1=(ETP(N-1)+ETP(N)+ETP(N+1))/3.
T2J=T2JP(N)
7001 IF(OMEGA.EQ. 0.) GO TO 684
IF(OMEGA.EQ. 1.) GO TO 6841
XLM1=1./(TM1** (1.-OMEGA))
XLPM1=(OMEGA-1.)*XLM1/TM1
GOTO625
6841 XLM1=1.
XLPM1=0.
GOTO625
684 XLM1=((1.+TR)*SQRT(TM1)/(TM1+TR))
XLPM1=XLM1*(TR-TM1)/(2.*TM1*(TM1+TR))
625 IF(ITCNT1.GT.1) GO TO 626
FY=(Y9*F0(N+1)/2.-Y10*F0(N)-Y8*F0(N-1)/2.)/DY
TY=(Y9*T0(N+1)/2.-Y10*T0(N)-Y8*T0(N-1)/2.)/DY
EYM1=(Y9*E0(N+1)/2.-Y10*EM1-Y8*E0(N-1)/2.)/DY
ETYM1=(Y9*ET0(N+1)/2.-Y10*ETM1-Y8*ET0(N-1)/2.)/DY
DT2J=(Y9*T2JO(N+1)/2.-Y10*T2JO(N)-Y8*T2JO(N-1)/2.)/DY
GO TO 627
626 FY=(Y9*FP(N+1)/2.-Y10*FP(N)-Y8*FP(N-1)/2.)/DY
TY=(Y9*TP(N+1)/2.-Y10*TP(N)-Y8*TP(N-1)/2.)/DY
EYM1=(Y9*EP(N+1)/2.-Y10*EM1-Y8*EP(N-1)/2.)/DY
ETYM1=(Y9*ETP(N+1)/2.-Y10*ETM1-Y8*ETP(N-1)/2.)/DY
DT2J=(Y9*T2JP(N+1)/2.-Y10*T2JP(N)-Y8*T2JP(N-1)/2.)/DY
627 IF(IDIFF.EQ.1) GO TO 7502
FM2=Y2*F0(N)-Y3*FN(N)
TM2=Y2*T0(N)-Y3*TN(N)
GO TO 7505
7502 FM2 =2.*F0(N)
TM2 =2.*T0(N)
7505 CONTINUE
IF(ITRAN.EQ.0) T2J=1.0
IF(ITRAN.EQ.0) DT2J=0.
A1(N,1)=Y3*XL*(2.*XLM1*EM1*T2J/DY-XLM1*EM1*DT2J-XLM1*T2J
1*EYM1+VM1-EM1*T2J*XLPM1*TY)
A1(N,2)=-4.*Y7*XL*XLM1*EM1*T2J/DY-2.*Y10*XL*(XLM1*EM1*
10T2J+XLM1*T2J*EYM1-VM1+EM1*T2J*XLPM1*TY)-2.*DX2*X8E*
2FM1*SEP-X*(2.*Y1*FM1-FM2)*SEP
A1(N,3)=XL*(2.*Y6*XLM1*EM1*T2J/DY+Y9*(XLM1*EM1*DT2J+XLM1
1*T2J*EYM1-VM1+EM1*T2J*XLPM1*TY))
B1(N,1)=-Y9*XL*EM1*T2J*XLPM1*FY

```



```

B1(N,2)=-2.*Y10*XL*EM1*T2J*XLPM1*FY+DX2*X9E
B1(N,3)=Y9*XL*EM1*T2J*XLPM1*FY
C1(N,1)=C1(N,3)=0.
C1(N,2)=-DX2*FY
A2(N,1)=-2.*Y8*FY*XL*XLPM1*EM1*T2J*XAL
A2(N,2)=-4.*Y10*FY*XL*XLPM1*EM1*T2J*XAL-X*(Y1*TM1-TM2)*SEP
A2(N,3)=2.*Y9*FY*XL*XLPM1*EM1*T2J*XAL
B2(N,1)=(XL*Y8/PR)*(2.*XLM1*ETM1*T2J/DY-XLM1*ETM1*DT2J-
1XLM1*ETM1*T2J+PR*VM1-2.*TY*XLPM1*ETM1*T2J)
B2(N,2)=-4.*Y7*XL*XLPM1*ETM1*T2J/(DY*PR)-2.*Y10*(XL/PR)*
1(XLM1*ETM1*DT2J+XLM1*ETM1*T2J-PR*VM1+2.*XLPM1*ETM1*
2T2J*TY)-X*Y1*EM1*SEP
B2(N,3)=(XL/PR)*(2.*Y5*XLM1*ETM1*T2J/DY+Y9*(XLPM1*ETM1*
1DT2J+XLM1*ETM1*T2J-PR*VM1+2.*TY*XLPM1*ETM1*T2J))
C2(N,2)=-DX2*TY
C2(N,1)=C2(N,3)=0.
A3(N,1)=A3(N,3)=0.
A3(N,2)=DX2*X*Y1
B3(N,1)=B3(N,2)=B3(N,3)=0.
C3(N,1)=-XL*Y9
C3(N,2)=-2.*XL*Y10
C3(N,3)=XL*Y9
D1(N)=DX2*FY*(EM1*T2J*XLPM1*TY-VM1)-FM1**2*(DX2*X9E+X*
1Y1)*SEP
D2(N)=DX2*TY*(XLPM1*ETM1*T2J*TY/PR-VM1)+DX2*XLPM1*EM1*T2J
1*XAL*FY**2-X*Y1*TM1*FM1*SEP
D3(N)=X*FM2

```

8014 CONTINUE

C  
C  
C  
C  
C  
C

THE FIELD POINTS EVALUATION

THE OUTER EDGE BOUNDARY CONDITION

```

DO 8015 I=1,3
8015 A1(IEDGE,I)=A2(IEDGE,I)=A3(IEDGE,I)=B1(IEDGE,I)=B2(IEDGE,I)=B3(
1 IEDGE,I)=C1(IEDGE,I)=C2(IEDGE,I)=C3(IEDGE,I)=0.
A1(IEDGE,3)=1.0
B2(IEDGE,3)=1.0
D1(IEDGE)=1.0
D2(IEDGE)=1.0
IF(SEPO.EQ.0.) GO TO 8016
XL=DX2/(2.*DYW*XXK*(IEDGE-1))
FM2=Y2*F0(IEDGE)-Y3*FN(IEDGE)
IF(IDIFF.EQ.1) FM2=2.*F0(IEDGE)
A3(IEDGE,3)=DX2*X*Y1
C3(IEDGE,1)=2.*XXK**3*XL/(1.+XXK)
C3(IEDGE,2)=-2.*XXK*(1.+XXK)*XL
C3(IEDGE,3)=2.*XXK*XL*(2.*XXK+1.)/(1.+XXK)
D3(IEDGE)=X*FM2
GO TO 8017
8016 VM1=V0(IEDGE)
IF(ITCNT1.GT.1) VM1=VP(IEDGE)
C3(IEDGE,3)=1.0

```

```

      D3(IEDGE)=VM1
8017 CONTINUE
C
C   THE OUTER EDGE BOUNDARY CONDITION
      RETURN
      END
C ///////////////////////////////////////////////////////////////////
C
      SUBROUTINE PRNCHS(ICOUN,IP,IG,IQ,MSTART,IIN,M,S,Y,BLT)
C
C ///////////////////////////////////////////////////////////////////
      COMMON S, PR, REY, XMINF, OMEGA, R0, TW, P10, T10, R10, VIS10, TE,
1  PE,RE,UE,VISINF,SU,EPS,OS,DYW,SI,ERROR,TC,TA,IEDGE,IEND1,INTACT,
2  PRT,XXX,BTRX,XLAM,VAPPT,XINTER,SEPO,ICHS(8),IPRN(3),EO(200),
3  EN(200),EP(200),ETO(200),ETN(200),ETP(200),FO(200),FN(200),J2DA,
4  FP(200),TN(200),TO(200),XNN(200),VN(200),VO(200),VP(200),TP(200),
5  D1(200),D2(200),D3(200),T2JP(200),T2JJ(200),T2JN(200)
      DIMENSION      Y(200),Z(7,16)
25  FORMAT (1H0,45X,23HPROFILE FOR STATION S=F14.8)
40  FORMAT (8H QN=      15F8.4 )
41  FORMAT (8H ETA=     15F8.4 )
42  FORMAT (8H F1=      15F8.4 )
43  FORMAT (8H T1=      15F8.4 )
44  FORMAT (8H V1=      15F8.2 )
45  FORMAT (8H E0=      15F8.2 )
507 FORMAT (8H Y/RLT=   15F8.4 )
509 FORMAT (8H R0/ROE=  15F8.4 )
510 FORMAT (8H MACH=    15F8.4 )
511 FORMAT (8H PT/POP=  15F8.4 )
512 FORMAT (8H PT/PE=   15F8.4 )
513 FORMAT (8H H/HE=    15F8.4 )
      IF(ICOUN-IPRN(IP)) 51,38,51
C
C   OUTPUT PROFILE DATA
C
38  KONT=IO-1
      J2=0
      WRITE(6,25) S
      D050J1=1,KONT,15
      J2=J2+1
      KON=J2*15
      WRITE (6,40) (XNN(N),N=J1,KON)
      WRITE (6,41) (Y(N),N=J1,KON)
      WRITE (6,42) (FO(N), N=J1,KON)
      WRITE (6,43) (TO(N), N=J1,KON)
      WRITE (6,44) (VO(N), N=J1,KON)
      WRITE(6,46) (EO(N),N=J1,KON)
      I=J1-1
      IF(M.EQ.MSTART) GO TO 50
      D0530JX=1,15
      I=I+1
      Z(1,JX)=XNN(I)/RLT
      Z(2,JX)=FO(I)
C   Z(3,JX)=TO(I)

```

```

      Z(3,JX)=1./T0(I)
      PTPED=(G-1.0)*TE*T0(I)
      IF (PTPED) 777,777,778
777 PTPED=1.
778 Z(4,JX)=UE*Z(2,JX)/(PTPED)**.5
      PTPD=Z(4,JX)*Z(4,JX)
      IF(Z(4,JX)-1.0)504,504,505
504 PTPD=(1.0+(((G-1.0)/2.0)*PTPD))**((G/(G-1.0)))
      GOT0506
505 PTPD=(((G+1.0)*PTPD/2.0)**(G/(G-1.0)))*(((G+1.0)/((2.0*G*PTPD)-(G-
11.0))))*(1.0/(G-1.0)))
506 Z(5,JX)=PTPD
      Z(6,JX) = PTPD*PE/P10
      Z(7,JX)=(TE*T0(I)/(UE*UE)+.5*F0(I)*F0(I))/(TE/(UE*UE)+.5)
530 CONTINUE
      WRITE(6,507) (Z(1,N),N=1,15)
      WRITE(6,509) (Z(3,N),N=1,15)
      WRITE(6,510) (Z(4,N),N=1,15)
      WRITE(6,511) (Z(6,N),N=1,15)
      WRITE(6,512) (Z(5,N),N=1,15)
      WRITE(6,513) (Z(7,N),N=1,15)
50 CONTINUE
      IF(IIN.EQ. 1) RETURN
      ICOUN=0
51 ICOUN=ICOUN+1
      IF(M+1-ICHS(IG)) 3601,3600,3601
3600 IP=IP+1
      ICOUN=IPRN(IP)
3601 CONTINUE
      RETURN
      END
C////////////////////////////////////////////////////////////////////////////////////////////////////////////////////////////////
C
      SUBROUTINE REYSTR(KON,TR,X,TREF,XNUE,XBE,S,ITCNT1,
1RCON,ALPHA,ITRAN)
C
C////////////////////////////////////////////////////////////////////////////////////////////////////////////////////////////////
      COMMON S, PR, REY, XMINF, OMEGA, BO, TW, P10, T10, R10, VIS10, TE,
1 PE,RE,JE,VISINF,SU,EPS,DS,DYW,SI,ERROR,TC,TA,IEDGE,IEND1,INTACT,
2 PRT,XXK,BTRX,XLAM,VARPRT,XINTER,SEPO,ICHS(8),IPRN(3),EO(200),
3 EN(200),EP(200),ETO(200),ETN(200),ETP(200),FD(200),FN(200),J2DA,
4 FP(200),TV(200),TO(200),XNN(200),VN(200),VO(200),VP(200),TP(200),
5 O1(200),O2(200),O3(200),T2JP(200),T2JO(200),T2JN(200)
      TTR=(TA+112.)/(TA*TREF+112.)
      CO=TP(1)
      DO=EP(1)=XNN(1)=TPI=RLT=0.
C
      SHEAR STRESS AT THE WALL AS THE SCALING FUNCTION
      Y11=((2.+XXK)*(1.+XXK+XXK**2)+1.+XXK)/((1.+XXK)*(1.+XXK+XXK**2))
      Y12=(1.+XXK+XXK**2)/XXK**2
      Y13=(1.+XXK+XXK**2)/(XXK**3*(1.+XXK))
      Y14=1./(XXK**3*(1.+XXK+XXK**2))
      FETW=(-Y11*FP(1)+Y12*FP(2)-Y13*FP(3)+Y14*FP(4))/DYW
      FETW=ABS(FETW)
      XLM1W=((1.+TR)*SQRT(TP(1)))/(TP(1)+TR))

```



```

C      PI2=XLM1W*FETW
C      SHEAR STRESS AT THE WALL AS THE SCALING FUNCTION
DO 1 N=2,KON
  DY=DYW*XXK**(N-2)
  XLM1=((1.+TR)*SQRT(TP(N))/(TP(N)+TR))
  C=TP(N)
  TPI=TP[+.5*DY*(C0+C)
  C0=C
  XNN(N)=EPS*TPI*SQRT(2.*X)/(RE*UE)
  IF(J2DA.NE.0) XNN(N)=XNN(N)/RCON
  IF(ITRAN.NE.0) XNN(N)=(PCON/COS(ALPHA))*(-1.+SQRT(1.+
12.*SQRT(2.*X)*EPS*COS(ALPHA)*TPI/(RE*UE*RCON**2)))
  IF(BLT.GT.0.) GO TO 2
  IF(FP(N).GE.0.995) BLT=XNN(N)-(FP(N)-.995)*(XNN(N)-XNN(N-1))
1 / (FP(N)-FP(N-1))
  IF(ITRAN.EQ.1) GO TO 12
  DD=DD+((1.-FP(N))*TP(N)+(1.-FP(N-1))*TP(N-1))*DY/2.
12 CONTINUE
  IF(ITRAN.NE.0) DD=DD+((1.-FP(N))*TP(N)/SQRT(T2JP(N))+(1.-FP(N-
11))*TP(N-1)/SQRT(T2JP(N-1)))*DY/2.
2  PI1=SQRT(2.*X*REY/(TREF**1.5*TTR))*TPI**2/(XNUE*TP(N)**3)
  IF(J2DA.NE.0) PI1=PI1/RCON
  IF(ITRAN.NE.0) PI1=((RE*UE)**2)*(XNN(N)**2)*PCON*SQRT(T2JP(N))
1 *(REY**1.5)/((TP(N)**3)*SQRT(2.*X)*(TREF**2.25)*(TTR
2 **1.5)*XNUE)
  DY=DYW*XXK**(N-1)
  DYM1=DY/XXK
  Y9=2./((DYM1/DY)*(1.+DYM1/DY))
  Y9=2./(1.+DY/DYM1)
  Y10=1.-DY/DYM1
C      PI2=XLM1*EP(N)*ABS(Y9*FP(N+1)/2.-Y10*FP(N)-Y8*FP(N-1)/2.)/DY
C
C      CEBICE-SMITH-MONSINKIS EDDY VISCOSITY MODEL
C      YPLUS=SQRT(PI1*PI2)/(25.*XLM1)
  IF(YPLUS.GT.50.) YPLUS=50.
  EP(N)=.15*PI1*(1.-EXP(-YPLUS))**2*ABS(Y9*
1 EP(N+1)/2.-Y10*FP(N)-Y8*FP(N-1)/2.)/(DY*XLM1)
C      CEBICE-SMITH-MONSINKIS EDDY VISCOSITY MODEL
C
C      TRUNCATE THE INNER REGION CALCULATION
  IF(EP(N).LE.EP(N-1)) EP(N)=EP(N-1)
C      TRUNCATE THE INNER REGION CALCULATION
C
1  CONTINUE
DO 3 N=1,KON
  XLM1=((1.+TR)*SQRT(TP(N))/(TP(N)+TR))
  DD1=.0158*SQRT(2.*X*REY/(TREF**1.5*TTR))*DD/(XNUE*XLM1*TP(N)**2)
  IF(J2DA.NE.0) DD1=DD1/RCON
  IF(DD1.LE.EP(N)) EP(N)=DD1
  ARGE=-.412*((S-3TRX)/XLAM)**2
  IF(ARGE.LT.-575.83) GO TO 9
  EP(N)=EP(N)*(1.-EXP(ARGE))
9 CONTINUE
  IF(XINTER.EQ.0.) EP(N)=1.+EP(N)

```



```

      IF(XINTER.EQ.1.) EP(N)=1.+ (1.75/(1.+5.5*(XNN(N)/BLT)**6)+1.)*
1  EP(N) /2.75
3  ETP(N)=1.+PR*(EP(N)-1.)/PRT
C
      RETURN
      END
C
C ///////////////////////////////////////////////////////////////////
C
      SUBROUTINE MATEON3 (X1,X2,X3,Y1,Y2,Y3,A11,A12,A13,A21,A22,A23,
$  A31,A32,A33,LC,LN,LQ)
C
C ///////////////////////////////////////////////////////////////////
C
      THIS SUBROUTINE SOLVES THE THREE SIMULTANEOUS BAND MATRIX
      EQUATIONS
C
      A11*X1 + A12*X2 + A13*X3 = Y1
      A21*X1 + A22*X2 + A23*X3 = Y2
      A31*X1 + A32*X2 + A33*X3 = Y3
C
      FOR X1, X2, AND X3
C
      AIJ ARE 9 BAND MATRICES OF LENGTH LQ, WORKING LENGTH LN,
      AND WIDTH LC
      (THESE MATRICES ARE ASSUMED TO BE CORNER ADJUSTED, I.E. THE
      CORNER ELEMENTS ARE STORED IN (1,1) AND (LN,LC), ETC.)
C
      XI AND YI ARE VECTORS OF LENGTH LQ AND WORKING LENGTH LN
C
      DIMENSION
$  X1(LQ),X2(LQ),X3(LQ),Y1(LQ),Y2(LQ),Y3(LQ),
$  A11(LQ,LC),A12(LQ,LC),A13(LQ,LC),
$  A21(LQ,LC),A22(LQ,LC),A23(LQ,LC),
$  A31(LQ,LC),A32(LQ,LC),A33(LQ,LC)
C
      INITIALIZATION
      -----
C
      LP=LN+1
      L=(LC-1)/2
      LM=LN-L-1
      IF(LC.GE.LN) L=LN
      DO 3 I=1,LN
      X1(I)=Y1(I)
      X2(I)=Y2(I)
      X3(I)=Y3(I)
3  CONTINUE
C
      DOWNWARD GAUSSIAN ELIMINATION WITH PIVOTING
      -----
C
      DO 401 K=1,LN
      IF(L.EQ.LM) L=LN

```

```

      IF(L.LT.LN) L=L+1
C
      U=ABS(A11(K,1))
      I=K
      M=1
      DO 113 J=K,L
      IF(J.EQ.K) GO TO 111
      V=ABS(A11(J,1))
      IF(V.LE.U) GO TO 111
      U=V
      M=1
      I=J
111  V=ABS(A21(J,1))
      IF(V.LE.U) GO TO 112
      U=V
      M=2
      I=J
112  V=ABS(A31(J,1))
      IF(V.LE.U) GO TO 113
      U=V
      M=3
      I=J
113  CONTINUE
      IF(I.EQ.K) GO TO 115
      IF(M.NE.1) GO TO 116
      DO 114 J=1,LC
      U=A11(K,J)
      A11(K,J)=A11(I,J)
      A11(I,J)=U
      U=A12(K,J)
      A12(K,J)=A12(I,J)
      A12(I,J)=U
      U=A13(K,J)
      A13(K,J)=A13(I,J)
      A13(I,J)=U
114  CONTINUE
      U=X1(K)
      X1(K)=X1(I)
      X1(I)=U
      GO TO 120
115  IF(M.EQ.1) GO TO 120
116  IF(M.NE.2) GO TO 118
      DO 117 J=1,LC
      U=A11(K,J)
      A11(K,J)=A21(I,J)
      A21(I,J)=U
      U=A12(K,J)
      A12(K,J)=A22(I,J)
      A22(I,J)=U
      U=A13(K,J)
      A13(K,J)=A23(I,J)
      A23(I,J)=U
117  CONTINUE
      U=X1(K)

```

```

X1(K)=X2(I)
X2(I)=U
GO TO 120
118 DO 119 J=1,LC
    U=A11(K,J)
    A11(K,J)=A31(I,J)
    A31(I,J)=U
    U=A12(K,J)
    A12(K,J)=A32(I,J)
    A32(I,J)=U
    U=A13(K,J)
    A13(K,J)=A33(I,J)
    A33(I,J)=U
119 CONTINUE
    U=X1(K)
    X1(K)=X3(I)
    X3(I)=U
120 CONTINUE
C
    DO 128 I=K,L
    IF(I.EQ.K) GO TO 123
    U=A11(I,1)/A11(K,1)
    DO 122 J=1,LC
    IF(J.NE.1) A13(I,J-1)=A11(I,J)-A11(K,J)*U
    A11(I,J)=A12(I,J)-A12(K,J)*U
    A12(I,J)=A13(I,J)-A13(K,J)*U
122 CONTINUE
    A13(I,LC)=0.
    X1(I)=X1(I)-X1(K)*U
123 CONTINUE
    U=A21(I,1)/A11(K,1)
    DO 125 J=1,LC
    IF(J.NE.1) A23(I,J-1)=A21(I,J)-A11(K,J)*U
    A21(I,J)=A22(I,J)-A12(K,J)*U
    A22(I,J)=A23(I,J)-A13(K,J)*U
125 CONTINUE
    A23(I,LC)=0.
    X2(I)=X2(I)-X1(K)*U
    U=A31(I,1)/A11(K,1)
    DO 127 J=1,LC
    IF(J.NE.1) A33(I,J-1)=A31(I,J)-A11(K,J)*U
    A31(I,J)=A32(I,J)-A12(K,J)*U
    A32(I,J)=A33(I,J)-A13(K,J)*U
127 CONTINUE
    A33(I,LC)=0.
    X3(I)=X3(I)-X1(K)*U
128 CONTINUE
C
    U=ABS(A21(K,1))
    I=K
    M=2
    DO 213 J=K,L
    IF(J.EQ.K) GO TO 212
    V=ABS(A11(J,1))

```



```

      IF(V.LE.U) GO TO 211
      U=V
      M=1
      I=J
211  V=ABS(A21(J,1))
      IF(V.LE.U) GO TO 212
      U=V
      M=2
      I=J
212  V=ABS(A31(J,1))
      IF(V.LE.U) GO TO 213
      U=V
      M=3
      I=J
213  CONTINUE
      IF(I.EQ.K) GO TO 215
      IF(M.NE.2) GO TO 215
      DO 214 J=1,LC
      U=A21(K,J)
      A21(K,J)=A21(I,J)
      A21(I,J)=U
      U=A22(K,J)
      A22(K,J)=A22(I,J)
      A22(I,J)=U
      U=A23(K,J)
      A23(K,J)=A23(I,J)
      A23(I,J)=U
214  CONTINUE
      U=X2(K)
      X2(K)=X2(I)
      X2(I)=U
      GO TO 220
215  IF(M.NE.3) GO TO 220
216  IF(M.NE.1) GO TO 218
      DO 217 J=1,LC
      U=A21(K,J)
      A21(K,J)=A11(I,J)
      A11(I,J)=U
      U=A22(K,J)
      A22(K,J)=A12(I,J)
      A12(I,J)=U
      U=A23(K,J)
      A23(K,J)=A13(I,J)
      A13(I,J)=U
217  CONTINUE
      U=X2(K)
      X2(K)=X1(I)
      X1(I)=U
      GO TO 220
218  DO 219 J=1,LC
      U=A21(K,J)
      A21(K,J)=A31(I,J)
      A31(I,J)=U
      U=A22(K,J)

```

```

A22(K,J)=A32(I,J)
A32(I,J)=U
U=A23(K,J)
A23(K,J)=A33(I,J)
A33(I,J)=U
219 CONTINUE
U=X2(K)
X2(K)=X3(I)
X3(I)=U
220 CONTINUE
C
DO 228 I=K,L
IF(I.EQ.K) GO TO 223
U=A11(I,1)/A21(K,1)
DO 222 J=1,L
IF(J.NE.1) A13(I,J-1)=A11(I,J)-A21(K,J)*U
A11(I,J)=A12(I,J)-A22(K,J)*U
A12(I,J)=A13(I,J)-A23(K,J)*U
222 CONTINUE
A13(I,L)=0.
X1(I)=X1(I)-X2(K)*U
U=A21(I,1)/A21(K,1)
DO 225 J=1,L
IF(J.NE.1) A23(I,J-1)=A21(I,J)-A21(K,J)*U
A21(I,J)=A22(I,J)-A22(K,J)*U
A22(I,J)=A23(I,J)-A23(K,J)*U
225 CONTINUE
A23(I,L)=0.
X2(I)=X2(I)-X2(K)*U
223 CONTINUE
U=A31(I,1)/A21(K,1)
DO 227 J=1,L
IF(J.NE.1) A33(I,J-1)=A31(I,J)-A21(K,J)*U
A31(I,J)=A32(I,J)-A22(K,J)*U
A32(I,J)=A33(I,J)-A23(K,J)*U
227 CONTINUE
A33(I,L)=0.
X3(I)=X3(I)-X2(K)*U
226 CONTINUE
C
IF(K.EQ.LN) GO TO 401
U=ABS(A31(K,1))
I=K
M=3
JL=K+1
DO 313 J=JL,L
V=ABS(A11(J,1))
IF(V.LE.U) GO TO 311
U=V
M=1
I=J
311 V=ABS(A21(J,1))
IF(V.LE.U) GO TO 312
U=V

```

```

M=2
I=J
312 V=ARS(A31(J,1))
    IF(V.LE.U) GO TO 313
    U=V
    M=3
    I=J
313 CONTINUE
    IF(I.EQ.K) GO TO 320
    IF(M.NE.3) GO TO 316
    DO 314 J=1,LC
    U=A31(K,J)
    A31(K,J)=A31(I,J)
    A31(I,J)=U
    U=A32(K,J)
    A32(K,J)=A32(I,J)
    A32(I,J)=U
    U=A33(K,J)
    A33(K,J)=A33(I,J)
    A33(I,J)=U
314 CONTINUE
    U=X3(K)
    X3(K)=X3(I)
    X3(I)=U
    GO TO 320
316 IF(M.NE.1) GO TO 318
    DO 317 J=1,LC
    U=A31(K,J)
    A31(K,J)=A11(I,J)
    A11(I,J)=U
    U=A32(K,J)
    A32(K,J)=A12(I,J)
    A12(I,J)=U
    U=A33(K,J)
    A33(K,J)=A13(I,J)
    A13(I,J)=U
317 CONTINUE
    U=X3(K)
    X3(K)=X1(I)
    X1(I)=U
    GO TO 320
318 DO 319 J=1,LC
    U=A31(K,J)
    A31(K,J)=A21(I,J)
    A21(I,J)=U
    U=A32(K,J)
    A32(K,J)=A22(I,J)
    A22(I,J)=U
    U=A33(K,J)
    A33(K,J)=A23(I,J)
    A23(I,J)=U
319 CONTINUE
    U=X3(K)
    X3(K)=X2(I)

```



```

      X2(I)=U
320  CONTINUE
C
      IL=K+1
      DO 328 I=IL,L
      U=A11(I,1)/A31(K,1)
      DO 322 J=1,LC
      IF(J.NE.1) A13(I,J-1)=A11(I,J)-A31(K,J)*U
      A11(I,J)=A12(I,J)-A32(K,J)*U
      A12(I,J)=A13(I,J)-A33(K,J)*U
322  CONTINUE
      A13(I,LC)=0.
      X1(I)=X1(I)-X3(K)*U
      U=A21(I,1)/A31(K,1)
      DO 325 J=1,LC
      IF(J.NE.1) A23(I,J-1)=A21(I,J)-A31(K,J)*U
      A21(I,J)=A22(I,J)-A32(K,J)*U
      A22(I,J)=A23(I,J)-A33(K,J)*U
325  CONTINUE
      A23(I,LC)=0.
      X2(I)=X2(I)-X3(K)*U
      U=A31(I,1)/A31(K,1)
      DO 327 J=1,LC
      IF(J.NE.1) A33(I,J-1)=A31(I,J)-A31(K,J)*U
      A31(I,J)=A32(I,J)-A32(K,J)*U
      A32(I,J)=A33(I,J)-A33(K,J)*U
327  CONTINUE
      A33(I,LC)=0.
      X3(I)=X3(I)-X3(K)*U
328  CONTINUE
C
401  CONTINUE
C
C      UPWARD GAUSSIAN ELIMINATION
C      -----
C
      L=1
      DO 507 K=1,LN
      I=LP-K
C
      U=X3(I)
      IF(I.EQ.LN) GO TO 502
      DO 501 J=2,L
      IJ=I+J
501  U=U-A32(I,J-1)*X1(IJ-1)-A33(I,J-1)*X2(IJ-1)-A31(I,J)*X3(IJ-1)
      IF(L.GE.LC) U=U-A32(I,LC)*X1(I+LC)-A33(I,LC)*X2(I+LC)
502  X3(I)=U/A31(I,1)
C
      U=X2(I)-A22(I,1)*X3(I)
      IF(I.EQ.LN) GO TO 504
      DO 503 J=2,L
      IJ=I+J
503  U=U-A23(I,J-1)*X1(IJ-1)-A21(I,J)*X2(IJ-1)-A22(I,J)*X3(IJ-1)
      IF(L.GE.LC) U=U-A23(I,LC)*X1(I+LC)

```

```

504 X2(I)=U/A21(I,1)
C
U=X1(I)-A12(I,1)*X2(I)-A13(I,1)*X3(I)
IF(I.EQ,LN) GO TO 506
DO 505 J=2,L
IJ=I+J
505 U=U-A11(I,J)*X1(IJ-1)-A12(I,J)*X2(IJ-1)-A13(I,J)*X3(IJ-1)
506 X1(I)=U/A11(I,1)
IF(L.LT,LC) L=L+1
C
507 CONTINUE
C
RETURN
END
C ///////////////////////////////////////////////////////////////////
C
SUBROUTINE CONST(ICON,IREF)
C
C ///////////////////////////////////////////////////////////////////
C
ICON=0 (AXISYMMETRIC BODY RADIUS IS COMPUTED FROM SURFACE
LOCATIONS)
1 (RADIUS POLYNOMIALS ARE INPUT TO THE PROGRAM BY READ
STATEMENTS LATER IN THIS SUBROUTINE)
COMMON/CONST/ R(30),Z(30),XP(30),A(30),B(30),C(30),J(30),E(30),
1F(30),CP(30),DP(30),INUM
COMMON G, PR, REY, XMINF, OMEGA, BO, TW, P10, T10, R10, VIS10, TE,
1 PE,RE,UF,VISINF,SU,EPS,DS,DYW,SI,ERROR,TC,TA,IEDGE,IEND1,INTACT,
2 PRT,XXK,BTRX,XLAM,VARPRT,XINTER,SEPO,ICHS(8),IPRN(9),EO(200),
3 EN(200),EP(200),ETO(200),ETN(200),ETP(200),FO(200),FN(200),J2DA,
4 FP(200),TN(200),TO(200),XNN(200),VN(200),VO(200),VP(200),TP(200),
501(200),02(200),03(200),T2JP(200),T2JO(200),T2JN(200)
IF(ICON.EQ.1) GO TO 25
WRITE(6,241)
241 FORMAT(5X,"R/L Z/L")
DO 32 IT=1,INUM
WRITE(6,801) R(IT),Z(IT)
801 FORMAT(2F15.9)
32 CONTINUE
KEND=INUM-2
N=1
DO 19 K=1,KEND
NEND=N+2
DO 12 M=N,NEND
D(M)=1.
E(M)=Z(M)
12 F(M)=Z(M)**2
DET =D(N)*E(N+1)*F(N+2)+E(N)*F(N+1)*D(N+2)+D(N+1)*E(N+2)
1*F(N)-F(N)*E(N+1)*D(N+2)-E(N)*D(N+1)*F(N+2)-D(N)*
2F(N+1)*E(N+2)
DO 14 M=N,NEND
14 D(M)=R(M)
DETA=D(N)*E(N+1)*F(N+2)+E(N)*F(N+1)*D(N+2)+D(N+1)*E(N+2)
1*F(N)-F(N)*E(N+1)*D(N+2)-E(N)*D(N+1)*F(N+2)-D(N)*
2F(N+1)*E(N+2)

```

```

      DO 16 M=N,NEND
      D(M)=1.0
16  E(M)=P(M)
      DETR=D(N)*E(N+1)*F(N+2)+E(N)*F(N+1)*D(N+2)+D(N+1)*E(N+2)
      1*F(N)-F(N)*E(N+1)*D(N+2)-E(N)*D(N+1)*F(N+2)-D(N)*
      2F(N+1)*E(N+2)
      DO 18 M=N,NEND
      E(M)=7(M)
18  F(M)=R(M)
      DETC=D(N)*E(N+1)*F(N+2)+E(N)*F(N+1)*D(N+2)+D(N+1)*E(N+2)
      1*F(N)-F(N)*E(N+1)*D(N+2)-E(N)*D(N+1)*F(N+2)-D(N)*
      2F(N+1)*E(N+2)
      A(K)=DETA/DET
      B(K)=DETR/DET
      C(K)=DETC/DET
      N=N+1
19  CONTINUE
      ZCON=0.0
      RCON=0.0
      S=0.0
      N=1
      KN=1
      DZ=DS
      Z2REF=Z(INUM)+DZ
22  CONTINUE
      IF(ABS(ZCON-Z(KN)).LE.DZ/2.) XP(KN)=S
      IF(KN.EQ.INUM) GO TO 25
      IF(ABS(ZCON-Z(KN)).LE.DZ/2.) KN=KN+1
25  CONTINUE
      IF(N.EQ.KEND) GO TO 24
      ZREF=Z(N+1)
      IF(ZCON.GE.ZREF) N=N+1
24  DRDZ=R(N)+2.0*C(N)*ZCON
      ALPHA=ATAN(DRDZ)
      DR=DS*STN(ALPHA)
      DZ=DS*COS(ALPHA)
      RCON=RCON+DR
      S=S+DS
      ZCON=ZCON+DZ
      IF(ZCON.LT.Z2REF) GO TO 22
      DO 83 KL=1,INUM
      D(KL)=0.
      E(KL)=0.
83  CONTINUE
26  CONTINUE
      IF(ICON.EQ.0) GO TO 41
      J=1
      K=1
      RCON=0.
      ZCON=0.
      S=0.
      KN=1
      DZ=DS
      READ(5,1000) IREF

```



```

1000 FORMAT(1I2)
1001 FORMAT(5F15.9)
1002 FORMAT(1F15.9)
      DO 27 I=1,IREF
      READ(5,1001) A(I),B(I),C(I),D(I),E(I)
      READ(5,1002) F(I)
27 CONTINUE
      F(IREF)=F(IREF)+DZ
36 IF(ABS(ZCON-Z(KN)).LE.DZ/2.) XP(KN)=S
   IF(KN.EQ.INUM) GO TO 29
   IF(ABS(ZCON-Z(KN)).LE.DZ/2.) KN=KN+1
29 DRDZ=B(J)+2.*C(J)*ZCON+3.*D(J)*ZCON**2+4.*E(J)*ZCON**3
   ALPHA=ATAN(DRDZ)
   DZ=DS*COS(ALPHA)
   S=S+DS
   ZCON=ZCON+DZ
   RCON=A(J)+B(J)*ZCON+C(J)*ZCON**2+D(J)*ZCON**3+E(J)*ZCON**4
   IF(ZCON.GE.F(J)) J=J+1
   IF(ZCON.LT.F(IREF)) GO TO 36
   WRITE(6,242)
242 FORMAT(10X,"CP          Z/L ")
      DO 3 KB=1,INUM
      WRITE(6,7112) CP(KB),Z(KB)
7112 FORMAT(2F15.9)
      3 CONTINUE
      41 CONTINUE
      RETURN
      END

```

### Vita

Charles R. Blake was born October 22, 1946 in Meridian Mississippi. He received his primary education in Hickory, Mississippi and graduated as valedictorian from Hickory High School in 1964. He received his undergraduate education at East Central Junior College and Mississippi State University. He was awarded a Bachelor of Science Degree in Aerospace Engineering from Mississippi State University in May 1969.

Upon graduation from college, Capt Blake was employed as an aerospace engineer for Brown Engineering Company, Huntsville, Alabama until entering the USAF in August 1969. He received a commission in November 1969 from the USAF Officer Training School and was then assigned to Undergraduate Pilot Training at Moody AFB, Georgia. He received his wings in December 1970.

Capt Blake then served as a C-130 pilot and flight instructor at Little Rock AFB, Arkansas, CCKAB, Republic of China, and Clark AB, Phillipines. He was then serving a second tour at Little Rock AFB immediately prior to entering the School of Engineering, Air Force Institute of Technology in May 1975.

Permanent address: Route 1,

Chunky, Miss., 39323

UNCLASSIFIED

SECURITY CLASSIFICATION OF THIS PAGE (When Data Entered)

REPORT DOCUMENTATION PAGE		READ INSTRUCTIONS BEFORE COMPLETING FORM
1. REPORT NUMBER GA/MC/76D-4	2. GOVT ACCESSION NO.	3. RECIPIENT'S CATALOG NUMBER
4. TITLE (and Subtitle) NUMERICAL SOLUTION OF THE COMPRESSIBLE BOUNDARY LAYER EQUATIONS OVER AXISYMMETRIC SURFACES		5. TYPE OF REPORT & PERIOD COVERED MS Thesis
7. AUTHOR(s) Charles R. Blake Capt USAF		6. PERFORMING ORG. REPORT NUMBER
9. PERFORMING ORGANIZATION NAME AND ADDRESS Air Force Institute of Technology (AFIT-EN) Wright Patterson AFB, Ohio 45433		8. CONTRACT OR GRANT NUMBER(s)
11. CONTROLLING OFFICE NAME AND ADDRESS		10. PROGRAM ELEMENT, PROJECT, TASK AREA & WORK UNIT NUMBERS
14. MONITORING AGENCY NAME & ADDRESS (if different from Controlling Office)		12. REPORT DATE Dec, 1976
		13. NUMBER OF PAGES 106
		15. SECURITY CLASS. (of this report) Unclassified
		15a. DECLASSIFICATION/DOWNGRADING SCHEDULE
16. DISTRIBUTION STATEMENT (of this Report)  Approved for public release; distribution unlimited		
17. DISTRIBUTION STATEMENT (of the abstract entered in Block 20, if different from Report)		
18. SUPPLEMENTARY NOTES  Approved for public release; IAW AFR 190-17 Jerral F. Guess, Captain, USAF Director of Information		
19. KEY WORDS (Continue on reverse side if necessary and identify by block number) Boundary Layer Compressible Axisymmetric		
20. ABSTRACT (Continue on reverse side if necessary and identify by block number) A numerical solution of the compressible boundary layer equations was developed for flows over either two-dimensional or axisymmetric surfaces. The solution method is capable of solving for boundary layer parameters in either laminar or turbulent flows. In the case of turbulent flow, closure is achieved by use of a two-layered eddy viscosity model. The boundary layer equations are solved by a numerical marching procedure. A Mangler-Levy-Lees transformation of independent variables is used to improve the efficiency of the		

DD FORM 1 JAN 73 1473

EDITION OF 1 NOV 65 IS OBSOLETE

UNCLASSIFIED

OVER

SECURITY CLASSIFICATION OF THIS PAGE (When Data Entered)



UNCLASSIFIED

SECURITY CLASSIFICATION OF THIS PAGE(When Data Entered)

20.  
numerical solution. The transformed boundary layer equations are then linearized by a three point finite difference scheme. The linearized equations are solved by a matrix solution technique. Comparisons of computed boundary layer parameters with experimentally determined parameters were made for both laminar and turbulent flows over axisymmetric bodies. The comparisons show the numerical solution to be very accurate.

UNCLASSIFIED

SECURITY CLASSIFICATION OF THIS PAGE(When Data Entered)